NUMERICAL STUDIES OF FIELD THEORIES ON RANDOM LATTICES

Simon Marcus Catterall

Department of Theoretical Physics
University of Oxford

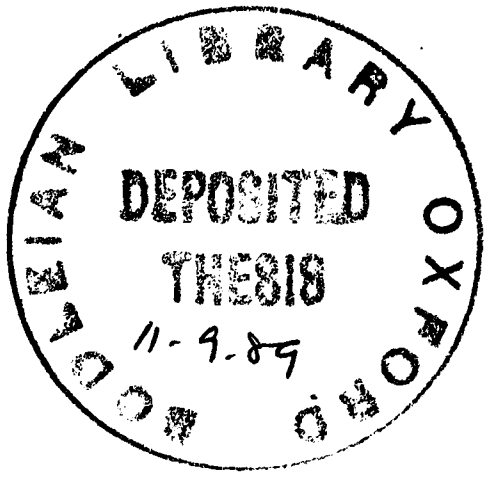

A Thesis submitted for the degree of
Doctor of Philosophy
at the University of Oxford

Christ Church

November 1988

NUMERICAL STUDIES OF FIELD THEORIES ON RANDOM LATTICES

Simon Marcus Catterall
Christ Church, Oxford

A Thesis submitted for the degree of Doctor of Philosophy
Michaelmas Term 1988

Abstract

In this thesis we shall be concerned with the study of models which arise as a consequence of adopting discrete regularisations for various Euclidean space quantum field theories. Specifically, we employ a random triangulation of the continuum space, and define the fields only over nodes or links of the mesh.

Lattice field theories, together with the Renormalisation Group, are introduced in the first chapter. Continuum physics is shown to depend on the positions and stabilities of zeroes of the β-function, which in turn requires a knowledge of the critical behaviour of the associated statistical model.

In Chapter 2. we examine a theory of Dirac fermions in $2+1$ dimensions on a random lattice. We investigate the behaviour of the 2-pt function and fermion condensate in the absence of any background gauge field. The results indicate certain doubling problems, generic to regular lattice formulations of fermion field theories, are evaded, at least at tree graph level. We then go on to examine the fermion vacuum currents in the presence of background fields with non-zero winding number. We are able to demonstrate the existence of a Chern-Simon's topological term in the gauge field effective action which yields parity violating vacuum currents. The magnitude of these are in agreement with certain continuum calculations.

The final chapter concerns the properties of random surfaces. The particular class of models chosen originate as discretisations of Polyakov's string. The partition function is approximated by a sum over all possible random triangulations and an integral over vertex positions. The sum over random lattices is intended to mimick the functional integral over intrinsic metrics encountered in the continuum, and the model may also be pictured as 2D quantum gravity coupled to a scalar field. We consider the phase structure of the models when two forms of extrinsic curvature are added to the standard action. Monte-Carlo simulation indicates that with one type of curvature term a strong 2^{nd} order phase transition exists at finite coupling, leading to a new continuum limit for the model possessing long-range correlation properties. With the other type a much weaker higher order transition is observed. In this case the surface will be crumpled at long distance. We discuss the implications of these results for continuum surfaces.

Acknowledgements

I should like to thank my supervisor John Wheater for his help and advice throughout my 3 years as a research student in Oxford. In addition I am grateful to Jack Paton for his interest and advice and to the S.E.R.C for the provision of a studentship. My thanks go especially to Don Ballance, Michael Bull, Paul Upton and Mike Wragg and to the many others who made my time in Theoretical Physics so enjoyable and worthwhile. Finally I should like to thank my family and Janette for their help, encouragement, and support at all times.

CONTENTS

Chapter One

Lattices and the Renormalisation Group

1.1 Introduction

In this thesis we shall be concerned with studies of discrete quantum field theories. For such models to be physically interesting we will require that their predictions for continuum physical quantities be independent of the precise form of discretisation, and specifically the size of the spacetime cut-off. That this is possible is dependent on two crucial facts. The first of these is related to existence of points in the parameter space of the models where cooperative effects couple many of the degrees of freedom in an essential way. At such points the presence of long range correlations ensure that the long distance properties of the theory become insensitive to the details of the lattice regularisation. The second depends on a non-trivial property of the theories termed renormalisability. This ensures that one may consistently parametrise the long distance theory in a way independent of the cut-off. We start with a brief summary of the essential features of continuum perturbative renormalisation which will motivate subsequent discussions of lattice renormalisation techniques and the extraction of continuum physics from discrete models.

1.2 Renormalisation in continuum field theory

In studying classical field theory we learn that all of the physics describing the spacetime evolution of, for example, some scalar field $\phi(x)$ is encoded in the action functional

$$S = S\left[\phi(x), \partial_\mu \phi(x), + \cdots\right] \tag{1.1}$$

where we might choose S to be

$$S = \int d^D x \, \frac{1}{2} \partial_\mu \phi(x) \, \partial^\mu \phi(x) - \frac{1}{2} m^2 \phi(x)^2 - \frac{\lambda}{4!} \phi(x)^4$$

the integral extending over all the D-dimensional spacetime. The expression inside the integral is termed the Lagrangian L. One defines the momentum field canonically conjugate to the ϕ-field by a derivative of the Lagrangian

$$\pi(x) = \frac{\partial L}{\partial(\partial_0 \phi)}$$

The equations of motion are obtained by finding extrema of S under variation of the field. In this case we obtain;

$$\partial^\mu \partial_\mu \phi(x) + m^2 \phi(x) = -\frac{\lambda}{3!} \phi(x)^3 \, .$$

The transition to a quantum theory is traditionally done by deriving a Hamiltonian and imposing commutation relations between the ϕ-fields, now regarded as operators, and their conjugate momenta. The physical content of the quantised theory is contained in its Green functions. These are vacuum expectation values of time ordered products of the fields $\phi(x)$;

$$G^N\left(\phi(x_1) \cdots \phi(x_N)\right) = \langle 0 | T\left(\phi(x_1) \cdots \phi(x_N)\right) | 0 \rangle \tag{1.2}$$

It proves expedient to calculate these from within the Feynman path integral formulation where the fields are once again c-number quantities and the probability amplitude for a given transition is obtained by a sum over all paths in field space,

weighted by e^{iS}. The Green functions may be obtained from a quantity known as the vacuum generating functional $Z[J]$.

$$Z[J] = \int D\phi \, e^{iS[\phi, \partial\phi, J]} \tag{1.3}$$

where a source term $J\phi$ is added to the standard action. If one functionally differentiates $\ln Z$ with respect to sources $J(x_1)$, $J(x_2)$, ..., and then sets the J's to zero one obtains averages or correlations of the fields with respect to the weight function e^{iS}. It may be shown that these are precisely the Green functions obtained in the canonical formalism. This path integral formulation requires a proper definition of the measure $D\phi$ and a subsequent demonstration of the convergence of the resulting integral. This proves extremely difficult in Minkowski space. In Euclidean space, obtained by the replacement $t \rightarrow -i\tau$, the suppression of paths far from the classical solution is manifest, the weight function now being e^{-S}. This substantially improves the convergence properties of the integral. However, as we shall see, the presence of an infinite number of degrees of freedom (the field at every spacetime point is to be regarded as an independent variable), leads to difficulties when calculating with the interacting theory.

The necessary functional integrals defining Z can only be performed for a free theory; one quadratic in the fields. Traditional methods of approach concentrate on a perturbative solution, in which the Green functions are developed as a power series in the (assumed small) coupling constant λ. These series are at best only asymptotic, and only useful for the calculation of physical amplitudes at energy scales where $\lambda \ll 1$. Even here important physics may be missed in such an approach and indeed for many theories of interest (e.g Q.C.D) the relevant coupling constant is large at the mass scales of interest (these theories are free only at asymptotically large mass scales) . This seems to preclude this type of approach. Indeed Renormalisation Group arguments lead to the conclusion that only theories with infrared fixed points at zero interaction stength behave at long distance like free theories, allowing for an identification of the asymptotic physical states with free

particles. It is only with these theories that an attempted expansion about a theory defined on the quadratic terms in the Lagrangian is valid at all. At present the best method of approach for theories without such properties is via a lattice description.

Eventually we will be interested in sending the spacing in our lattice theories to zero to recover continuum physics. To achieve this a non-trivial renormalisation of the bare parameters must be performed. In order to understand this process we will first summarise briefly the conventional methods of obtaining finite Green functions in continuum perturbation theory. We shall illustrate the process for the model we have already been discussing; scalar ϕ^4 theory.

The perturbative approach is most easily visualised diagrammatically with the aid of Feynman diagrams. A graph corresponding to some term in the perturbation series for a Green function in the interacting theory is built from lines (propagators of the free theory) which are joined at vertices determined by the interaction term $\lambda\phi^4/4!$. One particular method of approach attempts to evaluate the functional integral by an expansion about the saddle point corresponding to the classical solution. Successive terms in this expansion are the quantum corrections. Diagrammatically they correspond to graphs possessing internal loops leading to sums over all possible momenta of the intermediate state. For certain D the integrals representing their contributions diverge. Thus a perturbative approach apparently leads to nonsense. The essence of the technique of renormalisation is to reorganise the perturbation series in terms of a new set of parameters– the renormalised parameters in terms of which the Green functions can be made finite at all orders in the interaction. The first step in this process requires the identification of that subset of all possible graphs which are ultimately responsible for the divergences– these are termed the primitively divergent graphs. On inspection, one soon discovers that (except in certain massless theories) these divergences stem from the high energy modes of the kinetic operator.

The first job in the process of extracting something finite from these expressions consists of regulating the theory by, for instance, imposing a high-momentum cut-off

Λ. This truncation only allows the contribution of intermediate states with momenta less than Λ. The precise method of regularisation is unimportant as eventually we will want to remove the regulator to regain our original theory. It is merely a procedure which we follow to allow us to subsequently manipulate quantities which otherwise would be ill-defined. Other common methods include adding an opposite statistics Pauli-Villars regulator field, or analytically continuing the integrals in the dimension of spacetime (dimensional regularisation). In the former we subtract off the bad high energy behaviour of a graph by the contribution of some massive state of opposite statistics. The removal of the regulator then corresponds to letting the regulator mass $M \to \infty$, so that it decouples from the theory at physical mass scales. The essence of dimensional regularisation rests on the fact that the convergence properties of the graphs are improved in lower dimension. The diagrams can then be evaluated in general dimension by analytic continuation in D, poles corresponding to $1/\epsilon$ terms ($\epsilon = 4-D$) appearing in the resulting expressions in say $D = 4$, or at any other dimension where the original integral diverged. Dimensional regularisation has the advantage that it does not mutilate the structure of a graph, preserves symmetries of the classical theory, and is equally applicable to the infrared divergences, which are the major problem in critical phenomena.

Now that everything is finite and well-defined one calculates the amplitudes to some given order in the coupling constant, which now explicitly depend on the regulator Λ, or ϵ if we're employing dimensional regularisation. Typically the contribution will have a part, finite as the regulator is removed, plus potentially divergent pieces. Next one constructs counterterms, to be added to the original Lagrangian, whose job it is to cancel off these divergences. The finite part of these is arbitrary at this point. The ambiguity in the choice of the latter is a reflection of the arbitrariness in cancelling off the infinities. That the theory is independent of the choice of these finite pieces is the fact that is exploited in the Renormalisation Group. Counterterms which differ from each other by finite terms merely correspond to different parametrisations of the same theory with different renormalised parameters.

The process is continued order by order in the coupling λ, the Lagrangian containing terms of order λ^n being used to calculate the new Green functions to order λ^{n+1}, which are made finite by the addition of new counterterms at this order. The theory is termed renormalisable if the form of the counterterms needed to render the theory finite to arbitrary order correspond to terms present in the bare Lagrangian. The resulting Lagrangian may be written;

$$L_{ren} = L + L_{c.t}$$

where

$$L_{ren} = \frac{1}{2}(\partial_\mu \phi_0)^2 + \frac{1}{2}m_0^2\phi_0^2 + \frac{\lambda_0}{4!}\phi_0^4 \tag{1.4}$$

and

$$\begin{aligned} L =& \frac{1}{2}(\partial_\mu \phi)^2 + \frac{1}{2}m^2\phi^2 + \frac{\lambda}{4!}\phi^4; \\ L_{c.t} =& \frac{1}{2}(A\partial_\mu \phi)^2 + \frac{1}{2}Bm^2\phi^2 + \frac{1}{4!}C\phi^4 \end{aligned} \tag{1.5}$$

and A, B, C are constructed so that the Green functions generated by L_{ren} are finite as $\Lambda \to \infty$ or $\epsilon \to 0$. One may then sweep the infinities into redefinitions of the parameters in the Lagrangian and rescalings of the fields. At this point the cut-off may be removed. The finite part of the counterterms, within say a Pauli-Villars scheme of regularisation, are fixed by requiring that at some scale μ they are determined by certain normalisation conditions (also called prescriptions) on a small number of renormalised amplitudes. A similar, arbitrary, renormalisation scale enters in dimensional regularisation as the couplings of the theory have mass dimensions dependent on D, which leads to the introduction of an arbitrary mass parameter μ to absorb this dependence in general D. Thus we see that in rewriting the perturbation series in such a way as to eliminate the strong dependence on the cut-off Λ we are forced to introduce a compensating scale μ which is arbitrary but finite. Since the counterterms are now functions of this renormalisation scale, this implies that renormalised parameters (those in L) also develop a scale dependence. The statement of renormalisability implies the following relationship between the

Green functions of the bare and renormalised theories (we are using dimensional regularisation for convenience);

$$\Gamma_R^N\left(p_i,\lambda,m,\mu,\epsilon\right)=Z^{N/2}\Gamma_0^N\left(p_i,\lambda_0,m_0,\epsilon\right) \tag{1.6}$$

with Γ_R^N analytic in ϵ. We may express the invariance of the Green functions (strictly proper vertices) of the theory under changes in μ by noticing that the bare Green functions are independent of μ and hence;

$$\left(\mu\frac{\partial}{\partial\mu}+\beta\frac{\partial}{\partial\lambda}+\gamma_m m\frac{\partial}{\partial m}-\frac{n}{2}\gamma_d\right)\Gamma_R^N=0 \tag{1.7}$$

where

$$\begin{aligned}\beta\left(\lambda,\frac{m}{\mu},\epsilon\right)&=\mu\frac{\partial\lambda}{\partial\mu};\\ \gamma_d\left(\lambda,\frac{m}{\mu},\epsilon\right)&=\frac{1}{2}\mu\frac{\partial\ln Z}{\partial\mu};\\ \gamma_m\left(\lambda,\frac{m}{\mu},\epsilon\right)&=\frac{1}{2}\mu\frac{\partial\ln m^2}{\partial\mu}.\end{aligned} \tag{1.8}$$

These are analytic as $\epsilon\rightarrow 0$ and dimensionless–they depend only on λ and $\frac{m}{\mu}$. Γ_R^N has a canonical dimension d_N equal to

$$4-N+\epsilon(N-2)$$

and under a uniform scaling of the momenta from p to sp we have;

$$\left[\mu\frac{\partial}{\partial\mu}+s\frac{\partial}{\partial s}+m\frac{\partial}{\partial m}-(4-N+\epsilon(N-2))\right]\Gamma_R^N\left(sp,m,\lambda,\mu,\epsilon\right)=0$$

The β,γ functions are in general functions of the mass parameter. However it is possible to choose a renormalisation prescription where this dependence disappears–the minimal subtraction scheme. Neglecting also for the moment the mass term in the equations and eliminating $\frac{\partial}{\partial\mu}$, we arrive at a scaling equation for Γ_R^N

$$\left[-s\frac{\partial}{\partial s}+\beta\left(\lambda\right)\frac{\partial}{\partial\lambda}+d_N-N\gamma_d\left(\lambda\right)\right]\Gamma_R^N=0 \tag{1.9}$$

To solve this partial differential equation introduce the scale dependent or running coupling constant $\lambda\left(s\right)$. The solution then becomes;

$$\Gamma_R^N\left(sp,\lambda,\mu\right)=s^{-d_N}\Gamma^N\left(p,\lambda\left(s\right),\mu\right)e^{N\int_1^s\frac{ds'}{s'}\gamma_d\left(\lambda\left(s'\right)\right)}. \tag{1.10}$$

Thus under a change of momenta the Green functions scale in a non-trivial way. The coupling constant flows with scale s according to the β-function and the Green functions Γ^N develop, beside the canonical dimension d_N, an anomalous dimension γ_d for each external line. As we shall see, the asymptotic behaviour depends on the zeroes of the β-function or fixed points of the theory. Generic points in the parameter space flow into these points under repeated rescalings. At these points the coupling constants are invariant under further scale changes. Considerations of the sign of the β-function near these points allow one to infer the domain of attraction of the points in the limits of high and low momenta. Unfortunately one can only calculate the β-function in perturbation theory, and hence the only zeroes of it that may be relied on are those at zero interaction coupling corresponding to a free theory. Non-perturbative methods must be used if one is to investigate other non-trivial zeroes of this function. Of course in general the β- function is expressible as a double Taylor series in ϵ and λ, hence the fixed point structure is also dependent on ϵ. This dependence only disappears in a dimension where the coupling is dimensionless. However this ϵ-expansion allows one to study theories away from such critical dimensions within perturbation theory.

Having summarised this approach, let us consider its failings. Perhaps the most obvious is that already mentioned– that it is tied to perturbation theory. Secondly the usual continuum regulators do not possess any physical motivation– they are merely mathematical tricks used to render the graphs well-defined and to isolate the divergences. It would be nice to have a regulator which possessed a more direct physical interpretation. Such is the lattice (whether a regular or random discretisation of spacetime). This structure allows for non-perturbative studies to be carried out, the cut-off corresponding to some inverse average lattice spacing. Strong-coupling expansions are also rather natural on the lattice, and since we always deal with finite systems the problem may be translated onto the computer for numerical simulations to be performed.

It turns out that these discretised Euclidean space quantum field theories can

be interpreted as classical statistical models in one higher spatial dimension. Let the field $\phi(x)$ become the discrete set of variables ϕ_i, $i = 1 \cdots N$. Replace derivatives by some sort of nearest-neighbour coupling giving a matrix M_{ij}. The vacuum generating functional Z becomes a partition function and is represented by an ordinary, absolutely convergent, multiple integral

$$Z = \int \prod_{i=1}^{N} d\phi_i \, e^{-S_E} \tag{1.11}$$

where S_E now reads

$$S_E = \alpha \sum_{ij} \phi_i M_{ij} \phi_j + \gamma \phi_i^4$$

The Green functions map to correlation functions of the classical fields. This allows all the tools used by theorists in statistical mechanics and solid state physics to be employed in studying these models. It matters not (at least for scalar fields) whether we choose to regard the lattice spacing as some sort of fundamental scale (say the Planck length), Poincaré invariance being only an approximate symmetry valid on scales greater than this spacing, or merely as a cut-off required to define the quantum theory. One may expect that one can construct renormalised physical amplitudes which become independent of the cut-off at points where a continuum limit corresponding to a relativistic quantum field theory is obtained.

The degrees of freedom on the lattice are only coupled locally so it is a non-trivial problem to achieve correlations at finite fixed physical distance, as the lattice spacing tends to zero. It requires the inverse mass-gap of the theory to diverge in units of the lattice spacing. This is a feature of statistical models at so-called critical points of their parameter space, where a second or higher order phase transition occurs. Thus it is of some importance to understand the essential features of the critical properties of such models in order to understand how to take the continuum limit of any discrete quantum field theory.

1.3 Introduction to Critical Phenomena

As we have seen, in order to understand how we should approach the problem of taking the continuum limit of some lattice field theory, we must first acquaint ourselves with some of the phenomenology of statistical systems near critical points. Consider, for example, the 2-D Ising model, which is defined by the Hamiltonian (with N sites)

$$H = -J \sum_{\langle ij \rangle} \sigma_i \sigma_j$$

where the σ_i are discrete variables, constrained to the values $(+1\ , -1)$, and the sum runs over all bonds of the lattice. One may add a term coupling linearly to an external field B;

$$H \rightarrow H + B \sum_{i=1}^{N} \sigma_i$$

The partition function reads

$$Z = \sum_{\text{configs.}} e^{-\beta H}$$

with the corresponding free energy

$$F = -\frac{1}{\beta} \ln Z$$

where the sum runs over all 2^N possible spin configurations of the system. The model shows two qualitatively different phases. These are distinguished by a local order parameter – the average magnetisation per site

$$m = \frac{1}{N} \langle \sum_{i=1}^{N} \sigma_i \rangle$$

Alternatively we may write it as a derivative of the free energy with respect to the field B. The model defined by this Hamiltonian in the absense of the field term is invariant under the global symmetry

$$\sigma_i \rightarrow -\sigma_i$$

and the presence at large β of a non-zero value of the order parameter (which is not invariant) signals the spontaneous breakdown of this symmetry. It occurs because

the ground state of the theory in zero field is not invariant under the symmetry, even though the Hamiltonian is. Thus in the ground state spins must all point either up or down. One of the most difficult tasks, when analysing a general spin model for phase structure, may be the identification of the appropriate order parameter which develops a non-zero value in the non-symmetric phase. In some models (e.g 2-D continuous spin models, and theories with a local symmetry) such local order parameters may be absent, and the study of non-local quantities such as spin-spin correlation functions may be necessary to distinguish different phases.

The magnetisation vanishes as a power near the critical point

$$m \sim (\beta - \beta_c)^{\rho} .$$

The index ρ is termed a critical exponent. It is instructive to examine the fluctuations of this magnetisation;

$$\chi = \left\langle \frac{1}{N} \left(\sum_i \sigma_i - m \right)^2 \right\rangle \tag{1.12}$$

this becomes;

$$\frac{1}{N} \sum_{ij} \langle \sigma_i \sigma_j \rangle - m^2$$

if we choose a point where $m \sim 0$ then we see that this susceptibility χ measures the sum over correlation functions

$$\chi = \sum_i \langle \sigma_0 \sigma_i \rangle \tag{1.13}$$

and this may diverge if there are long-range correlations. As before we characterise this divergence in terms of some new exponent γ

$$\chi \sim (\beta - \beta_c)^{-\gamma} \tag{1.14}$$

Another thermodynamic function of interest is the specific heat or variance of the Hamiltonian;

$$\begin{aligned} C &= \langle H^2 \rangle - \langle H \rangle^2 \\ &\sim \frac{\partial^2 F}{\partial \beta^2} \end{aligned}$$

this may also diverge, sensitive as it is to large fluctuations in the spins, its singular part varying like;

$$C \sim (\beta - \beta_c)^{-\alpha}$$

If (as in the Ising model) the transition is continuous with singularities only occurring in second derivatives of the free energy, it is said to be of second order. Consider now the spin-spin correlation function. At a generic point in the parameter space of the model, it behaves as

$$\langle \sigma_i \sigma_j \rangle \sim e^{-r_{ij}/\xi(\beta)} \tag{1.15}$$

However, close to the critical point, β_c, the correlation length ξ diverges in units of the lattice spacing. This manifests itself in power law behaviour of the correlation function.

$$\langle \sigma_i \sigma_j \rangle \sim r_{ij}^{-(d-2+\eta)}$$

where η the anomalous dimension is a critical exponent. The divergence of ξ as $\beta \to \beta_c$ is controlled by another critical exponent ν

$$\xi \sim (\beta - \beta_c)^{-\nu}$$

Thus we have seen that the properties of typical statistical models near their critical points shows a universality manifested in the appearance of critical exponents which commonly are only sensitive to the dimensionality of the system and the nature of any symmetries of the Hamiltonian. The transition is pictured to be driven by the presence of a diverging correlation length (ξ), which becomes the only important length scale in the system, completely suppressing details of the interaction on scales of the lattice spacing. There is then an approximate scale invariance in the system.

The presence of power law behaviour of the singular part of the thermodynamic functions can be generalised to the more useful statement that these functions behave as generalised homogeneous functions of the variables used to describe the macroscopic state of the system (eg β and B). A generalised function of 2 variables is one such that

$$f(\lambda^p x, \lambda^q y) = \lambda f(x, y) \tag{1.16}$$

In order to see how the p and q relate to critical exponents consider writing the singular part of the free energy as such a function

$$f(\lambda^p t, \lambda^q B) = \lambda f(t, B)$$

where t is $\beta - \beta_c$. Differentiate with respect to B to obtain the magnetisation.

$$\lambda^q m(\lambda^p t, \lambda^q B) = \lambda m(t, B)$$

set $\lambda = (-t)^{-1/p}$ and put $B = 0$

$$m(t, 0) = (-t)^{\frac{1-q}{p}}$$

this leads one to identify the magnetisation exponent β with $\frac{(1-q)}{p}$. Similar arguments lead to all the critical exponents being determined in terms of p and q. Thus the hypothesis leads to so-called scaling laws relating the many critical exponents. These have experimental support.

Many tools have been developed for the study of such systems, for example high temperature expansions (strong coupling). These are based on expanding the Boltzman factor in the partition function and carrying out the configurational sums on the individual terms. Mean field methods can be employed, effectively evaluating the partition function by a saddle point approximation, whereby fluctuations are ignored and the expectation values of fields determined by minimising the resulting approximation for the free energy. At the other end of the coupling constant range low temperature expansions (weak coupling) also attempt to evaluate Z by a spin-wave expansion about some ground state of the model. All these methods fail to describe the critical point adequately, since they neglect the long-range correlations which are the all-important feature of systems at criticality. However as we shall see next, the methods of the Renormalisation Group work best near points where there is an approximate scale invariance.

1.4 Lattice Renormalisation Group arguments in spin models

As we have discussed, the search for continuum physics in lattice field theories must take place close to a critical point of the lattice model, where a diverging correlation length allows approximate scale invariance of the theory. We have seen in the continuum how the inclusion of fluctuations (i.e quantum corrections) induces a scale dependence in the physical parameters of the theory via renormalisation effects. This amounts to the statement that we can compensate for changes in the renormalisation scale (as seen in dimensional regularisation, for example), by an appropriate change of the coupling constants of the theory. An alternative approach, due to Wilson, exploits the arbitrariness in the parameterisation of a renormalisable theory in a more intuitive way. Instead of considering the variation of the renormalised parameters with renormalisation scale, holding the bare parameters and cut-off fixed, one chooses to vary the bare parameters and cut-off together in such away as to leave the renormalised parameters unchanged. This is the procedure usually effected in studies of critical phenomena and lattice gauge theories. Here the trick is to successively decrease some high-momentum cut-off, by integrating out degrees of freedom describing short distances, in such a way as to preserve the physics on long length scales. One finds a flow of the coupling constants under repeated applications of this transformation, and if the system is near criticality these flows may be attracted to a fixed point of the transformation. Such a point corresponds to a zero of a β-function which now gives the rate of change of the coupling with the cut-off. Notice that the central problem in critical phenomena corresponds to the divergence of correlation functions in the thermodynamic limit. It is thus the infrared properties that lead to the need for renormalisation here. In order to see these features in more detail we next summarise lattice renormalisation techniques, illustrating how they lead to critical exponents. It will be shown how considerations of stability of such points allow one to infer both the infrared and ultra-violet behaviours of the theory.

The basic idea of the lattice renormalisation group is that, close to a criti-

cal point, the spins fluctuate coherently over distances of the order the correlation length. The dominance of long-range fluctuations means that details of the interaction on the scale of the lattice spacing are irrelevant to the long-distance physics. One can consider thinning the number of degrees of freedom in the system by constructing "block spins", which represent some sort of average of the spins within some block of linear dimensions L, and systematically integrating out the interior spins. One is left with an effective Hamiltonian for the block spins, with renormalised coupling constants, which represents the same long-distance physics. This non-linear transformation of the coupling constants is termed an R.G transformation. Formally we perform the constrained sum

$$e^{-H_L(S_L)} = \sum_{\sigma_i} e^{-H(S_L,\sigma_i)} \tag{1.17}$$

where the sum on σ_i is over "interior" spins, consistent with some fixed configuration of the renormalised spins S_L. The partition function is an invariant by construction. In general, of course, such a procedure will induce new interactions not present in the bare Hamiltonian. If one imagines a space of all couplings, each of which is conjugate to to a possible interaction term, then the effect of repeated R.G transformations is to cause a flow in this space. Assembling the coupling constants into a vector K, the elementary transformation is pictured

$$K_L = T(K) \tag{1.18}$$

Fixed points in this parameter space correspond to points invariant under T. Call such a generic point the vector K^*. In order to examine the flow near such a point we linearise the transformation around K^*. Setting $\delta K = K - K^*$ we obtain

$$\delta K_L \sim T^* \delta K$$

where T^* is a matrix of partial derivatives of T with respect to the couplings, evaluated at K^*. By a sequence of transformations, one can bring this to diagonal

form, with a new set of couplings δk^r. Under n applications of the transformation T, these scale simply as

$$\delta k^r_{nL} \sim (\lambda^r)^n \, \delta k^r$$

where λ^r are the eigenvalues. Clearly interactions, corresponding to eigenvalues with $\lambda^r \leq 1$, run to their fixed point values and are termed irrelevant. Their vectors span a subspace termed the critical surface. Systems starting off on the critical surface are equivalent to ones at the fixed point. This partly explains the observation of universality among critical systems, as often the differences in the details of interactions in two systems correspond to irrelevant operators, which hence are unimportant on long-distance scales. The eigenvalues with $\lambda \geq 1$ are termed relevant as they grow under repeated application of T. Systems which start close to the critical surface initially move towards the fixed point, then out along the so-called renormalised trajectory corresponding to these coupling constants. These interactions alone are important in the infrared. We see that systems precisely at their critical point are exactly at a fixed point and remain there. The resulting theory is scale invariant. The relevant eigenvalues are related to the indices $p, q, \cdots$ introduced earlier, and hence to the critical exponents. Under a length rescaling by L, the free energy transforms (near β_c) as

$$f\left(k^1, k^2, \cdots\right) \sim L^{-d} f\left(\lambda^1 k^1, \lambda^2 k^2, \cdots\right) \tag{1.19}$$

Thus we recognise;

$$p = \frac{\ln \lambda^1}{d \ln L}$$
$$q = \frac{\ln \lambda^2}{d \ln L}$$
$$\cdots$$

This systematic integration out of degrees of freedom on small scales may be done either in real space or momentum space. We next illustrate these 2 techniques for 2 simple spin models.

Consider a 2-d Ising model on a triangular lattice. We may form block spins

associated to elementary triangles by the following rule;

$$S_L = \text{sgn} \sum_{\text{int } \sigma_i} \sigma_i.$$

Here the sum runs over spins bounding an elementary triangle of the lattice. These give a blocking factor $L = \sqrt{3}$. The block spin Hamiltonian is determined by the condition

$$e^{-H(K_L, S_L)} = \sum_{\sigma_i} e^{-H(K, S_L, \sigma_i)}$$

The summation over terms which do not involve coupling between blocks represents a harmless shift in the zero of energy and is not interesting. If we split the Hamiltonian into a piece $H_0\left(K, S_L, \sigma_i\right)$ which does not include interaction between blocks, and

$$V = -K \sum_{I \neq J} \sum_{i \in I} \sum_{j \in J} S_i S_j$$

then one can write the expression for the Boltzman weight on the scaled lattice as

$$e^{-H(K_L, S_L)} = \left[\sum_{\sigma_i} e^{-H_0(K, S_L, \sigma_i)} \right] \left\langle e^V \right\rangle$$

the brackets indicating an average over "interior" spins σ_i with respect to the "free" Boltzman factor

$$e^{-H_0}$$

Introducing a cumulant expansion

$$\left\langle e^V \right\rangle = e^{\langle V \rangle + \frac{1}{2}\left(\left\langle V^2 \right\rangle - \langle V \rangle^2\right) + \cdots}$$

we may obtain an expression for the perturbed Hamiltonian by retaining only the first few terms. At first order, retaining only the $\langle V \rangle$, a 2-spin term coupling adjacent block spins is obtained, with a renormalised coupling constant. Linearisation around the fixed point yields critical exponents close to those obtained by an exact solution.

To illustrate the momentum space approach, consider our original ϕ^4 model. Introduce the cut-off $\Lambda = 1/a$ and divide the momentum intervals into short-wavelength $\pi/La \leq k \leq \pi/a$ and long-wavelength $0 \leq k \leq \pi/La$ components.

Then separate the fields into their slow and fast components (i.e short-wavelength and long-wavelength).

$$\phi_L(x) = \left(\frac{1}{2\pi}\right)^D \int \cdots \int_{-\pi/La}^{\pi/La} dk a_k e^{ik.x}$$

$$\phi_S(x) = \left(\frac{1}{2\pi}\right)^D \int \cdots \int_{\pi/La}^{\pi/a} dk a_k e^{ik.x}$$

The quadratic part of the action (or Hamiltonian) is now diagonal, and in the absence of any self- interaction, the partition function factorises exactly, the integration over short-wavelength fluctuations being trivial. By appropriate rescaling of the momentum variable the integration over the long-wavelength components can be cast into a form identical to the original with renormalisations of the mass parameter.

$$k_L = Lk \qquad a(k_L) = Z^{-1}a(k)$$

with the identification $Z = L^{D/2+1}$. The fixed point corresponds to a massless field. In the more interesting case of self-interaction the solution can only be found in perturbation theory. The quartic coupling mixes fast and slow modes. This is analogous to the term V in the real space approach which couples block (renormalised) spins. Using a cumulant expansion and retaining terms to order λ^2, one can identify a renormalised action, which under rescaling leads to a set of renormalised parameters. In order to obtain a renormalised λ, independent of momentum, one must effect an expansion in $\epsilon = 4 - D$. The results are then only of quantitative use near $D = 4$ the so-called upper critical dimension for the model. This corresponds to the situation discussed in the section on continuum renormalisation. One finds 2 fixed points for general D. One corresponds to the Gaussian fixed point already discussed, and is the stable one for $D > 4$, whilst the other non-trivial fixed point depends on ϵ and is stable for $D < 4$. The stability criteria are reflected in the fact that one requires at least 1 negative relevant eigenvalue of the linearised R.G transformation at a fixed point for it to be physical (i.e for flows on it's critical surface to be attracted). Thus for dimensions greater than the upper critical dimension

corrections to mean-field theory are small as the theory behaves like a free theory at long distance. Conversely we expect critical exponents differing dramatically from mean-field predictions below this dimension where the inclusion of fluctuations generates new I.R stable fixed points.

As expected the approach has led to predictions for the scaling behaviour of bulk physical quantities, and an understanding of universality in statistical models. The final section of this chapter applies all these ideas to the important question of how to extract predictions for physical quantities, which are independent of the lattice spacing, in lattice models for field theories.

1.5 Continuum limits for lattice theories

As we have seen systems of many locally-coupled degrees of freedom may develop singularities in various bulk properties at so-called critical points, where a phase transition occurs. The theories are approximately scale invariant at these points, whilst deviations away from criticality are controlled by universal exponents, related to relevant operators in the R.G sense. In critical phenomena the potential divergences are associated with infrared divergences because of the thermodynamic limit, whilst as discussed, the generic problems in field theory relate to U.V divergences. However the conclusions remain the same. Physical quantities develop scale dependencies. One may change the cut-off and the couplings in such a way as to preserve the physical content of the theory. Such is renormalisability. One is led to introduce the so-called β-function, which describes the dependence of the coupling on the cut-off.

$$\beta(g) = -a\frac{d(g)}{da}$$

with a a measure of the average (for say a random system) lattice spacing. The β-function controls both the I.R and U.V behaviours of the theory. Zeroes of this function are points of global scale invariance corresponding to fixed points of the R.G transformation and critical points of the model. All conventional theories start

off with a Gaussian fixed point

$$\beta(g) = 0 \text{ at } g = 0$$

Theories where the β-function is always positive are termed infrared stable, the coupling always increases with increasing mass scale (this leads to the Landau singularity at sufficiently large momenta). Theories where the β- function starts off negative for small g are termed U.V stable, since the coupling is driven to zero at large mass scale. Asymptotic freedom is a phrase commonly used to label such theories. It is possible that other non-trivial zeroes of the β-function exist near each of which a continuum limit may be taken, but possessing different relevant operators and hence corresponding to different continuum physics. The stability of the fixed point is related to the sign of the derivative of the β-function there. Theories built near zeroes with a positive gradient are infrared stable, whilst a negative gradient indicates U.V stability. Note that the presence of fixed points provides another explanation of the universality observed in statistical systems. The values of coupling constants and mass parameters at long-distance are independent of their bare values at the scale of the lattice cut-off. They flow to the nearest I.R stable zero of the β-function. It may be possible to construct many different continuum limits from a given discrete statistical model, corresponding to a situation where the β-function possesses many zeroes with a variety of U.V and I.R stabilities. The full structure of this function is not available to perturbative approaches in the continuum, whilst, in principle, it may be studied numerically on a discrete system. Much of the work presented here is devoted to this aim.

In Chapter 3. we investigate random surface models with extrinsic curvature terms in their actions. Specifically we conduct a series of simulations on these models to search for possible new zeros of the corresponding β-function. The analysis in this chapter tells us that to each zero of the lattice β-function there may be a different continuum limit.

References:

D.J.Amit Field Theory, the Renormalisation Group and Critical Phenomena McGraw-Hill Inc (1978)

J.C.Collins Renormalisation C.U.P (1984)

M.Creutz Quarks, Gluons and Lattices C.U.P (1983)

Domb and Green Phase Transitions and Critical Phenomena vol.6 New York:Academic

R.D.Kenway and G.S.Pawley Proceedings of the 32nd Scottish Universities Summer School in Physics (1987)

J.B.Kogut Rev. Mod. Phys. vol.51 No.4 (1979)

P.Ramond Field Theory–A Modern Primer Benjamin/Cummings Publishing (1981)

D.J.Wallace and R.K.P.Zia Rep. Prog. Phys. Vol.41 (1978)

Chapter Two.

Parity Violating Vacuum Currents on the Random Lattice

2.1 Introduction

In this work we describe both the considerations which lead one to expect parity anomalous currents in the vacuum of a quantum field theory describing fermions in interaction with gauge fields in odd dimension spacetime, and our investigations of this phenomenon for a theory regulated on a random spacetime lattice. In the first section we discuss some of calculations which may be done in the continuum which illustrate important aspects of the problem. Later we explain our reasons for defining a discrete version of the theory on a random lattice, discuss questions of fermion doubling, and address the problems faced in devising suitable algorithms for a numerical study of these effects.

2.2 Anomalies in even and odd dimension

One speaks of an anomaly in a quantum field theory when a symmetry of the classical action is not preserved in the full quantum theory. Traditionally attention has centered on the so-called chiral anomalies which may occur in even dimension spacetime. We summarise the main conclusions here first;

The massless free fermion action is left invariant under global chiral rotations of the fermion fields;

$$\psi \rightarrow e^{i\alpha\gamma^5}\psi \qquad \overline{\psi} \rightarrow \overline{\psi}e^{i\alpha\gamma^5}$$

where

$$\gamma^5 = \prod_{i=1}^{2n} \gamma_i$$

Note that γ^5 plays the role of γ^{2n+1} in $D = 2n + 1$. This symmetry of the action remains when we add a vector coupling to, for example, a U(1) gauge field. Thus,

by Noether's theorem we expect a conserved current

$$\partial^\mu j_{\mu 5} = 0, \qquad j_{\mu 5} = \overline{\psi}\gamma_\mu\gamma_5\psi$$

but we find instead an anomalous Ward identity for the divergence of this axial current;

$$\partial^\mu j_{\mu 5} = const.\epsilon^{\alpha_1\beta_1\cdots\alpha_n\beta_n} F_{\alpha_1\beta_1}\cdots F_{\alpha_n\beta_n} \tag{2.1}$$

– the abelian anomaly [1]. In a topological background field this term contributes an anomalous part to the divergence. The anomaly manifests itself within the path integral formalism because of a non-trivial Jacobian factor which arises from the change in fermionic variables corresponding to the chiral transformation. The quantum theory is defined by integration over all field configurations. This requires the stipulation of a measure, and it is this which is not invariant under the chiral rotations. The main problems arise when we have a chiral gauge theory, in which V-A currents are coupled to gauge bosons. Here such anomalous changes in the fermion measure under gauge transformation lead to a breakdown in gauge invariance and renormalisability. For theories containing several species of fermion with differing axial charges one can arrange for a cancellation of the anomaly. The Weinberg-Salam model of the electroweak interactions is an example of the latter.

Here however I shall concentrate on the anomalies that occur in odd dimension. In a minimal representation of the Dirac algebra there is no γ_5 operator to generate a chiral symmetry. The important symmetry here is the discrete parity transformation. Consider $2+1$ Q.E.D and the transformation

$$x_1 \to -x_1 \qquad x_2 \to x_2 \qquad x_3 \to x_3$$

$$A_1 \to -A_1 \qquad A_2 \to A_2 \qquad A_3 \to A_3$$

$$\psi \to \sigma_1\psi \qquad \overline{\psi} \to \overline{\psi}\sigma_1$$

where σ_1,σ_2,σ_3 are a representation of the Dirac algebra. One may easily show that

$$\delta L_{kinetic} = 0$$

whilst any mass term $m\overline{\psi}\psi$ explicitly breaks this symmetry. Similarly in three dimensions a candidate mass term for the photon

$$\mu\epsilon^{\alpha\beta\gamma}A_\beta F_{\alpha\gamma} \tag{2.2}$$

is also odd under parity. Such a term is called a Chern-Simon's term [2,3]. In complete analogy to the situation in even dimension for chiral symmetry, this discrete symmetry will be seen to anomalous under quantisation. Furthermore, intimate connections may be drawn between these parity anomalies, and the possible chiral anomalies that may occur in one higher dimension spacetime.

If we integrate out the fermions in a background gauge field with non-zero winding number then at one loop order terms are generated in the effective gauge field action which break parity. These are just the Chern-Simon's terms (sometimes called Hopf terms) already mentioned. Furthermore the magnitude of such induced terms is independent of the fermion mass, varying like $\frac{m}{|m|}$. This already indicates, that if we include a fermion mass term, in order to control infrared divergences, we will generate anomalies in the effective gauge action. Our lattice calculations verify the existence of the associated vacuum currents. In the next section we shall see that in order to regulate the U.V. divergences of the theory in a gauge invariant fashion, we will be forced to add such a counterterm to the Lagrangian [2,3].

2.3 Gauge invariant regularisation of the fermion determinant

Let us consider the effective action obtained by integrating out the fermion fields (in 3D Euclidean space).

$$e^{-\Gamma} = \int D\overline{\psi} D\psi \exp\left(- \int d^3x \overline{\psi} \not{D} \psi \right) \tag{2.3}$$

this a non-local quantity–it may be that it is not invariant under gauge transformations which have a non-trivial topology, even though the action is invariant under local gauge transformations. In order to define this theory upon quantisation we must stipulate a method of regularisation which should attempt to preserve any symmetries of the theory. This presents us with a problem, since one cannot use say Pauli-Villars regularisation (which explicitly introduces a mass term), for fear of generating parity-anomalous terms in the effective action which remain even as the regulator mass is taken to infinity. Similarly, if we choose dimensional regularisation, one obtains vacuum polarisation graphs at one loop which generate a piece proportional to $\epsilon^{\alpha\beta\gamma}$. This tensor possesses no well-defined analytic continuation to arbitrary D. In an attempt to evade this problem let us write the effective action in the form [2]

$$\Gamma_{\text{eff}}(A) = -i \ln \det(\not{\partial} + \not{A}) \tag{2.4}$$

which may be written

$$\det \left(i \not{D}_4 \right)^{\frac{1}{2}}, \qquad \not{D}_4 = \gamma^\mu \left(\partial_\mu + A_\mu \right)$$

where

$$\gamma^\mu = \sigma_3 \otimes \sigma^\mu, \mu = 1,2,3$$

Now there exists a 4×4 matrix that anticommutes with iD_4–so the spectrum is symmetric about zero. Lets us define $\det(\not{D})$ as the product of the positive eigenvalues of $i \not{D}_4 (A_\mu)$. Since moreover $i \not{D}_4$ can be regulated by the introduction of a parity invariant mass term this procedure will maintain parity as a good symmetry. Consider now varying the gauge field along some path parametrised by τ

$$A_\mu (x^\mu, \tau) = 0, \tau = -\infty \quad \text{to} \quad A_\mu (x^\mu, \tau) = U_n^{-1} \partial_\mu U_n, \tau = +\infty$$

U_n belongs to the n^{th} homotopy class. Now the spectrum at $\tau = +\infty$ is identical to that at $\tau = -\infty$ (since it is gauge invariant). However somewhere along the path A must pass through configurations not pure gauge (if $n \neq 0$). The eigenvalues may become rearranged, and indeed some may pass through zero. Thus $\det^{\frac{1}{2}} i \not{D}_4$ may change sign if an odd number of eigenvalues flow from positive to negative values. Clearly $A_\mu(x^\mu, \tau)$ can be thought of as an instanton-like configuration in the gauge $A_4 = 0$ and 4 dimensions. Since the spectral flow is a topological object we may compute it in the adiabatic limit. Let us write $A(x_i) = \Xi(x_\mu)g(\tau)$ where $x_i = (x_\mu, \tau)$. We may show that the number of zero crossings is equal to the number of normalisable zero modes of some new d living in this even dimension space, where;

$$\not{d} = \gamma^i(\partial_i + A_i) \quad i = 1 \cdots 4 \quad \gamma^4 = \gamma^\tau = \sigma_2 \otimes I \tag{2.5}$$

To see this let us write the condition for a zero mode of this new operator

$$\not{d}\,\psi = 0$$

$$\frac{d\psi}{d\tau} = -\gamma^\tau \not{D}_4 \psi.$$

i.e writing

$$\psi = f(\tau)\phi(x^\mu)$$

$$\text{Thus} \qquad \frac{\mathrm{d}\psi}{\mathrm{d}\tau} = -\lambda(\tau)\,\mathrm{f}(\tau)\,\phi(\mathrm{x}^\mu)$$

$$f(\tau) = f(0)\exp\left(-\int d\tau'\lambda(\tau')\right)$$

Therefore only if $\lambda \geq 0$ at $\tau = +\infty$ and $\lambda \leq 0$ at $\tau = -\infty$ is this normalisable. Therefore, there is a $1:1$ correspondence between zero modes of d^{2n+2} and the spectral flow of the operator D_4 and hence $\det D^{2n+1}$. The index theorem allows us to relate the number of positive to negative chirality zero modes in this 4 dimensional space, corresponding to this new d, to the winding number of the instanton-like field we have constructed.

$$\text{number of zero modes } = 2n^+ - (n^+ - n^-) \tag{2.6}$$

Thus if the winding number is odd an odd number of eigenvalues flow through zero and the determinant changes sign. The instanton-like field corresponds to a large gauge transformation in the original space. Thus it appears that our carefully constructed regularisation scheme which maintains parity as a good symmetry leads to an effective action which is not invariant under large gauge transformations–a global anomaly. In order to restore gauge invariance one might add a photon mass term or Chern-Simons term to the action, since it is well-known that this term also changes sign under odd-winding number transformations [3] . However such a term breaks parity. If we naively employ Pauli-Villars regularisation we may show that the effective action, calculated as $M \to \infty$, contains an induced topological term proportional to the Chern-Simons term. This will give rise to a topological current in the ground state [2,3]

$$\langle J \rangle = 1/8\pi^* F$$

for an abelian theory. Thus we find that the ground state of the quantum theory does not respect the classical symmetry and parity is broken.

Indeed it appears to be a general conclusion that upon quantisation one is unable to maintain both symmetries and in order to keep gauge invariance one must necessarily give up parity. This in turn allows such theories to possess interesting vacuum structure. This is quite analogous to the situation in even dimension, where one finds an anomalous Ward identity for the divergence of the gauge-invariant axial current after renormalisation. Again one can construct a chirally-symmetric current which is conserved, but is now no longer gauge-invariant. Note also that there appear to be strong connections between the parity anomalies in odd dimension and the chiral anomalies in one higher dimension. We finish this discussion of the theory in the continuum by a generalisation of this analysis in 3 dimensions to any odd dimension.

2.4 Odd dimensional effective actions

Consider a generic fermion theory in $D = 2n + 1$. In order to extract physics from the quantised theory we must include a regulator. For simplicity add a Pauli-Villars regulator field with Lagrangian

$$L_{reg} = \frac{1}{2}\overline{\chi}\ \not{D}\ \chi + iM\overline{\chi}\chi \qquad D = 2n+1$$

where the imaginary mass term is needed to avoid tachyonic poles in the propagator after Wick rotation back to Minkowski space. So formally we can write [3];

$$e^{-\Gamma} = \prod_k \frac{\lambda_k}{\lambda_k + iM} \tag{2.7}$$

where we employ a regulator field of opposite statistics. Under P the eigenvalues are inverted about zero (in even dimension it is the operator γ_5 that is responsible for this symmetry in the spectrum, here the P operation plays an analogous role)

$$\lambda_k\left(A^P\right) = -\lambda_k\left(A\right)$$

so

$$\begin{aligned} e^{-\Gamma(A^P)} &= \prod_k \frac{-\lambda_k}{-\lambda_k + iM} \\ &= e^{-\Gamma(A)^*} \end{aligned} \tag{2.8}$$

So the anomaly is associated with the imaginary part of the effective action (or the phase of the determinant).

$$\begin{aligned} \Im(\Gamma) &= \lim_{M\to\infty} \Im\left(-\sum_k \ln\left(\frac{\lambda_k}{\lambda_k + iM}\right)\right) \\ &= \lim_{M\to\infty} \sum_k \arctan\left(M/\lambda_k\right) \\ &= \pi/2\left(\sum_{k\geq 0} - \sum_{k\leq 0}\right) \\ &= \eta \end{aligned} \tag{2.9}$$

η is termed the spectral asymmetry. To relate this to the anomaly in $D = 2n + 2$, consider an interpolation between field configurations A_0 and A_1 i.e A_s on M^{2n+1}–a

field on $M^{2n+1} \otimes R$. It will correspond to a gauge transformation between the two configurations. Now the number of normalisable zero modes of $\not{D}^{2n+2}$ gauged to $A^{2n+2} = 0$ equals the spectral flow of $\not{D}^{2n+1}$ (by a simple generalisation of our previous argument). So the difference in η is;

$$\begin{aligned} \eta(A_0) - \eta(A_1) &= 2\left(number\ of\ zero\ modes\ \not{D}^{2n+2}\right) \\ &= \int index\ density\left(D^{2n+2}\right) \end{aligned} \tag{2.10}$$

where the integral extends over the manifold $M^{2n+1} \otimes R$. Adopting for clarity the notation of differential geometry we have that the index density (TrF^n) is a closed form (i.e $dTrF^n = 0$ by the Bianchi identity), so there exists (by Poincaré's lemma) locally on $M^{2n+1} \otimes R$ a $2n+1$ form Q such that;

$$dQ(A) = TrF^n \qquad \text{since } \mathrm{d}^2 = 0$$

Therefore using Stoke's theorem we may write [1,3];

$$\eta(A) = \int Q(A) + const \tag{2.11}$$

where the integral extends over the boundary of the space M^{2n+2} i.e M^{2n+1} and we can successfully restrict Q to lie on this boundary. Q is clearly the generalisation of the Hopf term to arbitrary dimension. Indeed the content of the previous equation is that we may write the spectral asymmetry in the odd dimensional space as the integral of a local function over the space. Thus it is possible to eliminate this anomaly by the addition of a local counterterm of the form $-i\pi \int Q(A)$ provided Q (this Chern-Simons term) is gauge invariant globally. For spin 1/2 representations in $D = 2n+1$ we get a contribution when the winding number of the field A is odd.

We may extract the parity anomalous part of the gauge current by functionally differentiating the integrated Chern-Simon's form;

$$Z = \frac{\delta \Gamma_p}{\delta A} = F^* \quad \text{for } (2+1) \text{ Q.E.D}$$

This is in agreement with our earlier result. Note that this current is exactly conserved since the Chern-Simon's form is locally gauge invariant permitting a conserved Noether current. It is interesting to see that the existence of a spontaneous

breaking of parity, or equivalently the nonzero nature of the spectral asymmetry, is crucially dependent only on the properties of the zero modes of the corresponding Dirac operator in one higher dimension. It is only the zero modes that are sensitive to the global topology.

We have seen that the effective gauge field action contains topological terms in odd dimension as a result of integrating out fermionic fields. These may arise from explicit mass terms, or from attempts to regulate the theory's infrared and ultra-violet behaviour in a gauge invariant fashion. Instead of employing some standard continuum regulator it would be interesting to investigate such theories within a lattice approach. As we shall see, this is non-trivial with conventional approaches which utilise lattices endowed with an exact translational symmetry. Hence this work employs a random lattice. Such a lattice does not respect parity even in the massless case (there is no global reflection of coordinates which leaves the Dirac operator on a single lattice invariant). As such we might guess that even in the continuum limit one picks up an anomalous term in the action with the associated non-vanishing vacuum currents in topological gauge field backgrounds. The following section first describes, in more detail, the problems encountered in regular lattice formulations.

2.5 Doubling Problems

In studying a generic interacting quantum field theory one typically encounters divergences in the values of calculated physical quantities. These occur when a loop expansion is made about the classical theory and they can be classified into two types; infrared and ultra-violet. The first, arise in certain massless theories because of the infinite spatial extent of the system. The latter occur because of the necessity of including the contributions of products of fields in intermediate states whose arguments are arbitrarily close to one another. In momentum space this leads one to sum over arbitrarily large momenta which may formally give infinite results. To make sense of such a system one must first devise a method of regularising the theory in order to render all quantities finite and well-defined. One may then carry out the manipulations necessary to renormalise the theory. Of course eventually this regularisation must be removed. These steps have been reviewed in Chapter 1.

Clearly the central reason for the difficulties arises from the infinite number of degrees of freedom involved. A natural way to proceed, which is not tied to a perturbative approach, entails the replacement of a field defined over a spacetime continuum to a situation where the field variables are defined relative to a discrete lattice of points in spacetime. The field variables then live on local geometrical constructs of the lattice eg a spin-zero field could be defined at the lattice sites, a spin-one field on the links joining any pair of nearest neighbour points etc.

Since fundamental matter fields are believed to be of spin-1/2 character such an approach requires a prescription for discretising a fermion field on such a lattice. It turns out to be a highly non-trivial problem to devise a suitable method to do this which recovers standard continuum properties as we take the naive continuum limit. The generic problem in such approaches goes under the name of fermion doubling. When naive discretisations are chosen of the continuum Dirac operator one finds spurious states in the spectrum which contribute to physical observables and most importantly do not decouple from physics as the lattice spacing is taken to zero. These are the doubles [5]. An example illustrates the problem.

Consider a regular hypercubic lattice in D dimensions consisting of N sites. Let the spinor degrees of freedom sit on the lattice sites, replace derivatives by nearest neighbour differences. Then;

$$\partial_\mu \psi \to \frac{1}{2a}\left(\psi_{m_\nu + \delta_{\mu\nu}} - \psi_{m_\nu - \delta_{\mu\nu}}\right)$$

the lattice action reads

$$S = \sum_{m,n} \overline{\psi}_m M_{mn} \psi_n$$

where

$$M_{mn} = \frac{1}{2} a^{D-1} \sum_\mu \gamma_\mu \left(\delta^D_{m_\nu - \delta_{\mu\nu}, n_\nu} - \delta^D_{m_\nu + \delta_{\mu\nu}, n_\nu}\right) + a^D m \delta^D_{mn}$$

In momentum space this is diagonal

$$M_k = m + i a^{-1} \sum_\mu \gamma_\mu \sin\left(2\pi k/N\right) \tag{2.12}$$

a is the lattice spacing. The integer k varies in the range $\pm(1 \text{ to } N/2)$. Thus there is now a maximum momentum in the system corresponding to a wavelength equal to twice the lattice spacing. The space of all possible distinct wave-vectors becomes compactified to a region termed the Brillioun zone. The entire momentum space is obtained by translation through all reciprocal lattice vectors. If we write

$$q_\mu = \frac{2\pi k_\mu}{Na} \qquad Na = L, \text{ the lattice length}$$

then

$$M_k = m + i a^{-1} \sum \gamma_\mu \sin a q_\mu$$

Consider the 2-pt function. This is given by the inverse of the operator M

$$G \sim \frac{1}{-ima + \sum_\mu \gamma_\mu \sin a q_\mu} \tag{2.13}$$

$$\sim \frac{ima + \sum_\mu \sin a q_\mu}{\sum_\mu \sin^2 a q_\mu + (ma)^2}$$

The problem is now evident. As $ma \to 0$, the approach to the continuum limit, G picks up contributions both from the poles $aq_\mu \sim \pm ima$ but also from the poles at $\pi - ima$ and $-\pi + ima$. The lattice propagator has no suppression of momentum values near the zone boundaries. These are modes which oscillate in sign on the scale of the lattice spacing which preclude a simple continuum limit. In each spacetime direction we have two independent regions where the theory gives a free fermion propagator in the continuum limit. In D dimensions we have 2^D fermion species [5].

One might think that this problem is merely an artefact of our simple discretisation scheme and that by cleverly choosing our derivative term we can avoid the extra zeros of M. In fact the problem is much more fundamental than that and can be seen to be unavoidable in a rather general class of theories. To show this consider a regular lattice formulation in $D = 1$. The Dirac operator is a first order operator and hence changes sign under inversion of the coordinate. Thus its Fourier transform contains only antisymmetric terms in momentum space. If the discrete form is to represent a Dirac operator then $M_k \sim k$ at small k. Now M is periodic in momentum space with period $2\pi/a$, so that if the dispersion relation is continuous, there must be another zero of M somewhere in the Brillioun zone i.e $-\pi/a$ to $+\pi/a$.

If we allow for a non-local expression for the derivative in real space we can generate a discontinuous dispersion relation with no species doubling– the so-called SLAC derivative. However it proves difficult to reproduce the correct results in weak-coupling perturbation theory with such a term. Other lattice formulations add terms to the action which ascribe masses to the doubled sector of the order the cut-off which hence do not contribute in the continuum limit;

$$M_k = m + ia^{-1} \sum_\mu \gamma_\mu \sin aq_\mu + ra^{-1} \sum_\mu (1 - \cos aq_\mu)$$

This procedure explicitly breaks the chiral symmetry present in the massless Dirac action in even dimension and that of parity in odd dimension. The situation is complicated by the fact that both these symmetries are anomalous in the continuum,

and it is by no means clear whether the correct Ward identities are obtained in the continuum limit with this so-called Wilson fermion prescription. An alternative approach due to Kogut and Susskind diagonalises the Dirac operator in spinor space by a sequence of unitary transformations on the γ matrices. One then simply throws away 3 of the spinor components on each site leaving a single component fermionic object in the theory. This reduces the number of species from 16 to 4 in $D = 4$. However constructing operators for the original degrees of freedom in terms of the new fields is difficult. Furthermore one is forced to describe the residual degeneracies as different flavours.

To summarise any local, hermitian, chirally symmetric and translationally invariant lattice regularised fermion field theory is guaranteed to suffer from doubling problems. The doubles come in equal numbers of positive and negative chirality species ensuring that the axial anomaly identically vanishes in this scheme. This in turn means that the continuum limit can never reproduce the correct anomalous Ward identity for the divergence of the axial current [5]. Previous work in 2 [6] and 4 [7] dimensions on random lattices indicates that the formulation of fermion theories on such lattices avoids these problems at least at tree level. It is shown that in even dimension a spontaneous breaking of the chiral symmetry of the doubles occurs, the doubled sector acquiring masses of the cut-off the inverse of the average lattice spacing. A goldstone boson is present in the spectrum. In the continuum limit the correct anomalous Ward identities are obtained. However if one considers radiative corrections then the doubles contribute to primitively divergent graphs, even in the continuum limit. It is found that the form of these divergences differ from the continuum case and a careful fine-tuning is required to extract finite answers as the average lattice spacing goes to zero [8].

The object of this work is partly to test the random lattice as a suitable framework for building fermion theories in odd dimension and secondly to investigate topological currents in these theories . Conventional schemes preclude such studies as the doubles always conspire to render the net current zero.

In order to give a specific example of the presence of doubles in a physical correlation function, we calculate the transverse propagator on a regular lattice in $3-D$. This will also be of interest when we later obtain the corresponding random lattice result.

Consider the transverse fermion propagator;

$$G^{\alpha\beta}(z) = \int dz_1 dz_2 dx_1 dx_2 dy_1 dy_2 \delta(z_1 - z_2 - z) \langle \overline{\psi^{\alpha}_{(x_1,y_1,z_1)}} \psi^{\beta}_{(x_2,y_2,z_2)} \rangle \qquad (2.14)$$

We diagonalise the Dirac operator by Fourier transformation and obtain the following expression for the transverse propagator

$$G(z) = \sum_{q_z} \frac{e^{iq_z z}}{\sigma_z \sin aq_z - ima} \qquad (2.15)$$

where the sum over q_z is

$$q_z = \pm(1 \cdots N/2)\frac{2\pi}{Na}$$

Here $Na = L = 1$. The evaluation of this sum is detailed in appendix A. The results for G^{11} and G^{22} when $z \geq 0$ are

$$G^{11}(z) = \frac{1}{1 - e^{-mL}} \left(e^{-mz} + (-1)^{n+1} e^{-mL} e^{mz} \right)$$
$$G^{22}(z) = \frac{1}{e^{mL} - 1} \left(e^{mz} + (-1)^{n+1} e^{mL} e^{-mz} \right)$$

There are two interesting features to these equations. Let $L \to \infty$ then G^{11} becomes the standard expression (in Euclidean space) for the fermion propagator

$$e^{-mz}$$

However G^{22} is not zero (corresponding to no amplitude for antiparticle propagation foward in time) but

$$(-1)^{n+1} e^{-mz}$$

This is the doubled mode. Figure (2.1). illustrates G^{11}, showing the oscillating contribution of the doubles.

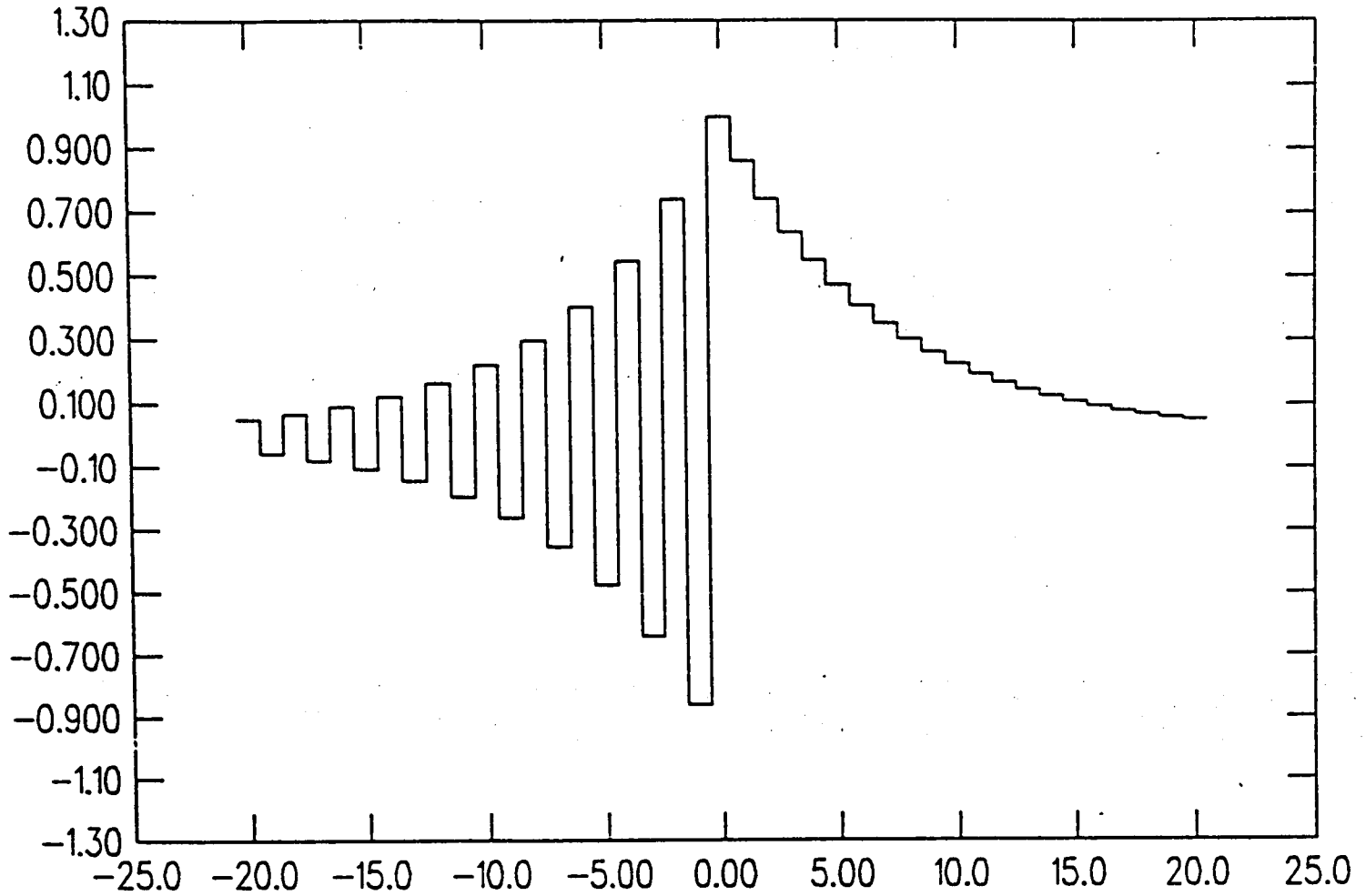

Figure 2.1 Regular lattice propagator $G^{11}(z)$ at $ma = 0.15$.

One may also write the expressions for the two components of the propagator as

$$G^{11}(z) = \begin{cases} \dfrac{-\sinh m(z - L/2)}{\sinh mL/2}, & \text{n even;} \\ \dfrac{\cosh m(z - L/2)}{\sinh mL/2}, & \text{n odd.} \end{cases} \tag{2.16}$$

$$G^{22}(z) = \begin{cases} \dfrac{\sinh m(z - L/2)}{\sinh mL/2}, & \text{n even;} \\ \dfrac{\cosh m(z - L/2)}{\sinh mL/2}, & \text{n odd.} \end{cases} \tag{2.17}$$

Having motivated the use of a random lattice to investigate the vacuum structure of these fermion theories, hopefully with a view to reproducing some of the results obtained with continuum techniques, the next section discusses the methods used to construct the lattice and the discrete counterpart to the Dirac operator.

2.6 Construction of the random lattice Dirac operator

In order to develop a discrete analogue of the Dirac operator over a random distribution of sites we require an algorithm that provides us with rule for generating a set of nearest neighbours to every site which is in some sense optimal, permits no crossed links, and assigns bond-strengths in a way consistent with the local structure. Such an algorithm was proposed by Christ, Friedberg and Lee [9]. To triangulate a set of points in D dimensions pick every distinct set of D+1 points and draw the hypersphere defined by them. If this sphere contains no other points the set of D+1 points forms a cluster. Each site is then connected to every other site in the cluster by a link and all are nearest neighbours to each other. Repeat this for all other sets of points. Such a procedure sets up the nearest neighbour information and the link lengths l_{ij} . The clusters are termed D-simplices. It is important to note that every D-1 simplex is bounded by two D-simplices. In D=3 the clusters are tetrahedra, the 2-simplices are the triangular faces of the tetrahedra and form the boundary between 2 neighbouring tetrahedra. The algorithm completely fills the system volume , usually taken to be a unit cube, with non-overlapping D-simplices.

The calculation of the Dirac operator involves a knowledge of the dual lattice. Every link l_{ij} is dual to (D-1)-dimensional volume σ_{ij} which lies in the hyperplane orthogonal to the link. The union of these volumes as one sweeps round all links to a site enclose a D-volume–the dual cell volume ω_i , which is conjugate to the site i.

A naive implementation of the search procedure outlined above proves inordinately time-consuming as the work required scales like N^{D+2}. Instead we exploit the fact that every triangle bounds two and only two tetrahedra. Given some starting tetrahedron one loads its faces into some array which eventually will contain all the triangles, flagged by a logical bit that tells us that the face is active, in the sense of being a potential source of another tetrahedron. The links are stored in a sequence of linked lists, successive members of the list for site i holding the site indices of any links attached to site i, where a link ordering is imposed in order that any given link appears only once in the lists. As for any linked list a pointer

is included in the field of the data item giving the address of the next link attached to site i. This allows for the subsequent efficient insertion of new links as the only disruption to a given list involves reconnecting the pointers of data items adjacent to the insertion. It also proves an efficient way of storing link information given that with the algorithm we use we are continually comparing a potential new link with existing ones to check if we have seen it before. Initially all the links of the first tetrahedron are loaded.

The algorithm proceeds by the continual removal of active triangles from the triangle array, the search for a new tetrahedron complementary to the the one which generated the triangle initially, the comparison and possible insertion of the potential new links and triangles with those already found, and the subsequent removal of the triangle from those flagged active. It proves useful for the later dual lattice calculation to store all the tetrahedra attached to a given link.

The search for a new tetrahedron from a triangular face is the search for only one new vertex. It is effected by a bisection method. One constructs the normal to the triangle passing through the point of intersection of the perpendicular bisectors of any two of the triangle sides **n**. The circumcentre of a cluster must lie somewhere along this. If **c1** represents the circumcentre of the 'old' tetrahedron, the circumcentre of the new tetrahedron we are trying to find may be represented as

$$\mathbf{c2} = \mathbf{c1} + \lambda \mathbf{n}$$

where λ (the distance along the normal away from the old vertex) is determined by a simplex bisection. That is, at any stage we write

$$\lambda = \frac{1}{2}(a_{min} + a_{max})$$

We start the search with $a_{min} = 0$, $a_{max} = 4\bar{a}$ say. The distances of all points from this trial circumcentre are computed (we set the distance of the old tetrahedron vertex to infinity). The radius of this trial circumsphere is determined by the distance of the circumcentre to a vertex of the triangle. If more than 1 point lies

within this radius, then we are looking too far along the normal, we set a_{max} to λ and try again. Conversely if we find less than 1 point within the radius we set a_{min} to λ and try again. If we find just 1 point we have a candidate for a fourth point to a new tetrahedron. We check this explicitly and if not, go back to the search and increase the initial a_{max}.

One can refine this so that when distances are being computed in order to check for points inside the search sphere we consider only those guaranteed to be 'close' . This we do by dividing the lattice volume into boxes with say roughly 3 or 4 points per box. Arrays giving the box numbers of neighbouring boxes to a given box are set up. Then when we do the distance search we include only neighbouring boxes. If the simplex method fails to converge after some number of iterations, then we consider the next layer of boxes out from the box containing the triangle. This is continued indefinitely and ensures we do not do excessive amounts of useless work.

When a new tetrahedron is located its vertices are loaded into an array and the links examined for new additions. A similar procedure is followed for the triangles (where again an ordering of the vertices is decided upon, in order to ensure that any triangle appears only once). The 'old' triangle is flagged inactive and the next active triangle is examined. In this way we 'grow' tetrahedra from some seed until there are no active triangles left.

We apply periodic boundary conditions on all faces. We implement this in the code by replacing any vector between say sites in the lattice by a new vector which takes care of the toroidal boundary conditions, allowing simplices to wrap around the boundaries. Specifically

$$\mathbf{X} \rightarrow \mathbf{X} - anint\,(\mathbf{X})$$

where the intrinsic FORTRAN function *anint* is defined below.

$$anint\,(\mathbf{X}) = \begin{cases} 0, & \text{if } |\mathbf{X}| \leq \mathbf{0}; \\ -1.0, & \text{if } \mathbf{X} \leq -\mathbf{0.5}; \\ +1.0, & \text{if } \mathbf{X} \geq +\mathbf{0.5}. \end{cases}$$

All the most frequently used parts of the code were written to facilitate efficient vectorisation on the CRAY-XMP/48. The CPU time taken to triangulate a 10^3

system, together with a calculation of the dual lattice, being of the order 4 seconds, whilst the program scales only as the system size. The triangulation can be checked by summing the tetrahedron volumes and the dual cell volumes. These should be unity. The Euler characteristic is also calculated to check the boundary conditions have been implemented correctly.

$$\chi = \sum_{all\ simplices} N_m (-1)^m \tag{2.18}$$

where N_m is the number of simplices of order m. χ should be zero on a torus.

In D=3 the σ_{ij} themselves are constructed as follows: First restrict attention to a site i and its nearest neighbours. For every link l_{ij} retain the site indices of the tetrahedra attached to it. Take any 3 non-coplanar links in a cluster. These define a tetrahedron. Construct the unique point of intersection of the planes perpendicular to these links. Do the same for the other tetrahedron sharing a common face with the last and joined along the same link l_{ij}. One can construct a small triangle from these 2 points and the mid-point of the link. This is a contribution to σ_{ij}. Now continue sweeping round the link summing all the elemental triangular areas associated with pairs of neighbouring tetrahedra to obtain the total σ_{ij}. An elemental contribution to the dual cell volume is obtained by multiplying this area by 1/3 the link length. Summing over all links to site i generates all the σ's and ω_i.

Now we have triangulated the lattice it remains to calculate the Dirac operator. First though we must examine the question of how to impose topological fields on the system.

2.7 Topological background fields

Here we describe different methods for imposing background gauge fields with arbitrary winding number. Consider the field

$$A_1 = \omega x_2 \qquad A_2 = 0 \qquad A_3 = 0$$

The only non-zero components of the field tensor are $F_{12} = -F_{21} = -\omega$. However we need to identify opposite faces of the lattice in order to create the toroidal boundary conditions. Thus there is a potential discontinuity at say $x_2 = L$ of ωL in A_1. This is allowed provided we can interpret it as a gauge transformation. Now a gauge transformation transforms the potential as;

$$A_\mu \rightarrow A_\mu - \partial_\mu \Lambda$$

where we must have

$$\Lambda = -\omega L x_1$$

and the fermion field transforms as

$$\psi \rightarrow e^{i\Lambda}\psi$$

Such a gauge transformation must be strictly periodic in x_1, so

$$\omega L^2 = 2\pi n \qquad \omega = \frac{2\pi n}{L^2} \tag{2.19}$$

We see that the flux must be quantised. The integer n is of course just the winding number of the field. In practice we found it convenient to use a singular representation of the gauge field with trivial boundary conditions on the fermion field, as opposed to the trivial gauge field plus non-trivial fermion boundary conditions described above. Specifically we examined the theory in the background field [6]

$$A_z = 0 \qquad A_x = -\frac{2\pi n y \delta(x)}{L} \qquad A_y = \frac{2\pi n x}{L^2} \tag{2.20}$$

which yields the same constant field stength everywhere, including $x = 0$. Gauge field variables, living on the links of the lattice U_{ij} are then calculated in the usual way

$$U_{ij} = e^{i \int A_\mu dx^\mu}$$

2.8 The Dirac operator

The fermion action is chosen to be [10]:–

$$S = \frac{1}{2}\sum_{i,j}\overline{\psi}_i\lambda_{ij}l^{\mu}_{ij}\gamma^{\mu}U_{ij}\psi_j + m\sum_i \omega_i\overline{\psi}_i\psi_i \tag{2.21}$$

where

$$\lambda_{ij} = \begin{cases} \sigma_{ij}, & \text{if i,j linked;} \\ 0, & \text{otherwise.} \end{cases}$$

$\overline{\psi}_i$,ψ_i are independent (in Euclidean space) 2-component spinors, U_{ij} is the gauge field variable and m is the mass. The lattice analogue of the Dirac operator is:–

$$\not{D}_{ij} = \frac{\lambda_{ij}\gamma^{\mu}l^{\mu}_{ij}U_{ij}}{2\sqrt{\omega_i\omega_j}}$$

The complex matrix operator D_{ij} is sparse and we store only the nonzero entries together with indexing information. We are interested in obtaining elements of the inverse matrix, since this contains all the information on the system in a fixed background. The total storage for a matrix of order 8000 is about 2.5 megawords, so fits easily into the fast memory of the XMP.

2.9 Inversion algorithm

To obtain matrix elements of the inverse operator we use a simple conjugate gradient scheme, which tackles the general problem of the solution of linear systems of the type

$$AX = b$$

where A is a positive definite hermitian matrix of order N, by minimising the functional;

$$F\left(z, z^{\dagger}\right) = \left(b - Az\right)^{\dagger} A^{-1} \left(b - Az\right)$$

This is effected by the following algorithm;

At each iteration a change in z, the approximate solution vector, is made which maximises the change in F. Thus we track down the line of greatest slope, hence the name. At each step a new approximation to z is obtained by simple matrix operations;

$$F\left(z^{n+1}\right) = min\ F\left(z^{n} + \alpha_0 r_0 + \cdots + \alpha_n r_n\right)$$

where the minimisation takes place in the space of the α's. The r_i are termed the residuals at step i. They are constructed to be orthogonal (in the absence of roundoff). The algorithm is implemented as shown below;

initial guess z_0

$$p_0 = r_0 = b - Az_0$$

loop while $(r_k, r_k).ge.\epsilon\ k = 0, 1, \cdots$

$$\alpha_k = \left(r_k, r_k\right) / \left(p_k, Ap_k\right)$$

$$z_{k+1} = z_k + \alpha_k p_k$$

$$r_{k+1} = r_k - \alpha_k A p_k$$

$$\beta_k = \left(r_{k+1}, r_{k+1}\right) / \left(r_k, r_k\right)$$

$$p_{k+1} = \beta_k p_k + r_{k+1}$$

end loop

This has a global minimum at $Az = b$ and local minima are encountered whenever the residual vector $r = b - Az$ is an approximate eigenvector of A. This leads to oscillations in the magnitude of r and a slowing down of the convergence rate of the algorithm. In principle the procedure, like the Lanzcos algorithm to which it is closely related, is exact in the sense that in the absence of roundoff errors it is guaranteed to converge within N iterations. As such the algorithm has advantages over other iterative and relaxation methods. The conjugate gradient algorithm effectively never discards any of the information acquired at previous iterative passes. It converges well for diagonally dominant matrices whilst the rate falls off exponentially as the mass is decreased – the function F has a local gradient which decreases with the mass, consequently the changes in z are correspondingly smaller. Another way to see this is to notice that as the mass decreases the correlation length increases and we experience critical slowing down. This occurs because at each iterative step only local changes are made in the z vector so that information is only propagated across the lattice at finite speed measured in units of iteration time. Clearly the Dirac operator is not positive definite so one works instead with $-\not{D}^2 + m^2$ by applying our operator twice in succession. Since almost all the work is spent in doing the matrix-vector multiplication, we optimised this in such a way that row on vector operations are pipelined on the XMP with the code achieving close on 50 megaflops in spite of the necessary indirect addressing. The number of iterations required depends essentially on the so-called condition number of the matrix which is approximately the ratio of largest to smallest eigenvalue.

$$\kappa \sim \lambda_{max}/\lambda_{min}$$

Due to the increased coordination number (typically 16 links per site as opposed to 6 on a regular lattice in D=3), and the much larger condition number of the operator on a random system, it requires a considerable number of iterations to obtain a good approximation to a column of the inverse matrix (eg $\epsilon \leq 1E-10$).

Figure 2.2. Propagator on $10 \times 10 \times 20$ *lattice at* $ma = 0.2$.

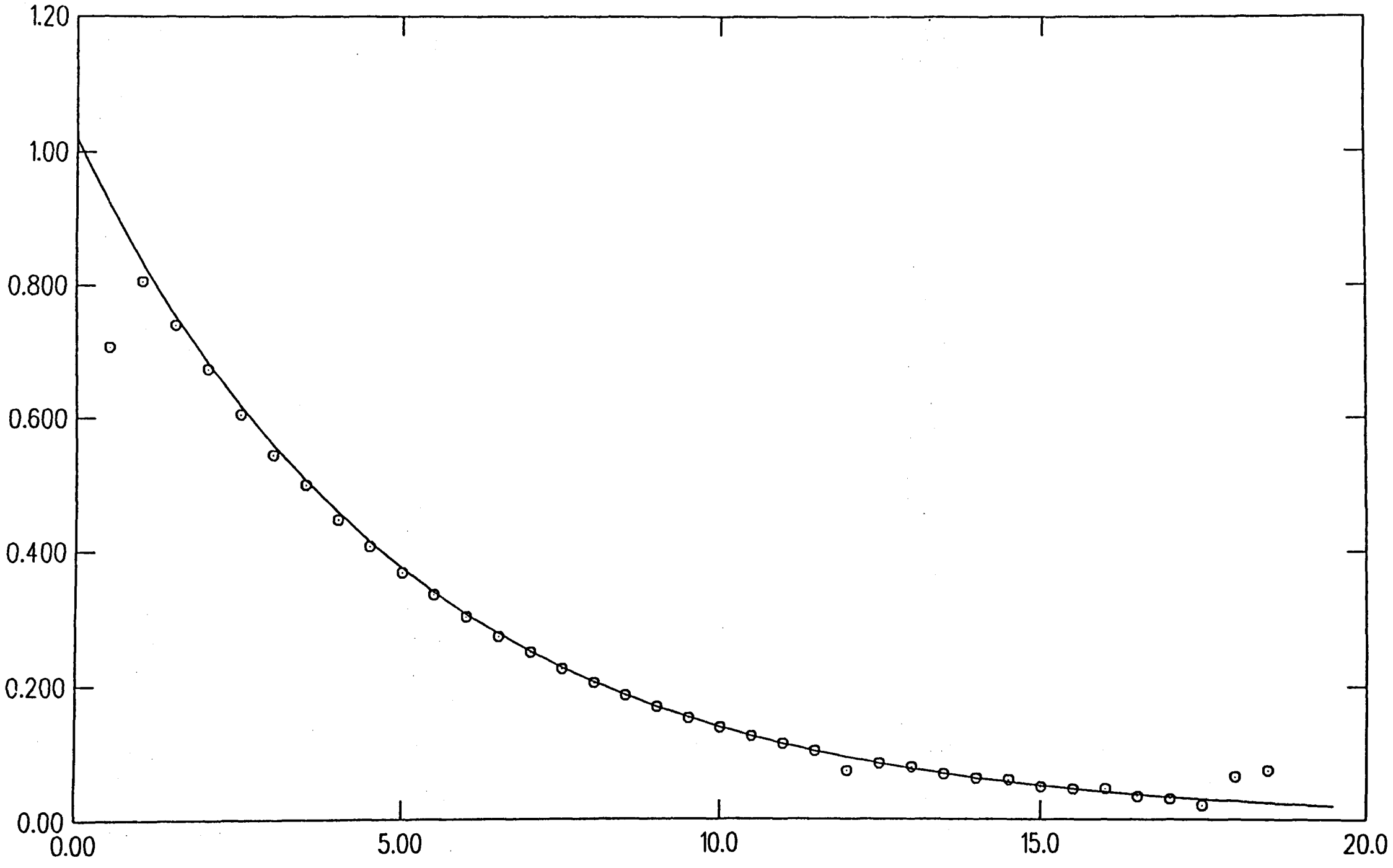

Typically we need 150 iterations at $ma = 0.1$. It proves unnecessary to obtain the entire inverse, something in the region of 4 timeslices proves sufficient to calculate the currents.

2.10 Results

Firstly we examined the theory in the absence of any background gauge field. The results confirm that only the primary fermion contributes to the 2-pt function. Specifically we calculated the transverse propagator as discussed previously. If we adopt a representation of the γ matrices such that $\gamma_z = \sigma_3$, then by rotational symmetry $G^{\alpha\beta}(z)$ has zero off-diagonal elements. As we have seen we can extract the continuum propagator in a periodic box of sidelength L as

$$G^{11}(z) = \frac{e^{-mz}}{1 - e^{-mL}}$$

Again as $L \to \infty$ we recover the expected propagator e^{-mz}. On a random lattice this goes over to [11];

$$G^{\alpha\beta}(z) = \frac{1}{V} \sum_{i,j} \sqrt{\omega_i \omega_j} \frac{1}{a} \Delta\theta_a \left[\left(\not{D} + m \right)^{-1} \right]_{ij}^{\alpha\beta} \tag{2.22}$$

where

$$\Delta\theta_a = \theta(z_i - z_j - (z - a/2)) - \theta(z_i - z_j - (z + a/2))$$

a is the average lattice spacing $a = N^{-1/3}$. The random lattice propagator has the correct symmetries and the coefficients of γ_x and γ_y are small and look like noise. Figure (2.2). shows the 2-pt function on a 2×1000 site lattice. The only deviations occur for separations less than 2/3 lattice spacings where the contribution of the doubles is evident.

We also studied the fermion condensate $\langle \overline{\psi}\psi \rangle$. In the continuum this is;

$$Tr \int \frac{d^3p}{(2\pi)^3} \frac{1}{i \not{p} + m}$$

$$= \frac{2m}{(2\pi)^3} \int_0^\Lambda \frac{d^3p}{p^2 + m^2}.$$

where Λ is a cut-off. Therefore we find:–

$$\langle\overline{\psi}\psi\rangle = \frac{4m}{(2\pi)^2}\left(\Lambda - \frac{m\pi}{2}\right)$$

Thus we expect

$$\int d^3x\langle\overline{\psi}\psi\rangle \sim \frac{ma}{a^2}$$

or

$$\frac{1}{Na}\sum_i \omega_i\langle\overline{\psi}_i\psi_i\rangle \sim ma \tag{2.23}$$

unless there are extra heavy fermions present. Figure (2.3). shows a plot of this quantity against ma for several lattices. The results confirm that, as expected there are extra particles in the spectrum with mass$\sim 1/a$ contributing. This conclusion survives the continuum limit, and indicates that we have a breaking of parity.

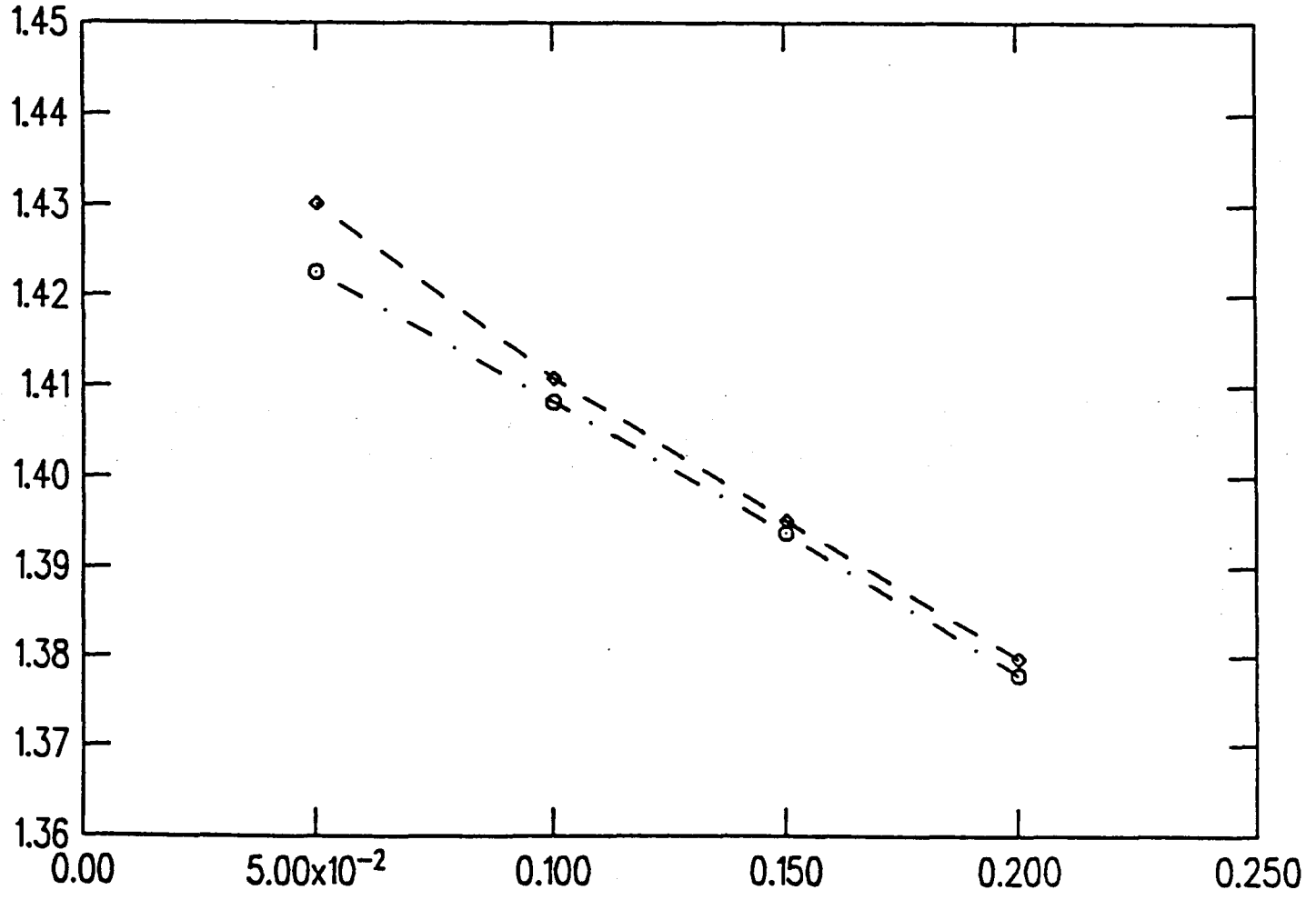

Figure 2.3. $\langle\overline{\psi}\psi\rangle$ *vs* ma *for N=1000 (◇), N=2000 (○) sites.*

It is now of interest to examine the electromagnetic current in the background of fields with winding number 1 and 2. In the continuum the vacuum charge is

$$Q_\mu = \int d^3x \langle \overline{\psi} \gamma_\mu \psi \rangle$$

With the topological field introduced earlier, the continuum charge is

$$Q_z = n/2$$

On the random lattice we must first determine the form of the gauge invariant current. This is done by the following trick [11]. In the continuum replace A_μ as follows

$$A_\mu(x) \to A_\mu(x) + a_\mu$$

then

$$Q_\mu = i \frac{\partial}{\partial a_\mu} \ln Z|_{a^\mu = 0}$$

On the random lattice

$$S = \frac{1}{2} \sum_{i,j} \overline{\psi}_i \sigma_{ij} \hat{l}^\mu_{ij} \gamma^\mu U_{ij} e^{i a^\nu l^\nu_{ij}} \psi_j + m \sum_i \omega_i \overline{\psi}_i \psi_i$$

so

$$\begin{aligned} Q^\nu &= i \langle \frac{\partial S}{\partial a_\nu} \rangle |_{a_\nu = 0}, \\ &= \langle \frac{i}{2} \sum_{i,j} \sigma_{ij} \hat{l}^\mu_{ij} U_{ij} i l^\nu_{ij} \overline{\psi}_i \gamma^\mu \psi_j \rangle, \\ &= -\frac{1}{2} \sum_{i,j} \frac{\sigma_{ij} \hat{l}^\mu_{ij} U_{ij}}{\sqrt{\omega_i \omega_j}} \left(Tr \gamma^\mu \left(\not{D} + m \right)^{-1} \right). \end{aligned} \tag{2.24}$$

We also calculated the naive current

$$j_z = i \sum_m Tr \gamma_z \left(\not{D} + m \right)^{-1}_{mm}$$

which is expected to give identical results as $ma \to 0$.

We experimented with both periodic and antiperiodic boundary conditions on the fermion field. The results for periodic boundary conditions show strong finite size effects, due to the contribution of the (approximate) zero mode, rendering

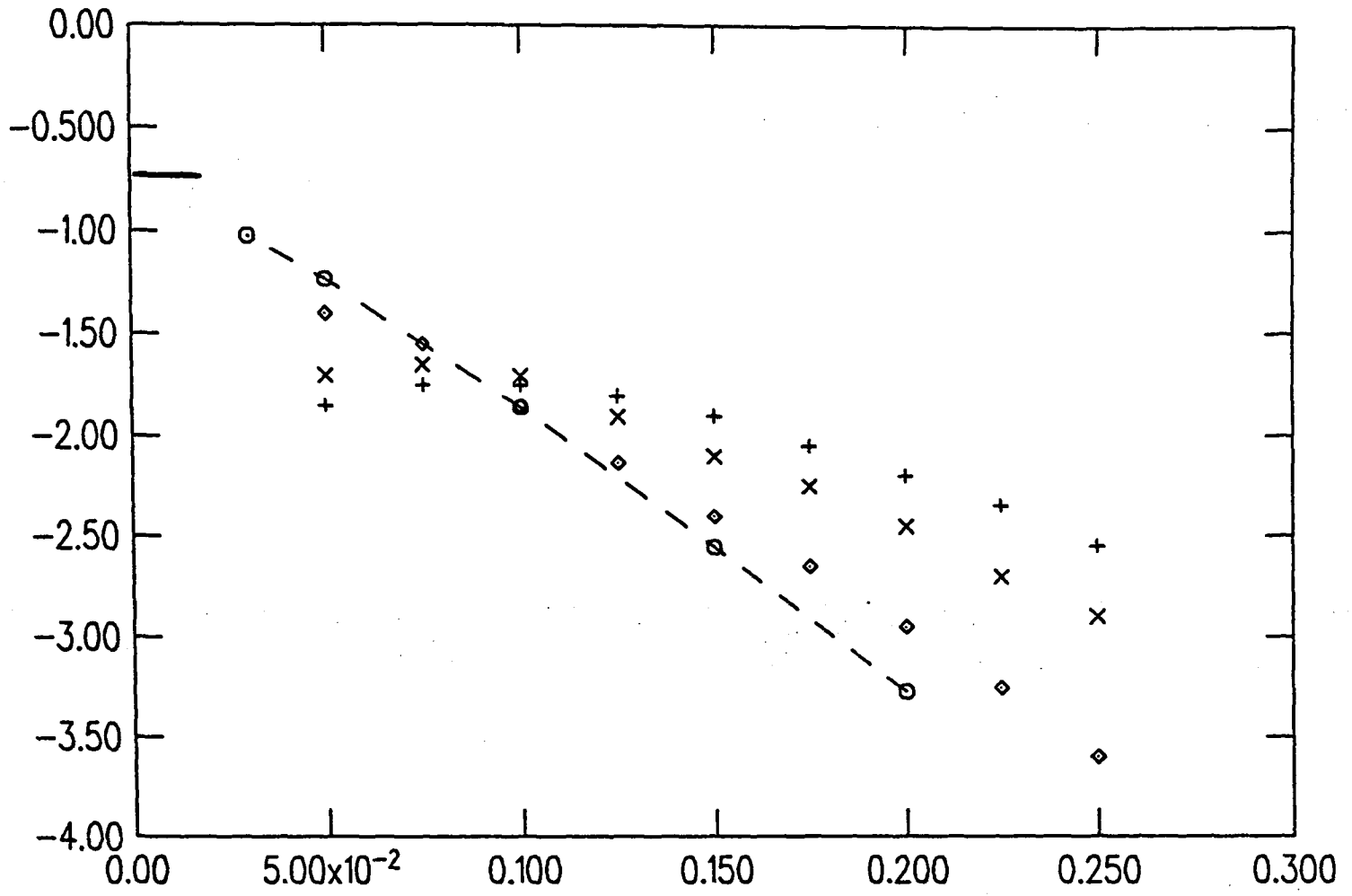

Figure 2.4. Log vacuum charge vs ma for N=500 (+), N=1000 (×), N=2000 (◇), and N=4000 (○) sites. The continuum prediction $\ln 1/2$ *is also shown.*

extrapolation to the limit $ma \to 0$ impossible on the relatively small lattices we employed. Those for anti-periodic boundary conditions with unit winding number field show much improved behaviour. In Figure (2.4). we plot $\ln Q_z$ against ma for 4 lattice sizes.

On the figure the continuum prediction is shown and we see that the data are consistent with a charge of one half in the continuum limit $ma \to 0$. Note that at small enough ma the curves turn over to give vanishing charge at $ma = 0$, so our extrapolations must be done at points before these finite size effects become important. We also compared the results of a winding number 2 field on a 1000 site lattice (Figure (2.5).), the measured charge indeed being close to twice that for the $n = 1$ field on the same system.

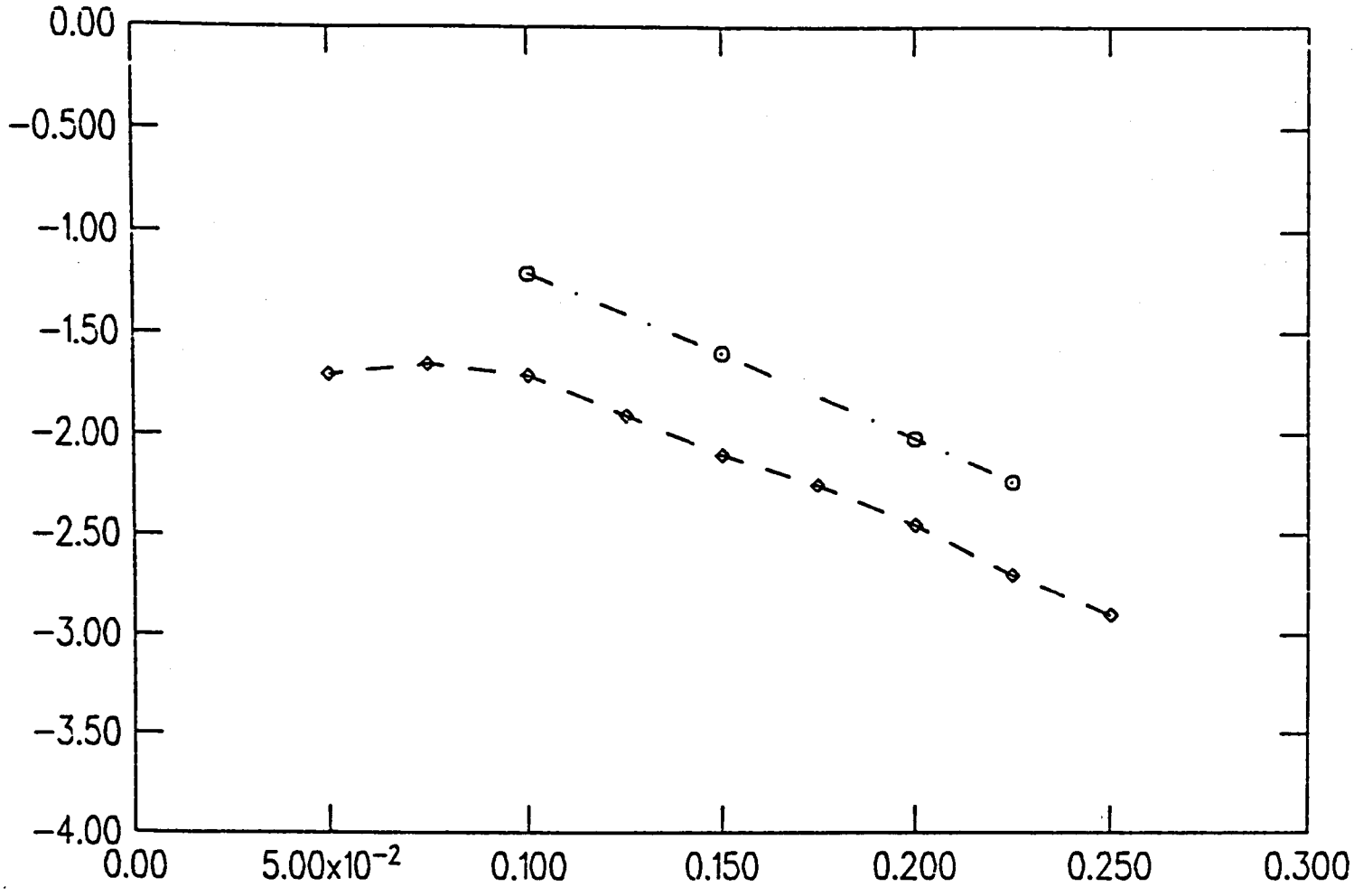

Figure 2.5. Log vacuum charge vs ma for N=1000 sites and winding number 1 (◇), winding number 2 (○) fields.

2.11 Conclusions

In conclusion it appears that random lattices provide a suitable regulator for fermionic theories in odd dimension, at least at tree level, the doubled modes do not contribute to correlation functions beyond a few lattice spacings and appear to acquire masses of order the cut-off. That this is so signals a breaking of parity in the system. This is in agreement with other methods of regularisation which are forced to induce parity anomalies in order to maintain gauge invariance. In particular, our results are in agreement with those obtained by Dagotto using Wilson fermions [12].

We are able to demonstrate the existence of a topological term in the effective action for the gauge fields, which yields parity-violating currents in the vacuum, whose magnitude depends only on the sign of the bare fermion mass term. This is in agreement with earlier work using Wilson fermions, and the measured charge

agrees well with continuum predictions. The fact that a non-zero value is found is another indication that in the continuum limit, the doubles decouple from the theory. Any even number of fermion species are believed to pair up with equal and opposite signs of the mass in odd dimension, their contributions to the current cancelling [13]. We have not considered the situation with dynamical gauge fields. The calculations were done on the CRAY-XMP/48 at the Rutherford laboratory under SERC grant GR/E/3209.0.

References:

[1] B.Zumino, W.Yong-Shi and A.Zee Nucl. Phys. B239 (1984) 477

[2] A.Niemi and G.Semenoff, Phys. Rev. Lett 51 2077 (1983);
A.N.Redlich, Phys. Rev. D 29 2366 (1984)
R.Jackiw, Phys. Rev. D 29,2375 (1985);
J.F.Schonfeld, Nucl.Phys. B185 157 (1981);
S.Deser, R.Jackiw and S.Templeton, Phys.Rev.Lett 48,975 (1982)

[3] L.Alvarez-Gaumé, S.Della-Pietra and G.Moore,
Annals.Phys. 163 288-317 (1985)

[4] R.Blankenbecler and D.Boyanovsky, Phys.Rev. D 34 2612 (1986)

[5] L.H.Karsten and J.Smit, Nucl. Phys. B183 (1981) 103;
H.B.Nielson and M.Ninomiya, Nucl. Phys. B185 (1981) 20;
H.B.Nielson and M.Ninomiya, Nucl. Phys. B193 (1981) 173;
D.Friedan, Comm. Math. Phys. 85 (1982) 481

[6] D.Espriu, M.Gross, P.E.L.Rackow and J.F.Wheater, Nucl.Phys.
B275 (1986) 39

[7] Yang Pang and Hai-cang Ren, Colombia University preprint (1987)
CU-TP-369

[8] S.J.Perantonis and J.F.Wheater Nucl. Phys. B295 [FS21] (1988) 443

[9] N.H.Christ, R.Friedberg and T.D.Lee, Nucl.Phys. B202(1982) 89;

[10] N.H.Christ, R.Friedberg and T.D.Lee, Nucl.Phys. B210 [FS6] (1982) 310

[11] S.M.Catterall and J.F.Wheater, in publication

[12] E.Dagotto Phys. Rev. D 34 2457 (1986)

[13] T.Appelquist, M.J.Bowick,Dimitra Karakali and L.C.R Wijewardna
Phys.Rev. D 33 3774 (1986);
G.Semenoff Phys.Rev.Lett 53 2449 (1984)

Figure Captions

Figure 2.1 Regular lattice propagator $G^{11}(z)$ at $ma = 0.15$.

Figure 2.2. Propagator on $10 \times 10 \times 20$ lattice at $ma = 0.2$.

Figure 2.3. $a^2\langle\overline{\psi}\psi\rangle$ vs ma for N=1000 ($\diamond$),

N=2000 (o) sites.

Figure 2.4. Log vacuum charge vs ma for N=500 (+), N=1000 ($\times$),

N=2000 ($\diamond$), and N=4000 (o) sites. The continuum

prediction $\ln 1/2$ is also shown. The dashed line through the

(o) points is to guide the eye.

Figure 2.5. Log vacuum charge vs ma for N=1000 sites and winding

number 1 ($\diamond$), winding number 2 (o) fields.

Appendix A.

In order to evaluate this sum consider the following contour integrals in the complex ω plane;

$$I_1 = \oint_C ima \frac{e^{i\omega z} d\omega}{(e^{i\omega L} - 1)\left(\sin^2 a\omega + (ma)^2\right)}$$

$$I_2 = \oint_C \sigma_z \sin a\omega \frac{e^{i\omega z} d\omega}{(e^{i\omega L} - 1)\left(\sin^2 a\omega + (ma)^2\right)}$$

where $z \geq 0$. The contour C can be drawn such that it encloses both a series of poles along the real axis corresponding to the allowed values of q_z in the first Brillouin zone (and no others) and the 4 isolated poles arising from the second factor in the denominator. Furthermore it can be arranged that the value of the integral is zero corresponding to a careful choice of contour. Thus the sum of the residues of the poles along the real axis is just the negative of the sum of the other poles in the complex plane. Thus our transverse propagator becomes the sum of I_1 and I_2. I_1 contributes;

$$\frac{1}{2}\left[\frac{e^{-mz}}{e^{-mL}-1}(1-(-1)^n) + \frac{e^{mz}}{e^{mL}-1}(-1+(-1)^n)\right]$$

I_2 contributes;

$$\frac{1}{2}\left[\frac{e^{-mz}}{e^{-mL}-1}(1+(-1)^n) + \frac{e^{mz}}{e^{mL}-1}(1+(-1)^n)\right]$$

where $z = na$ with n integral. Adding and subtracting these terms gives the appropriate diagonal components of the transverse propagator.

$$G^{11}(z) = \frac{1}{1-e^{-mL}}\left(e^{-mz} + (-1)^{n+1} e^{-mL} e^{mz}\right)$$

$$G^{22}(z) = \frac{1}{e^{mL}-1}\left(e^{mz} + (-1)^{n+1} e^{mL} e^{-mz}\right)$$

A similar procedure allows us to calculate the propagator G for $z \leq 0$ and shows analagous structure.

Chapter Three

Random Surfaces with Extrinsic Curvature

3.1 Introduction

Random surfaces appear to be important in understanding many diverse areas of theoretical physics. These include solution of the 3-D Ising model, a description of the confining phase of non-abelian gauge theory, and topics in polymer membranes and interface physics. In addition such models are crucial to the problem of constructing discrete regularisations for bosonic string theory.

When constructing an action for these objects it is appealing to incorporate only those terms which are independent of the way we parametrise the surface and possess some geometrical significance such as the surface area. In the case of string theory this area is the invariant area of the world sheet swept out by the string as it moves through spacetime. The motion of point-like excitations provides a useful analogy. As a particle propagates through spacetime it sweeps out a line. It is the invariant length of this world line which is taken as an action. In the continuum we may write;

$$S = m_0 \int d\tau \left[\left(\frac{dx^\mu}{d\tau} \right)^2 \right]^{1/2}$$

This action is invariant under reparametrisation of the world line;

$$x^\mu(\tau) \rightarrow x^\mu(f(\tau))$$

To construct the quantum mechanical amplitude for such a particle to start at x and go to x' we must sum over all possible intermediate trajectories. This amounts to an functional integration over the x coordinates, where we must be careful to include each path only once by dividing out the volume of the gauge (reparametrisation) orbit. If we attempt to discretise the paths (thus breaking this invariance explicitly),

and rotate to Euclidean space, then the quantum mechanics of such excitations becomes a problem in the statistical mechanics of random curves.

Similarly, we may adopt the surface area as an action for Euclidean string propagation (the Nambu-Goto formulation). The quantum amplitude for loop-loop propagation is obtained by performing the necessary functional integrals over spanning surface configurations. Again the measure for defining the integrals must be defined carefully in order to sum only over inequivalent surfaces. It is then interesting to devise discrete regularisations of the theory with the aim of eventually studying non-perturbative physics. In Euclidean space the models will involve the statistical mechanics of fluctuating, random surfaces. The work discussed here is largely a numerical study, via Monte-Carlo simulation, of the properties of such random surface models.

We shall see that naive discretisations of an area-like action fail to reproduce a satisfactory continuum limit. We explore the possibility of adding curvature terms to the action, and investigate the resulting phase diagram. It may be that such terms, whilst rendering our discrete regularisation well-defined, are irrelevant for the long-distance properties. Alternatively there may exist new critical points, in the vicinity of which a continuum limit corresponding to smooth surfaces exists.

3.2 Review and Introduction to the Model

Models of random surfaces fall into two main categories; those based on a simple area action plus possible rigidity terms which we discuss below, and others related to Polyakov's partition function for bosonic strings. These latter types (discussed in section 3.2.2) treat the internal metric as a new, separate degree of freedom and prove more tractable in the continuum. All the simulation work presented later concerns discretisations of this second type.

3.2.1 Actions with an area term

As we have discussed, the simplest approach is take the action proportional to the invariant area (the Nambu-Goto form). A microcanonical ensemble of surfaces with fixed area has partition function

$$Z = \sum_{\text{surfaces}} \delta(A - A_0)$$

It usually proves expedient to replace the microcanonical ensemble with a canonical ensemble allowing for fluctuations in the area [1–4]. The partition function now reads

$$Z = \sum_{\text{surfaces}} e^{-\mu^2 A} \tag{3.1}$$

The parameter μ^2 corresponds to the bare string tension. Such models have been studied on rigid hypercubic lattices [1,2]. Unfortunately they correspond to a free scalar field in the continuum limit. At the critical point the partition function is dominated by tree-like, branched polymer configurations. These prohibit the long-wavelength collective excitations which are needed to force a vanishing of the renormalised string tension (in units of the inverse lattice spacing) at the critical point.

In an effort to avoid this problem the Nambu-Goto form of area action has also been studied on models arising from a discrete triangulation of the surface. Here, the continuum surface is approximated by a set of random triangles, glued pairwise along their edges [5,6]. A given triangulation comprises a set of vertices, links and triangles. Any vertex is connected to a fixed number of neighbours by links which are the sides of elementary triangles. The vertices are then given an embedding in some D dimensional space. The sequence of surfaces corresponding to the canonical ensemble is then generated by an integration over vertex positions, keeping the triangulation fixed, weighted by the exponential of minus the area. The partition function for a surface of N sites is;

$$Z = \int \prod_{i=1}^{N\ \prime} dX_i^\mu \, e^{-\mu^2 A(X_i)} \tag{3.2}$$

where the prime indicates that one of the integrations over the embedding coordinates is suppressed to kill off the zero mode due to translational invariance. Typical surfaces from this ensemble are highly crumpled with the mean square size of the surface increasing only logarithmically with area. We shall see (section 3.7) that this result may be obtained within a mean-field approach. Furthermore it can be shown that the models contain certain pathologies related to the growth of spikes [7]. Consider the p^{th} moment of the probability distribution for the surface

$$\langle X^p \rangle = \int DX\, X^p e^{-\mu^2 A}.$$

It may be shown that for some finite p, dependent on the triangulation and the precise form of A, this moment diverges, even for a finite system. These divergences stem from the existence of certain zero mode deformations of the area action, which correspond to the growth of spikes. These are configurations of the discrete surface where one or more vertices is displaced an arbitrary distance from the bulk of the surface, in such a way that the area remains constant. Moreover, a simple counting argument shows that such configurations are entropically favoured over smooth ones. The existence of such zero modes tends to destabilise any mean field solution and ensures that there is no characteristic length scale attributable to the surface. Thus the problem here is not that the surfaces are crumpled in the infra-red, but that they are crumpled on all scales (they are self-similar).

As a consequence it can be seen that it is necessary to go beyond the simple area action, if we wish to consider models with satisfactory scaling behaviour. Clearly terms involving the curvature of the surface are ideal candidates for suppressing extremely crumpled configurations, or ones possessing large spikes [6].

3.2.2 Models based on the Polyakov string

This formulation is entirely equivalent to the Nambu-Goto at the classical level. In the continuum the Nambu-Goto action takes the form;

$$S = \int d^2\xi \sqrt{\det\left(\frac{\partial X^\mu}{\partial \xi_a}\frac{\partial X^\mu}{\partial \xi_b}\right)} \tag{3.3}$$

The coordinates X^μ are functions of the world sheet parameters ξ_a, $a = 1, 2$. In order to rid the action of this cumbersome square-root of a determinant, we introduce another set of degrees of freedom– the intrinsic metric on the surface g_{ab}, and write Z as;

$$Z = \int Dg_{ab}DX^\mu\, e^{-\mu^2 S_P} \tag{3.4}$$

where

$$\begin{aligned} S_P &= \int d^2\xi \sqrt{g} g^{ab}\partial_a X^\mu \partial_b X^\mu \\ &= -\int d^2\xi \sqrt{g} X^\mu \Delta X^\mu \end{aligned} \tag{3.5}$$

where Δ is the covariant Laplacian on the world sheet and g the determinant of g_{ab}. The model possesses two important symmetries; reparametrisation invariance (general coordinate invariance on the world sheet)

$$\xi_1' = f(\xi_1, \xi_2);$$

$$\xi_2' = g(\xi_1, \xi_2)$$

and Weyl invariance, corresponding to local rescalings of the metric;

$$g_{ab} \to \lambda(\xi_1, \xi_2)\, g_{ab}.$$

Any discrete model will necessarily break these symmetries at the outset, and it is a highly non-trivial problem to show that they are recovered in the continuum limit (if indeed such a limit exists). Alternatively the model may be pictured as two dimensional quantum gravity coupled to a D-component scalar field X^μ. The discrete model corresponding to this formulation is represented by the partition function (N sites) [8–13]

$$Z_N = \sum_T \frac{1}{C(T)} \int \prod_{i=1}^{N\,\prime} d^D X_i e^{-S} \tag{3.6}$$

where

$$S = \mu^2 \sum_{\langle ij \rangle} (X_i - X_j)^2 \,. \tag{3.7}$$

Z_N comprises a series of terms, corresponding to a sum over vertex positions, and the contribution of all possible triangulations T. The action S contains a discrete version of the continuum Laplacian for a given triangulation acting on the coordinates X^μ of the vertices in some D-dimensional space. The triangulations are restricted so a given link bounds two and only two triangles, and any two vertices are connected by at most one link. The surface is said to be self-avoiding. It is important to realise that this is a restriction purely on the intrinsic geometry—it does not prevent the folding of the surface upon itself in the embedding space. The sum over triangulations T is intended to mimic the sum over smooth Riemannian metrics encountered in the continuum. Note that we are summing over only equivalence classes of triangulation, differing only in a relabelling of some given triangulation (this freedom is the vestige of reparametrisation invariance left in the model)– this accounts for the division by $C(T)$ – the order of the symmetry group of T. If some universality holds it is expected that this discrete sum over singular metrics will give results similar to the full sum over smooth metrics in the scaling limit.

As seen by examining the form of the gaussian action, the internal geometry corresponds to a set of equilateral triangles. Fluctuations of intrinsic geometry at the level of the cut-off are reflected only in the variation of the coordination number of the vertices. We expect that this restriction will not be important near a critical point, where the long-distance fields will not be so restricted. The topology of the triangulation (labelled by its Euler number) is fixed throughout, partly for simplification, and secondly as there exist arguments that show that the partition function diverges, if summed over all topologies. Specifically, we have only considered closed topologies with toroidal or spherical boundary conditions.

One may also add to the action a term depending on the intrinsic curvature

(not to be confused with the extrinsic curvature to be introduced later).

$$R_i^{\rm int} = \pi \frac{(6 - q_i)}{q_i}$$

of the form;

$$R^{\rm int} = -\alpha \sum_{i=1}^{N} \ln q_i$$

where q_i is the coordination of vertex i. On expanding the logarithm we find terms depending on $R, R^2, R^n, \cdots$. The first of these has integral proportional to the Euler characteristic for the manifold and is hence just a constant, whilst the higher terms correspond to higher-derivative terms in the continuum and are expected to be irrelevant operators on dimensional grounds. Thus a naive application of universality leads to the conclusion that such a term should not change the nature of any continuum limit. In fact, results already obtained indicate that the critical exponents do indeed seem to depend continuously on the coefficient α [8–12]. In section 3.5 we will see this explicitly. As $\alpha \to \infty$ this term favours a locally flat intrinsic geometry with the majority of the vertices 6-fold coordinated.

In principle we may extend our model from a fixed number of vertices to a grand canonical ensemble of surfaces where the number of vertices may change [10,12,13]

$$Z = \sum_{N=3}^{N=\infty} e^{-\gamma N} Z_N. \tag{3.8}$$

Here γ plays the role of a chemical potential. However, in all the work I shall describe we are working in the canonical ensemble. In addition, although most of what is said will be applicable to all embedding dimensions, the work presented here is in the fixed bulk space dimension $D = 3$. This is a physically interesting case and if adopted reduces the computational effort considerably, especially with the inclusion of extrinsic curvature terms to the standard action. In all the numerical work the string tension μ^2 is set to unity. In section 3.5 we examine this Polyakov formulation with intrinsic curvature, both to confirm results obtained by other groups, and to check our codes before extending them to allow for extrinsic curvature terms. First

we discuss some important properties of surface models near criticality, indicating the expected scaling behaviour if such models are to have a non-trivial continuum limit.

3.3 Critical Properties of Random Surfaces

Consider a generic random surface model with a purely area-like action

$$Z = \sum_{\text{surfaces}} e^{-\alpha A}$$

It can be shown that the number of surfaces pinned to a given boundary increases like [4]

$$e^{\alpha_0 A}$$

so that the partition function may be written as

$$Z = \sum_{A} e^{-(\alpha-\alpha_0)A} \tag{3.9}$$

Clearly Z and indeed all loop-loop correlation functions will diverge for $\alpha < \alpha_0$ i.e the entropy associated with surfaces overwhelms the Boltzman factor. The point α_0 itself is a candidate for a critical point of the model since it separates two qualitatively different phases.

One may define general loop-loop correlation functions in the following manner

$$G(\gamma_1 \cdots \gamma_N) = \sum_{\text{surfaces}\,\gamma_1 \cdots \gamma_N\,\text{fixed}} e^{-\alpha A} \tag{3.10}$$

It is convenient to let the loops $\gamma_1 \cdots \gamma_N$ contract to points $x_1 \cdots x_N$ and we are left with the following n-pt functions

$$G(x_1 \cdots x_N)$$

The mass gap of the model is defined as

$$m(\alpha) \sim - \lim_{|x_1 - x_2| \to \infty} \frac{\ln G(x_1, x_2)}{|x_1 - x_2|}$$

whilst the string tension is

$$\tau(\alpha) \sim -\lim_{L,M\to\infty} \frac{\ln G(\gamma_0)}{LM}$$

where γ_0 is some fixed loop of area LM.

If the mass vanishes at the point α_0, we may characterise the singular parts of various observables near α_0 as follows

$$m(\alpha) = (\alpha - \alpha_0)^{\nu}$$

$$\tau(\alpha) = (\alpha - \alpha_0)^{\delta}$$

$$\chi(\alpha) = (\alpha - \alpha_0)^{-\epsilon}.$$

where the susceptibility χ is defined as

$$\chi = \sum_{\gamma_i} G(\gamma_0, \gamma_i)$$

It is the integral of the 2-pt function over the surface. If we have long range correlations then the susceptibility may diverge. The mass gap may be extracted from the asymptotics of the 2-pt function

$$G(x_1, x_2) \sim e^{-m(\alpha)|x_1 - x_2|} |x_1 - x_2|^{2-d+\eta}$$

which also defines the anomalous exponent η. It may also be shown that the inverse mass-gap exponent ν is just the Hausdorff dimension.

For a sensible scaling limit we require that

$$m\overline{a} \to 0, \qquad \tau\overline{a}^2 \to 0$$

with

$$m^2/\tau \sim \text{const} \tag{3.11}$$

$\overline{a}$ is the average bond length determined by the bare string tension . The generic problem for these naive models is the non-vanishing of the string tension (in units of the inverse bond length) at α_0. We shall see that the addition of extrinsic curvature may well generate new critical points in the vicinity of which we may hope that such a scaling behaviour is true.

3.4 Simulations

Our numerical simulation of the partition function (3.6) involved two independent Monte-Carlo schemes, in order to generate both the sum over triangulations and the integral over embedding coordinates. If vertices are labelled by some site index i, then data structures are needed to hold information on all N_L links (ij) and N_T triangles (ijk). Since this information is necessarily continually changing, it is very inefficient to store the data in static arrays. Instead we employ a sequence of linked lists. As we show in appendix B, this facilitates rapid scanning for local link or triangle information, and allows rapid insertion and deletion of links or triangles. The price paid is the inherent difficulty of vectorising the resultant code. Whilst it proves relatively easy to pipeline the vertex updating (even with extrinsic curvature in the action), the operations to generate new triangulations are serial in character. Effectively two vertices which start out at the beginning of some sweep many bonds apart, may end up as nearest neighbours by the end of the sweep. Thus the usual locality criteria, which are traditionally required for a successful vector or parallel algorithm, are missing. It is a highly non-trivial problem to devise a really efficient algorithm for these random surface models, which maps readily onto parallel architectures. In consequence of this our simulations utilise a maximum of 144 sites. This was not too limiting for obtaining a merely qualitative picture of the phase diagram (which was our main task), but would prove to be a nuisance in studies requiring more detailed measurements. The bulk of the work was carried out on the CRAY-XMP/48 at the Rutherford labs.

The first problem to be addressed is the construction of a triangulation with a given topology, characterised by its Euler number. Those simulations employing only intrinsic curvature were carried out on a lattice possessing toroidal topology, and the lattices in this case are started out in a regular configuration with all vertices 6-fold coordinated and with periodic boundaries. For the simulations with extrinsic curvature we choose a spherical topology (Euler number 2). Here a lattice of N sites is constructed from some starting tetrahedron by inserting new vertices at the

centre of randomly chosen triangular faces. Between successive additions a number (typically 50) of sweeps of the lattice are made to thermalise the new insertion, the process continuing until N vertices are attained. A further $10N$ sweeps are then made to allow for complete relaxation to equilibrium.

A single vertex updating step comprises the addition of a gaussian random vector to the vertex position vector.

$$X_i \rightarrow X_i + \eta_i$$

The shift is accepted or rejected according to the usual Metropolis algorithm. First the change in the action δS under such a potential change is made. If this is negative the change is accepted, and the lattice information updated. If, however, δS is positive it is accepted only conditionally. Specifically compute $e^{-\delta S}$. Choose a random number r in the range $0 \rightarrow 1$. If $e^{-\delta S} \geq r$ then we accept the change again, otherwise it is rejected. Such a Markovian process is guaranteed to eventually generate a sequence of configurations representative of those which dominate the partition function.

It proved effective to hit a given vertex more than once before moving on to the next, in order to approach a heat bath-like update. This had to be balanced against the increased time for the process. A compromise of 6 hits was used in the production runs. For the simulations with extrinsic curvature, characterised by the coupling β, the size of the gaussian step is reduced as β increases to maintain the acceptance rate close to $\frac{1}{2}$.

Retriangulations are generated from the basic link flip operation. Every link $\langle ij \rangle$ borders 2 triangles, the other 2 vertices of which define a complementary link $\langle kl \rangle$. This is illustrated below in Figure (3.1)

We imagine flipping the link to its complement. The change in the action under such a flip is then subjected to a Metropolis test. This operation is ergodic in the sense that it allows all possible triangulations to be accessible to the system with a priori equal probability. For efficiency we store the complementary link within

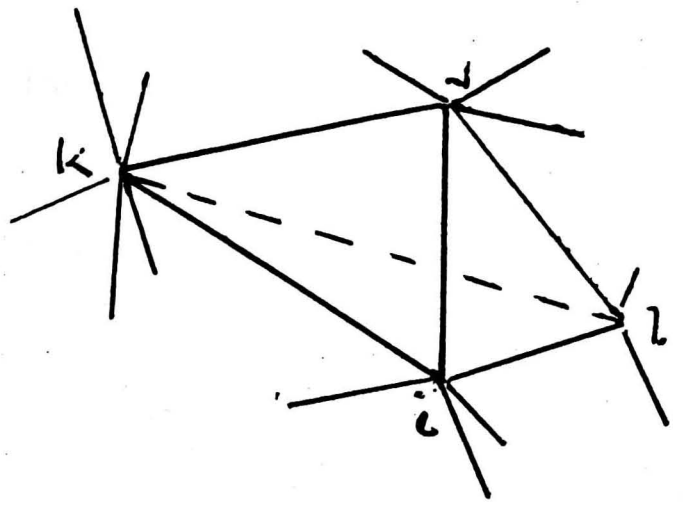

Figure 3.1 Elementary link flip

a given link record. After every successful update, it is necessary to change the information stored in the records of neighbouring links and triangles.

A single sweep of the lattice commences with the attempted flip of $2N_L$ links chosen at random. This is followed by the random update of $N-1$ sites (we fix one vertex to eliminate the contribution of the zero mode). For the runs with intrinsic curvature we utilise at large coupling $810 \times N$ sweeps for each data point, whilst $50 \times N$ sweeps are used for the simulations with extrinsic curvature. Measurements are made every second sweep.

As we shall show in section 3.5 we may calculate the mean and variance of the gaussian term analytically, independent of T. Monitoring their values in the simulation runs provides us with a check that we are sampling the equilibrium distribution for the vertices correctly. It is much harder to be sure that we are seeing the correct distribution of linking structures. It would be very easy for the links to fall out of equilibrium with the vertices, if the characteristic relaxation times were markedly different. The internal geometry would then be akin to a glassy structure. In order to check for this we ran the simulations over a wide range of the relative frequency f for link to vertex updating, examining the mean gyration radius for systematic drift. We were able to increase f to 25 at $\alpha = 0$. For the runs with rigidity terms in the action we measured the extrinsic curvature and its variance in order to look for the singular behaviour characteristic of phase transitions of varying orders. The mean gyration radius (see section 3.5) is calculated in order to test for

a transition from the scaling behaviour associated with crumpled surfaces to that of smooth surfaces. In addition the mean dot product between normals is stored as a naive order parameter to characterise possible differing phases of the models.

$$\langle n.n \rangle = \frac{1}{N_L} \sum_{\langle ij \rangle} (n^\alpha . n^\beta)$$

where the normals n^α and n^β border the link $\langle ij \rangle$. It is also of some interest to measure the distribution of internal curvature, or equivalently the coordination number. Some of our measured results can later be compared with the results of various mean-field and continuum predictions (see section 3.7).

The results are distributed into 10 bins. In order to eliminate correlations between successive measurements we store the moving average of a quantity Q and subsequently reaverage the moving averages with weight $\sqrt{t}$ (see [8]) . We measure;

$$Q_t = \frac{1}{t} \sum_{k=1}^{t} Q_k$$

then

$$\langle Q \rangle = \frac{\sum_{t=1}^{\tau} \sqrt{t} Q_t}{\sum_{k=1}^{\tau}} \tag{3.12}$$

The error bars are computed by taking the root mean square of the deviations in the means measured within each bin from their global averages. It sometimes proved useful to employ a jack-knife method when computing the error bars on a quantity like $\langle X^2 \rangle$, which suffers large fluctuations in the vicinity of a phase transition. Here a set of 10 new means are obtained from the binned quantities, by averaging them in sets of 9. The root mean square deviation is then recalculated in order to assess the errors. The method is useful when there are few measurements within each bin, or where large systematic fluctuations occur which overlap between bins. For quantities distributed normally it is equivalent to the usual methods.

3.5 Results with Intrinsic Curvature

In this section we present results for the discretised Polyakov model with the addition of intrinsic curvature to the gaussian action. First, consider the result of explicitly integrating out the X coordinates. The gaussian integral yields;

$$Z = \sum_T \frac{1}{C(T)} \left(\frac{1}{\det M} \right)^{D/2} \tag{3.13}$$

where M is the connection matrix (essentially the discrete Laplacian);

$$M(i,j) = \begin{cases} q_i, & \text{if } i = j; \\ -1, & \text{if } i,j \text{ linked}; \\ 0, & \text{otherwise.} \end{cases}$$

q_i is the coordination number of vertex i. Now the determinant can also be written

$$\det(M) = \text{number spanning trees in the lattice}$$

where a tree is defined as a connected graph linking all vertices of the lattice such that there are no closed loops on the tree. Asymptotically as $D \to \infty$ the partition function is saturated by configurations with a minimal number of spanning trees. This occurs for branched tree-like structures. Thus we might expect branched polymers to dominate in these models for sufficiently large D, in contrast to the fixed triangulation models, where $D \to \infty$ corresponds to the mean field limit with infinite Hausdorff dimension (section 3.7). In the formal limit $D \to -\infty$ a maximal number of spanning trees is preferred, corresponding to a regular triangulation with the majority of vertices having coordination number 6.

The scale invariance of the intrinsic curvature term allows us to determine the mean and variance of the gaussian term. Consider

$$Z = \sum_T \int DX e^{-\mu^2 XQX - \alpha R^{\text{int}}} \tag{3.14}$$

Let us rescale the X variables

$$X' = \mu X;$$

$$DX' = \mu DX.$$

then

$$Z = \mu^{-(N-1)D} \sum_T \int DX' e^{-X'QX' - \alpha R}$$

i.e

$$Z(\mu^2) = Z(1)\mu^{-(N-1)D}$$

Now

$$\begin{aligned} \langle XQX \rangle &= -\frac{\partial}{\partial \mu^2} \ln Z(\mu^2); \\ &= \frac{1}{2}(N-1)D. \end{aligned}$$

Similarly

$$\left\langle (XQX)^2 \right\rangle - \langle XQX \rangle^2 = \frac{1}{2}(N-1)D$$

where we have set μ to unity in the last two expressions (in order to compare with our numerical results). Note that this trick will also work later when we consider extrinsic curvature terms, as these will also be globally scale invariant.

We simulated the partition function (3.6) numerically as detailed in section 3.4 on system sizes with $N = 49, 64, 81, 100, 121, 144$, the coupling α varying in the range $0 \rightarrow 15.0$

The important observables are the mean gyration radius, and the distribution of coordination number. The former is defined as;

$$\left\langle X^2 \right\rangle = \frac{1}{N} \left\langle \sum_{i=1}^{N} (X_i - \langle X \rangle)^2 \right\rangle \tag{3.15}$$

where N is the number of sites in the surface. Asymptotically we expect;

$$\left\langle X^2 \right\rangle \sim N^{2/d_H}$$

which defines the Hausdorff dimension d_H. This quantity is extremely sensitive to the long-wavelength fluctuations of the surface. The results shown were obtained using toroidal boundary conditions, but the code was checked on systems with spherical topology, and beyond a slight renormalisation of the coefficient of the power law the results for the scaling behaviour were unaltered (this is to be expected as $\left\langle X^2 \right\rangle$ is sensitive to the smallest eigenvalue modes of the Laplacian on

Figure 3.2. $\ln X^2$ *vs* $\ln N$ *for* $\alpha = 0, 1.5, 3.0, 4.5, 6.0, 9.0, 15.0$.

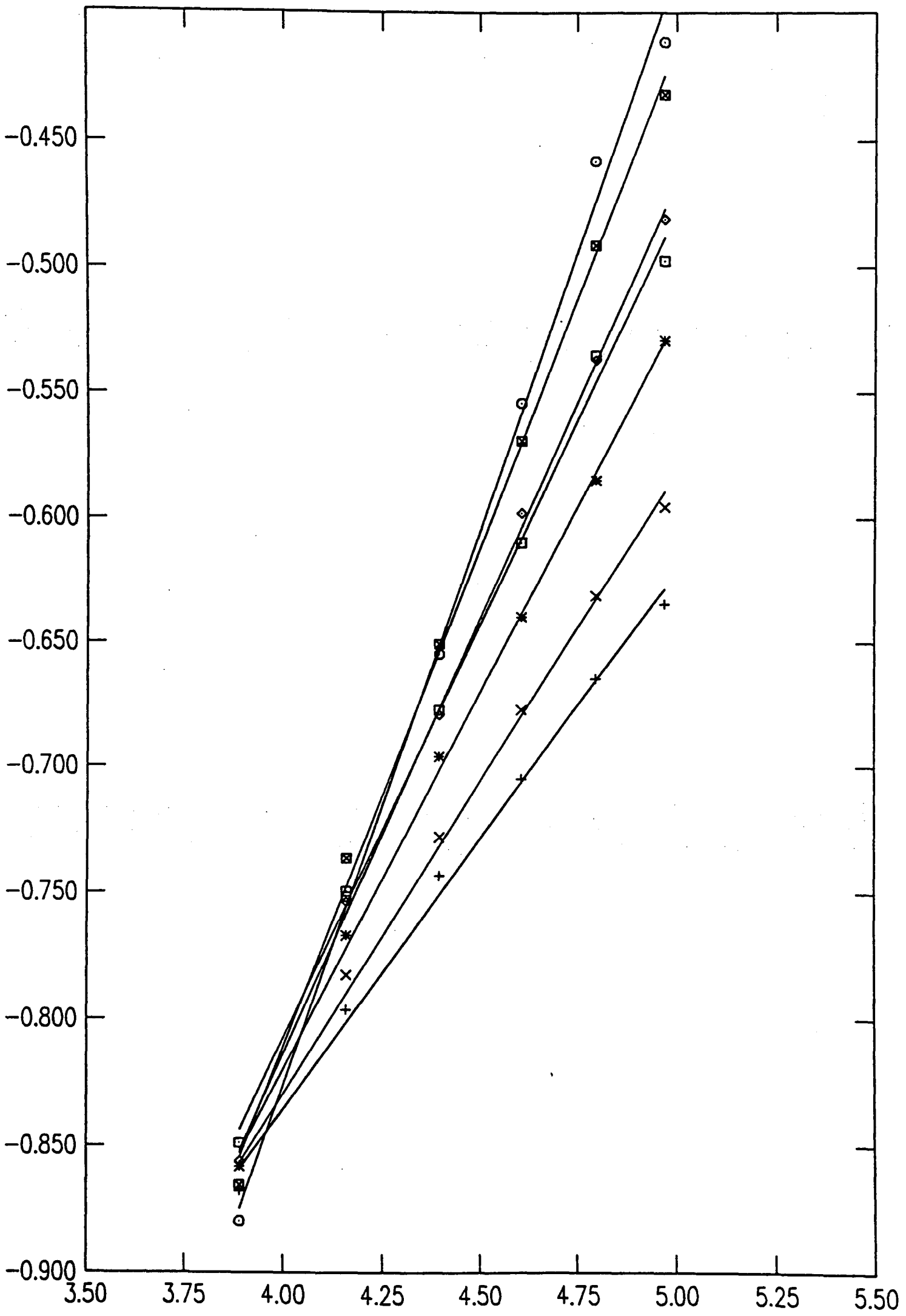

the triangulation, which vary with topology). Figure (3.2). shows a plot of $\ln X^2$ versus $\ln N$ for a variety of α. The straight lines are least square fits to the points. From this we may extract a picture of how the Hausdorff dimension varies with α. $2/d_H$ is plotted as a function of α in Figure (3.3).

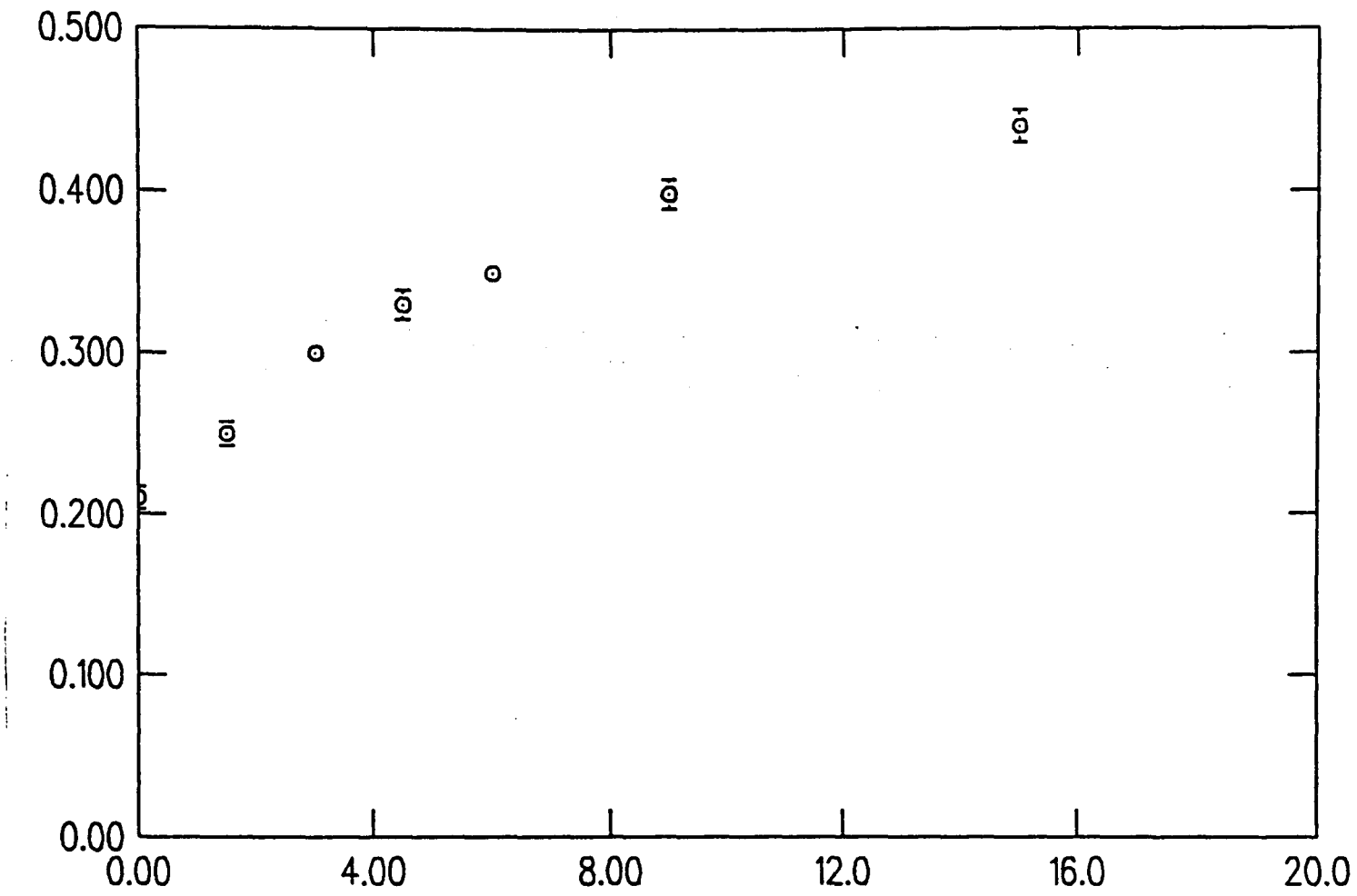

Figure 3.3. Inverse Hausdorff dimension ($2/d_H$) as a function of α.

The results indicate that this critical exponent apparently depends continuously on α– there is no sign of a discontinuity in the curve (which might indicate a possible phase transition). At $\alpha = 0$ the Hausdorff dimension is large ~ 10, the small power being consistent with logarithmic scaling, which is the mean-field result expected for fixed triangulations. As α increases the Hausdorff dimension tends to decrease steadily towards the value of 4, indicating, it seems, an increasing dominance of branched polymer configurations. As the system sizes barely vary over one order of magnitude, and we consider only 6 different sizes of lattice, one should not take

the exponents in the scaling laws too literally as those of a continuum surface. As we mentioned in the previous section, we may test for the equilibration of the triangulations by increasing f, the link to vertex updating frequency. For the small lattices employed it is hard to draw definite conclusions from this study. It appears that there is a systematic drift upwards in the values of the mean gyration radius, this effect increasing with larger N. The data at $\alpha = 0$ are consistent with a Hausdorff dimension significantly less than the value $O(10)$, obtained before. It is tempting to speculate that perhaps the true scaling behaviour corresponds to $d_H = 4$, independent of α, and that the region where this critical exponent is continually varying between this limits disappears as $f \to \infty$. Presumably this would mean that the continuum limit is described by a free scalar field again.

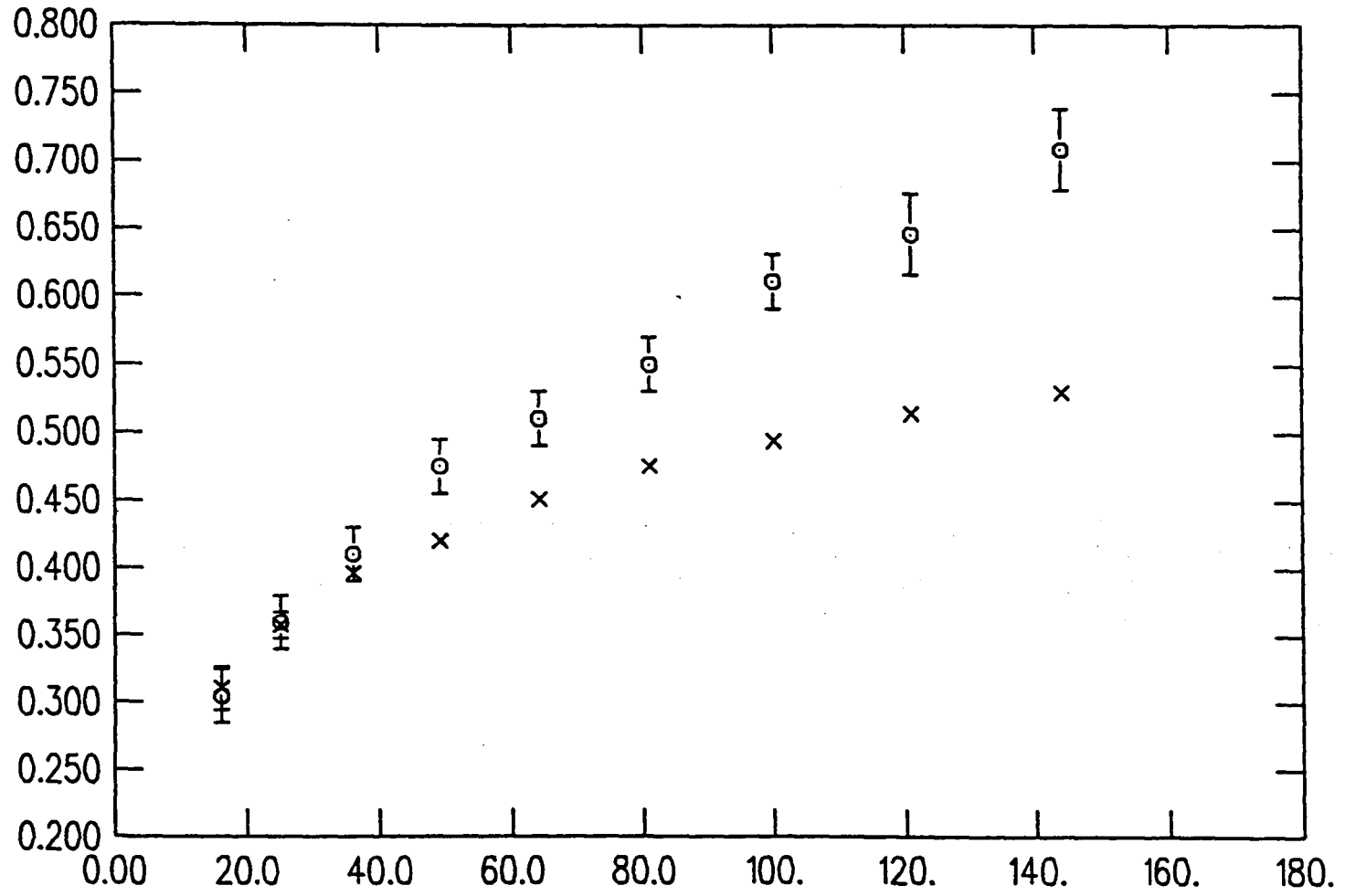

Figure 3.4. $\langle X^2 \rangle$ vs N for random ($\times$) and biased (o) update.

Whilst trying various methods of link updating it was noticed that a systematic

Figure 3.5. Histogram showing distribution of coordination number at $\alpha = 0$.

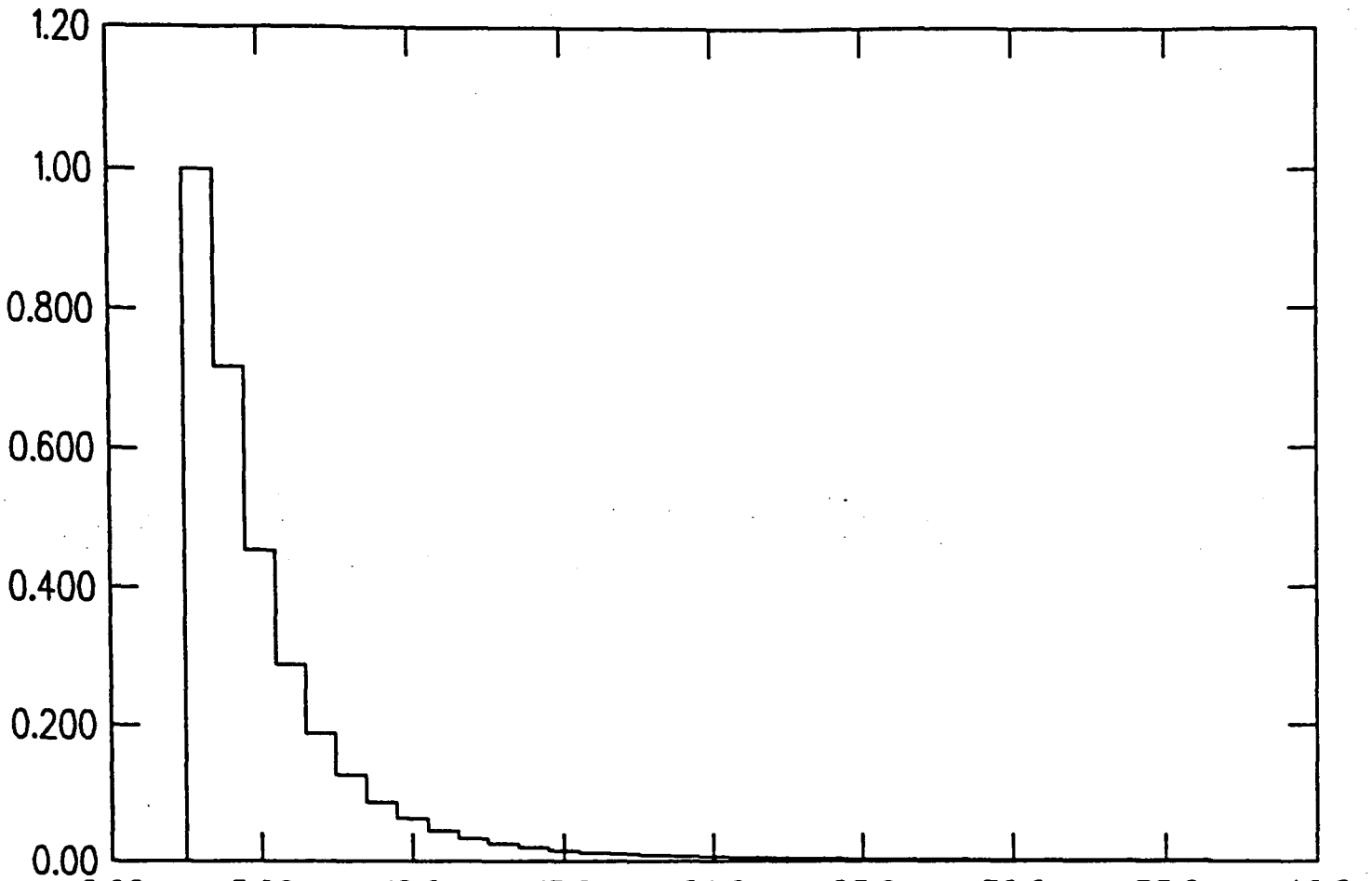

Figure 3.6 Distribution of coordination number for $\alpha = 15.0$.

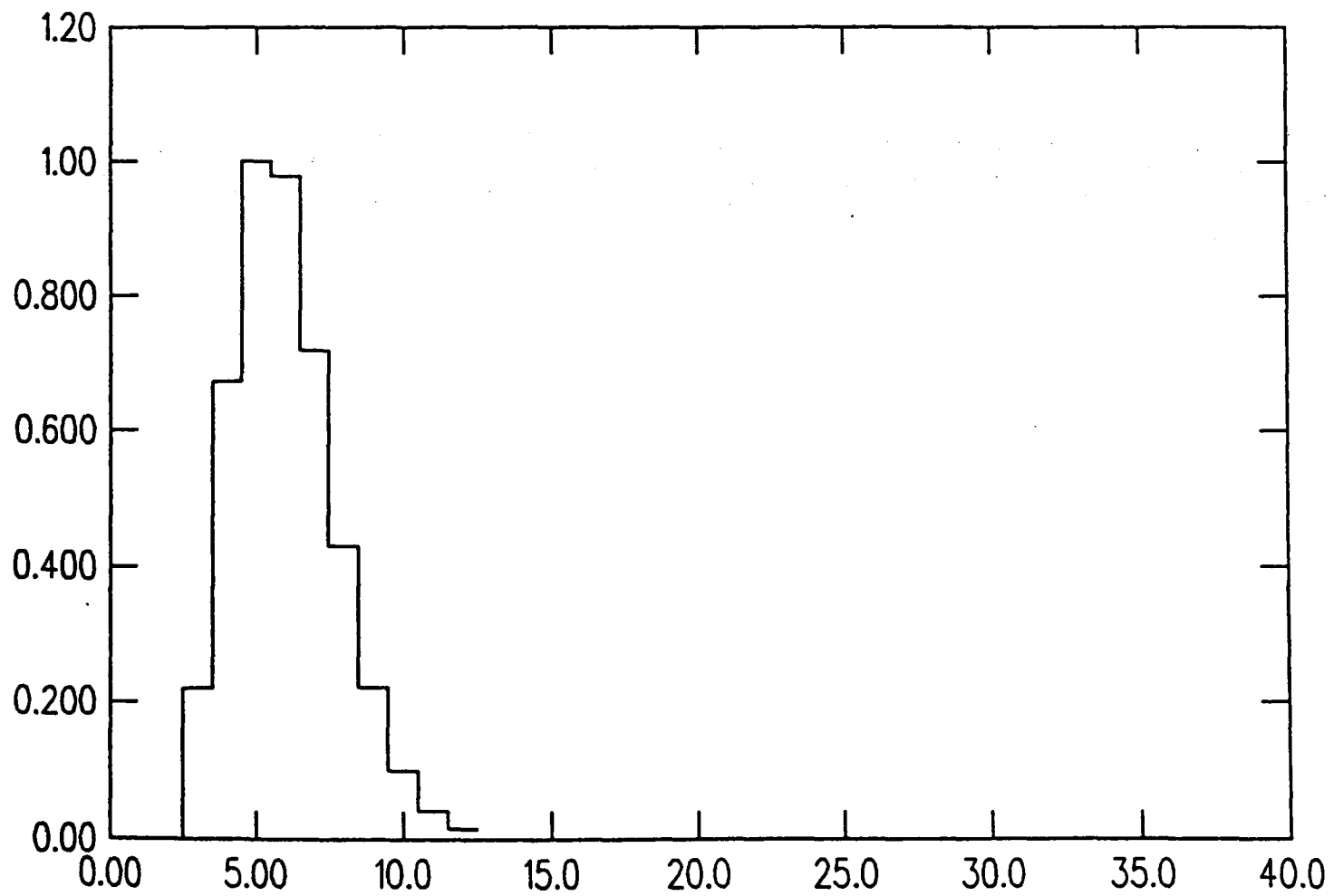

disagreement occurred between the purely random link update, and one which, having selected a site at random, attempted to update all links attached to that site before moving on. Figure (3.4) shows a plot of $\langle X^2 \rangle$ against N at $\alpha = 0.0$ for the two forms of update. It appears that this biased form of update induces far larger fluctuations in the mean gyration radius. Fits to scaling laws lead to a Hausdorff dimension much closer to 4, which is at variance with the results for random updating. It appears to promote a degeneration into branched polymers. Such anomalous effects in two dimensional systems have been observed before [14]. The biased update does not respect detailed balance, which although not absolutely required, is certainly a sufficient condition for the sampling to follow the equilibrium distribution. The effect is thought to disappear for extremely large numbers of sweeps and much bigger system sizes. Throughout the rest of this chapter we shall adopt the random link update, which has the virtue of being (computer)time reversal invariant.

As $\alpha \to \infty$ only configurations with $q_i = 6$ are allowed. This is shown in figure (3.5) and figure (3.6), where the distribution of coordination number for $\alpha = 0.0$ and $\alpha = 15.0$ is plotted.

In conclusion, it appears that the models based on the Polyakov formulation with actions containing intrinsic curvature terms in addition to the gaussian term are unacceptable as discretisations of smooth continuum surfaces. In small D and neglecting intrinsic curvature, they have large Hausdorff dimensions and in addition a small fraction of the vertices have high coordinations. The latter problem may be improved by the addition of intrinsic curvature, which forces locally flat configurations (internally) as the associated coupling $\alpha \to \infty$. The scaling behaviour then seems consistent with a dominant contribution to Z of branched polymer-like surfaces. This situation is also expected at large D. At intermediate α the Hausdorff dimension varies continuously with α which seems at variance with conventional wisdom– universality in these models seems to be poorly understood.

As Migdal has argued, it is perhaps not so surprising that problems appear in

trying to formulate sensible regularised statistical models for bosonic string theories. The free bosonic string has a tachyon in its spectrum. Any random surface model will have difficulties in producing a tachyon in the scaling limit i.e as the mass goes to zero through positive real values and it is tempting to speculate that the degeneration into branched polymers is a manifestation of the instability of the corresponding continuum surface to tachyon emission. It appears that we must consider the addition of other curvature terms (depending explicitly on the X coordinates) in order to try to retrieve the situation– these are, of course, just the extrinsic curvature forms already mentioned. This we do in section 3.6 and onwards.

3.6 Extrinsic Curvature Terms

First, let us summarise the situation with intrinsic curvature terms. We have seen that the Einstein term R does not contribute for two dimensional manifolds of fixed topology, whilst higher powers of R are naively expected to be irrelevant in the continuum limit as they correspond to couplings of negative mass dimension. In fact such terms do seem to influence the critical behaviour, but in a rather poorly understood manner. Furthermore we do not seem to be able to generate models with the correct scaling behaviour even with these terms (indeed it appears that the old problem associated with branched polymer behaviour reasserts itself).

The other possibility, to which most of the present work is devoted, relates to the inclusion of extrinsic curvature terms in the action. These encode an explicit dependence on the embedding dimension. Our studies concentrate on two possible types of extrinsic curvature which can be shown to be equivalent up to total divergences in the continuum [15]. It will turn out that their discrete counterparts have quite different properties determining quite contrasting phase structures. The two terms will, from now on, be referred to as type 1. and type 2. In the continuum type 1. has the form

$$R_1 = \beta \int d\sigma d\tau \sqrt{g} \left(\frac{1}{\sqrt{g}} \partial_b \left(g^{ab} \sqrt{g} \partial_a \right) X \right)^2 \tag{3.16}$$

The square of the covariant Laplacian acting on X. The second form is

$$R_2 = \beta \int d\sigma d\tau \sqrt{g} g^{ab} \nabla_a n^i \nabla_b n^i \tag{3.17}$$

where ∇_a is the covariant derivative and n^i are the $i = 1 \cdots D-2$ normal vectors to the surface. Polyakov [15] has shown that the inverse coupling (which is dimensionless) is asymptotically free so the term is important in smoothing the short scale structure but should become unimportant in the infrared (in the absence of any critical points between weak and strong coupling). For type 1. we adopt the discrete form [16]

$$R_1 = \beta \sum_i \frac{1}{\Omega_i} \left(\sum_j^{n.n} (X_i - X_j) \right)^2 \tag{3.18}$$

where Ω_i is the union of the areas of triangles around vertex i and the inner sum runs over all nearest neighbours of i. The form for the type 2. rigidity term is taken to be [17,18,19]

$$R_2 = \beta \sum_{\langle ij \rangle} \left(1 - n_i^\alpha n_i^\beta \right) \tag{3.19}$$

where the unit normals n_i^α,n_i^β correspond to the normals to the two triangles bordered by each link $\langle ij \rangle$. Note that both of these terms are globally scale-invariant, so that the mean bond length a is determined only by the gaussian term.

In an attempt to try to attain some preliminary understanding of these discrete models we next discuss their mean-field solution. It will be seen that even at the level of mean-field theory, one can start to understand our Monte-Carlo results in terms of a difference in the effective action for the two models. This leads to the possibility of a zero mass-gap theory at some finite value of the curvature coupling for the type 2. form.

3.7 Mean Field Solutions

Here we examine some mean-field approaches to the discrete surface models described above. It is hoped that this will allow a qualitative picture of the phase diagram to be inferred. This may be then compared with the results from the simulations, both providing a check on these, and serving to test the validity of the mean-field approximation. It would be expected that at least some of the features of the mean-field solution survive. It will turn out that the suppression of fluctuations will become exact only in the limit $D \to \infty$. As all the work here is carried out in $D = 3$, we may well expect significant quantitative deviations. The treatment will truncate the full sum over all triangulations to only those which are approximately regular. In the continuum this might be viewed as a gauge-fixing of the metrical degrees of freedom. The consequence of summing over triangulations will be essentially unknown, but hopefully will not dramatically alter the conclusions. Certainly as $\beta \to \infty$ only locally flat (in the sense of their internal geometry) configurations contribute to the partition function, so in this limit the summation should become unimportant.

Firstly we consider the models with type 1. curvature. We argue that the partition function may be evaluated approximately by a saddle-point method, the resulting free energy may then be used to calculate mean values for the extrinsic curvature and specific heat as a function of β. We may also examine the propagator for the X fields within mean-field theory, and deduce the behaviour of the mean gyration radius for the surface in the limits $\beta = 0$ and $\beta \to \infty$. It will be seen that mean-field theory predicts no finite order phase transition between these limits. The same methods may then be applied to type 2. curvature actions, although crucial differences in the form of the effective action allow for the possibility of a phase transition at finite β.

3.7.1 Type 1.

Consider first models possessing type 1. extrinsic curvature. The action reads;

$$S = \mu^2 XQX + \beta R_1$$

where Q is the connection matrix (essentially the Laplacian operator) , and R_1 the extrinsic curvature

$$R_1 = \sum_i \frac{1}{\Omega_i} \left(\sum_j^{n.n(i)} (X_i - X_j) \right)^2 .$$

Add the Lagrange multiplier term, which fixes the length of the bond $\langle ij \rangle$ at l_{ij}

$$S_L = \sum_{i,j} i\lambda_{ij} \left[(X_i - X_j)^2 - l_{ij}^2 \right]$$

and integrate over the λ_{ij} and l_{ij} in order to recover the original partition function. At the mean field level all bond lengths become equal to some constant l, and all triangles are equilateral. If q is the coordination then;

$$\Omega_i = \frac{\sqrt{3}}{4} l^2 q.$$

Setting

$$\lambda_{ij} = \lambda \qquad l_{ij} = l$$

we have

$$Z = \int D\lambda Dl DX' e^{-S'}$$

where

$$\begin{aligned} S' &= S + S_L \\ &= XMX + \mu^2 3(N-\chi) l^2 - 3(N-\chi) i\lambda l^2. \end{aligned}$$

with

$$M = \left[i\lambda Q + \frac{4\beta}{\sqrt{3} l^2 q} Q^2 \right] \tag{3.20}$$

On integrating out the embedding coordinates, and setting $(N - \chi) \sim N$ we arrive at an effective action S_{eff} of the form;

$$S_{\text{eff}} = D/2 \,\text{Tr} \ln M + 3Nl^2\mu^2 - 3Ni\lambda l^2 \tag{3.21}$$

Since every term depends linearly on D, the validity of a subsequent saddle point expansion depends on $D \to \infty$ (note that we may compute l^2 straightforwardly from the mean of the gaussian term $l^2 = D/6\mu^2$). The interesting Tr term may be evaluated by first bringing the operator M to diagonal form. It then reads;

$$S_{\text{eff}} = D/2 \sum_{i=2}^{N} \ln \left(i\lambda e_i + \frac{4\beta}{\sqrt{3} l^2 q} e_i^2 \right).$$

In order to evaluate this sum, assume that the eigenvalues are distributed linearly from $O(1/N)$ to $2q$, where $q \sim 6$, the mean coordination.

$$e_i \sim \frac{2q}{N} i$$

As the number of vertices becomes large, with some fixed triangulation, replace the sum by an integral over the equivalent range. Carrying out the integrals, and dropping some constant terms we arrive at an expression for the effective action of the form;

$$\begin{aligned} S_{\text{eff}} =& 3Nl^2\mu^2 - 3Ni\lambda l^2 + \\ & \frac{D}{2} \left(\frac{\sqrt{3} l^2 N}{8\beta} \right) [(\delta + i\lambda) \ln (\delta + i\lambda) - (\delta + i\lambda) - \\ & (\gamma + i\lambda) \ln (\gamma + i\lambda) + (\gamma + i\lambda)]. \end{aligned}$$

where

$$\delta = \frac{8\beta}{\sqrt{3} l^2}, \qquad \gamma = \delta / N$$

Setting $\frac{\partial S_{\text{eff}}}{\partial \lambda} = 0$ at the saddle-point allows us to solve for λ

$$i\lambda = \frac{1}{(1 - e^{\kappa})} (e^{\kappa}\gamma - \delta)$$

$$\kappa = \frac{48\beta}{\sqrt{3} D}.$$

Using these values for λ and l^2 we may obtain an expression for the free energy in this approximation.

$$F = \frac{ND}{2} \left[1 + \ln \left(\mu^2 \kappa \frac{1}{(1 - e^{-\kappa})} \right) \right] \tag{3.22}$$

Here we have also dropped γ terms as they are of order $1/N$ relative to δ. To find the expectation value of the extrinsic curvature differentiate F with respect to κ. This leads to

$$\left(\frac{48}{\sqrt{3}D}\right)^{-1}\langle R_1\rangle = ND/2\left(1/\kappa - \frac{e^{-\kappa}}{(1-e^{-\kappa})}\right) \tag{3.23}$$

As $\kappa \to 0$ the extrinsic curvature approaches a constant (which we shall calculate next), whilst as $\kappa \to \infty$ it appears to approach zero. However this latter result is clearly wrong and comes from dropping the γe^{κ} term. For any finite N there will always be a point, as we increase κ, where the exponential wins out over the γ coefficient and it is incorrect to drop the term relative to δ. If this retained a piece, linear in β and independent of N is found in the free energy, giving a contribution to R as $\beta \to \infty$. However, in this limit it proves more convenient to calculate the extrinsic curvature in the continuum, by using its defining formula, assuming a regular sphere. This gives a value of 16π for R_1. To calculate the extrinsic curvature at $\beta = 0$ we may expand (3.23) in powers of κ. However it is also possible to determine this result by adding a source term coupling to QX in the partition function for the gaussian action.

$$Z = \int DX' e^{-XQX+JQX}$$

Thus

$$\langle R\rangle = \frac{1}{Z\Omega}\sum_i \frac{\partial^2}{\partial J_i^2} Z\left[J_i\right]|_{J_i=0}$$

Completing the square and doing the gaussian integrals allows us to write;

$$\begin{aligned}\langle R_1\rangle &= \frac{D}{2\Omega}\mathrm{TrQ};\\ &= \frac{D}{\Omega}3(N-\chi);\\ &= 4\sqrt{3}N.\end{aligned}$$

In this result we have set $\mu^2 = 1$, and $D = 3$. The variance of the extrinsic curvature is related to the specific heat [17]. Specifically we have

$$C = D/2 + \beta^2/N\left(\langle R^2\rangle - \langle R\rangle^2\right). \tag{3.24)}$$

Taking a second differential of F with respect to β gives a contribution as $\beta \to \infty$ of $ND/2$. Thus the total specific heat per site, including the contribution from the gaussian term (already calculated), as $\beta \to \infty$ is D.

Before we turn to type 2 terms, let us consider the propagator in the mean-field approximation

$$\left\langle X_i^\mu X_j^\nu \right\rangle = \delta_{\mu\nu} M_{ij}^{-1}$$

In order to evaluate this expression, consider the corresponding expression in the continuum, obtained by replacing the connection matrix by the Laplacian.

$$Q \sim \Delta$$

This may be diagonalised in k-space with the result;

$$M_{k,k'} = \delta_{k,k'} \left(-i\lambda k^2 + \frac{4\beta}{\sqrt{3}l^2} k^4 \right)$$

Using the mean-field values for l^2 and $i\lambda$ we obtain;

$$M_{k,k'} = \frac{24\beta\mu^2}{\sqrt{3}D} \left(-\frac{k^2}{1-e^\kappa} + k^4 \right) \delta_{k,k'}$$

Thus the expectation value of the mean gyration radius (the trace of the propagator) takes the form;

$$\left\langle X^2 \right\rangle = \kappa\mu^2 \int d^2k \frac{1}{k^4 - k^2/(1-e^\kappa)}$$

Putting $M^2 = 1/(e^\kappa - 1)$ then this may be written;

$$\left\langle X^2 \right\rangle = \frac{\kappa\mu^2}{M^2} \int d^2k \left(\frac{1}{k^2} - \frac{1}{k^2 + M^2} \right) \tag{3.25}$$

Thus the effective mass $M \to \infty$ as $\kappa \to 0$ – this corresponds to a crumpled surface with a vanishing correlation length for the normals to the surface. In this limit

$$\xi \sim \sqrt{\kappa}$$

In the continuum the propagator is dominated by the infrared singularity of a massless 2D field. On the lattice the lowest eigenvalue of the connection matrix is the important one;

$$\left\langle X^2 \right\rangle \sim \int_{1/N} d^2k/k^2 \sim \ln N$$

Thus we expect logarithmic scaling or infinite Hausdorff dimension. In the opposite limit as $\kappa \to \infty$ the propagator behaves like $1/k^4$, the effective mass $M^2 \to 0$ so that;

$$\xi \sim e^{\kappa/2}$$

Here

$$\langle X^2 \rangle \sim \int_{1/N} d^2k/k^4 \sim N$$

This the behaviour expected of smooth surfaces with Hausdorff dimension $d_H = 2$. We may calculate the mean gyration radius in the limits $\beta \to 0$ and $\beta \to \infty$, in order to compare to our measured values. For $\beta = 0$ then, using the results of Gross [5], we find;

$$\frac{\langle X^2 \rangle}{l^2 \ln N^2} \sim \frac{\sqrt{3}}{4\pi}.$$

This leads to

$$\langle X^2 \rangle \sim \frac{\sqrt{3}}{4\pi} \ln N$$

At the other limit $\beta \to \infty$, then, assuming a rigid sphere geometry, we have;

$$2(N - \chi)\frac{\sqrt{3}}{4} l^2 = 4\pi \langle X^2 \rangle$$

So

$$\langle X^2 \rangle = (N - \chi)\frac{\sqrt{3}}{16\pi}. \tag{3.26}$$

Note that mean-field predicts no finite order phase transition between the limits $\kappa \to 0$ and $\kappa \to \infty$. The first corresponds to a scale invariant I.R stable fixed point with vanishing correlation length. The second to a U.V stable fixed point with infinite correlation length. Physically one there appears to be a smooth evolution between crumpled and smooth surfaces as we move from large to short distance scales.

3.7.2 Type 2.

Now let us turn our attention to the type 2. extrinsic curvature term. Consider the expression for the dot product between normals to triangles in the mean-field approximation. Using elementary vector algebra this can be cast into the alternative form;

$$n_i.n_j = \frac{(w.v)(v.u) - v^2(w.u)}{uwv^2 \sin^2 \pi/3}$$

where the neighbouring normals n_i, n_j are formed from triangles whose sides are given by the vectors u, v, w. Calling the angle between the non-adjacent vectors u, w by α we obtain in this limit;

$$R_2 = \sum_{\text{links } \langle ij \rangle} \frac{2}{3}(1 + 2\cos\alpha) \tag{3.27}$$

The angle α varies in the range $0 \rightarrow 2\pi/3$. The limit $\alpha = 2\pi/3$ corresponds to neighbouring triangles being coplanar and minimises the extrinsic curvature term. If k, l label the vertices of the complementary link to $\langle ij \rangle$, then this becomes;

$$\frac{1}{2l^2} \sum_i \sum_j^{n.n(i)} (X_i^2 - 2X_i.X_j + X_k.X_l) \tag{3.28}$$

Thus the curvature part of the action contains the term XPX and the total quadratic operator becomes now

$$M' = i\lambda Q + \frac{\beta}{2l^2} P$$

The expression (3.28) is to be compared with the analogous expression for type 1.;

$$\frac{4}{\sqrt{3}l^2 q} \sum_i q_i \sum_j \left(X_i^2 - 2X_i.X_j + 1/q_i \sum_l X_l.X_j \right) \tag{3.29}$$

where the sum on l runs over all nearest neighbours to i, and the corresponding operator to P is simply Q^2. The difference at the level of mean-field theory between the two operators lies in the last term. When the X coordinates are integrated out, we are left with an effective action which involves the term

$$D/2 \text{ Tr } \ln M'$$

Contrast this with M for type 1. The operator M contains two terms– M interpolates between the Laplacian term at $\beta = 0$ and its square as $\beta \to \infty$. The resultant operator is always positive definite at all β and the eigenvalue spectrum evolves smoothly between the two limits. For type 2. however the picture is different. Here M' contains the Laplacian term at $\beta = 0$ and a new operator, say P, which dominates as $\beta \to \infty$. This is not positive definite. It may thus possess negative eigenvalues. At intermediate β there will, in general, be at least one point where an eigenvalue goes through zero – leading to the possibility of a phase transition. As we shall show, such a phase transition is indeed seen in the Monte-Carlo results.

It is difficult to develop the mean-field solution further in the absence of explicit knowledge of the eigenvalue spectrum at general β of M'. Note that we can no longer simultaneously diagonalise the two operators composing M'. However we can calculate R_2 in the two limits $\beta \to 0$ and $\beta \to \infty$. In the absence of extrinsic curvature the angle α can be expected to vary uniformly in the range $0 \to 2\pi/3$. Thus we may calculate R_2 as

$$\langle R_2 \rangle = \sum_{ij} \frac{2}{3} (1 + \langle \cos \alpha \rangle)$$

This leads to $R_2 = 3.6N$ at $\beta = 0$. In the opposite limit, we may calculate R by simple geometrical considerations from the defining formula. We expect asymptotically $(\beta \to \infty)$;

$$R_2 = \pi (\pi + 2)$$

The asymptotic form of the specific heat can be estimated by the following argument. In $D = 3$, the dominance of the curvature term as $\beta \to \infty$ allows only coherent fluctuations of the 2D surface. It effectively restricts the geometry to the remaining one dimension. Thus by simple equipartition this term gives an asymptotic contribution to the specific heat per site of $1/2$.

This concludes that portion of the work concerned with the analytic solution of the models. In order to test which features of the mean-field solutions survive at small D, we have employed simulation techniques.

Figure 3.7. $\langle R_2 \rangle$ *on lattices with N=48(+),N=72(×), N=96(◇), and N=144(○) sites. Mean-field predictions are also shown at* $\beta = 0$ *and* $\beta \to \infty$.

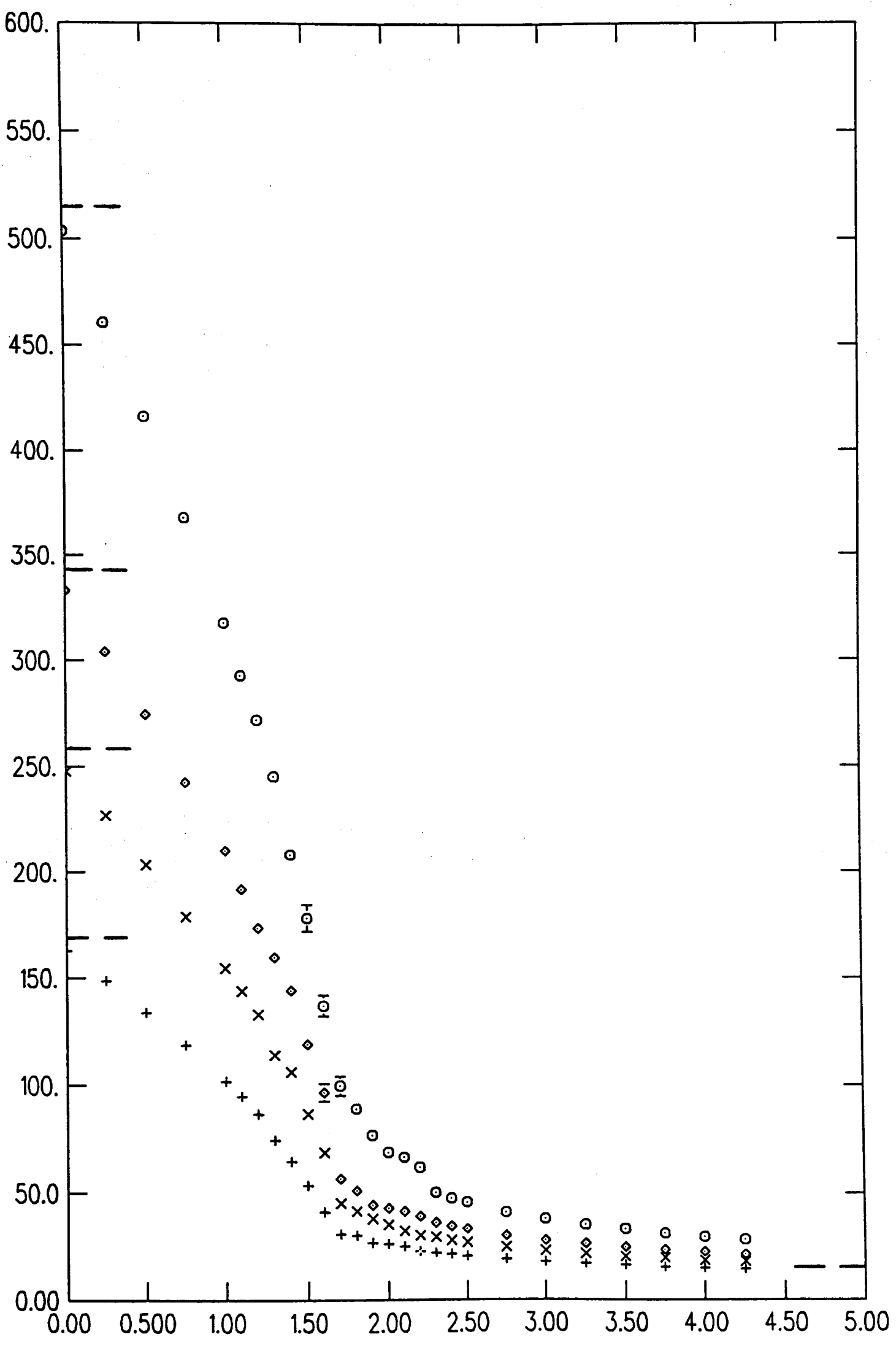

3.8 Results and Discussion

In this section we examine the results of the Monte-Carlo simulations for both forms of extrinsic curvature.

3.8.1 Type 2.

In fig.(3.7) we show the mean extrinsic curvature $\langle R_2 \rangle$, measured on lattices with $N = 48(+)$, $N = 72(\times)$, $N = 96(\diamond)$, $N = 144(\circ)$ sites. The curves show no sign of a discontinuity out to large β, where they approach the continuum rigid sphere result. As $\beta \to 0$ they agree fairly closely with the mean-field prediction, which is reassuring. Clearly then, there are no first order transitions in the model, but notice that the gradient is changing rapidly in the vicinity of $\beta \sim 1.5$.

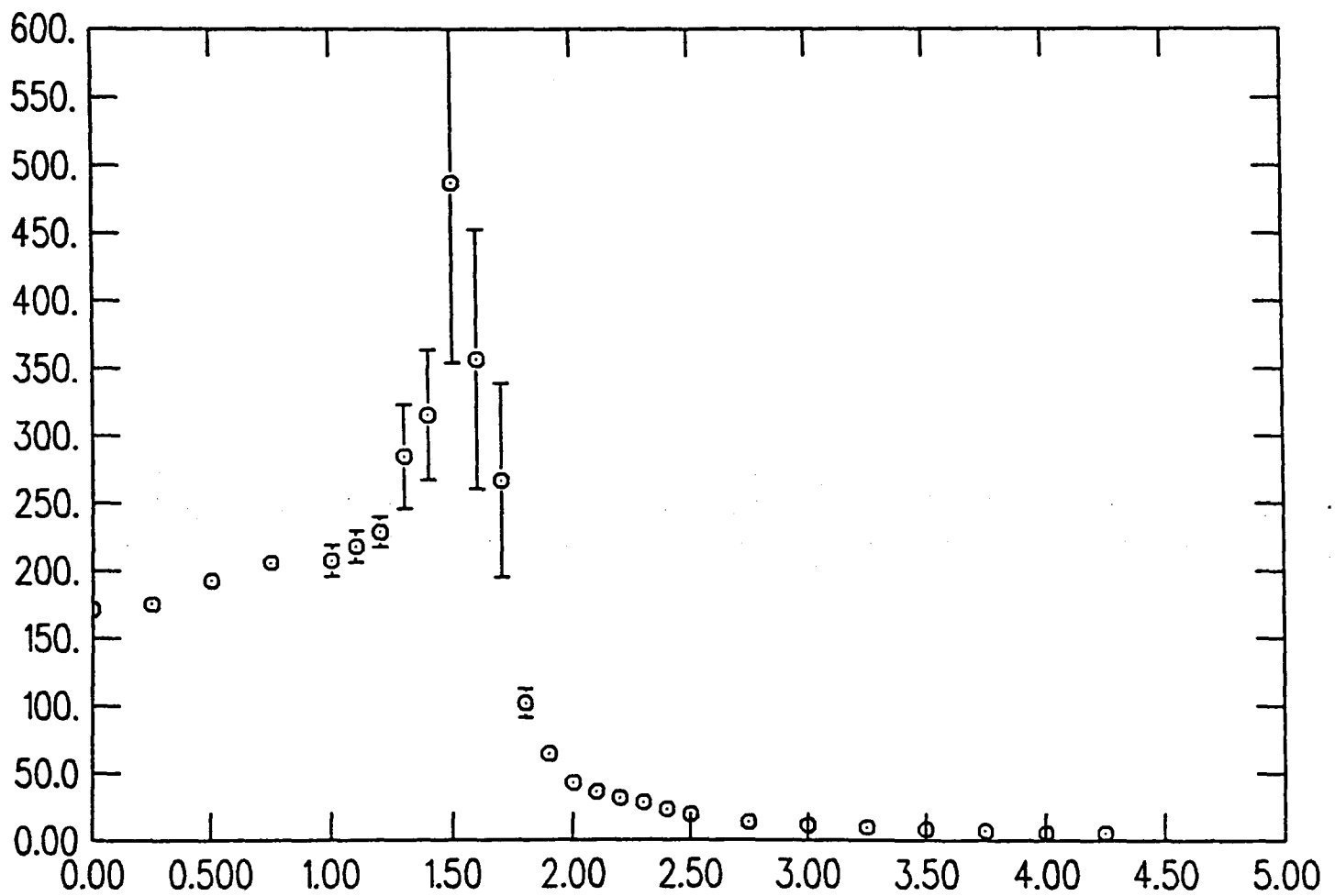

Figure 3.8. $\langle \frac{\partial R_2}{\partial \beta} \rangle$ *for N=144 sites.*

Indeed fig.(3.8) shows that the variance of the extrinsic curvature $\langle \frac{\partial R_2}{\partial \beta} \rangle$ for

Figure 3.9. $C - D/2$ for type 2. models with N=72.

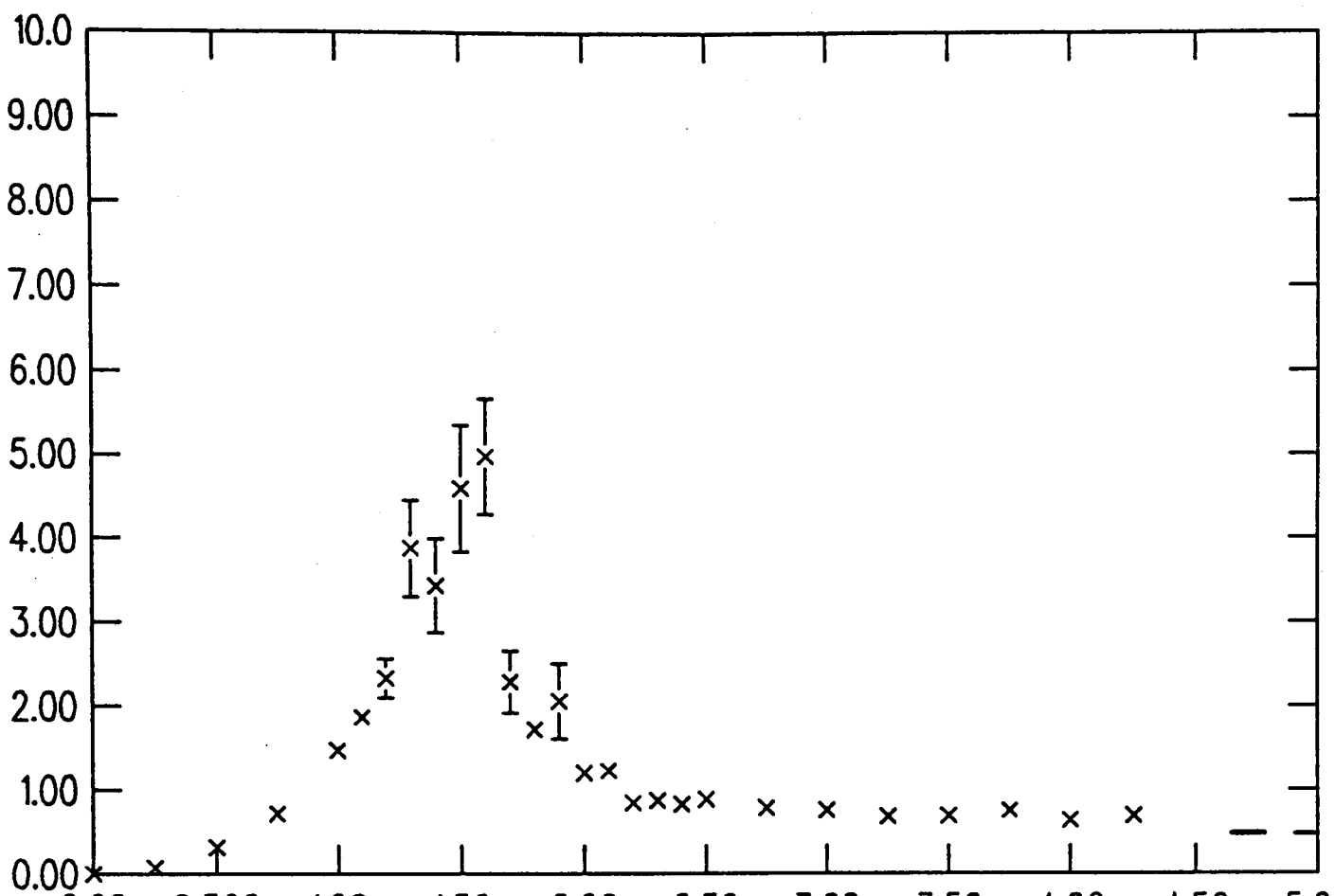

Figure 3.10. $C - d/2$ for type 2. models with N=96.

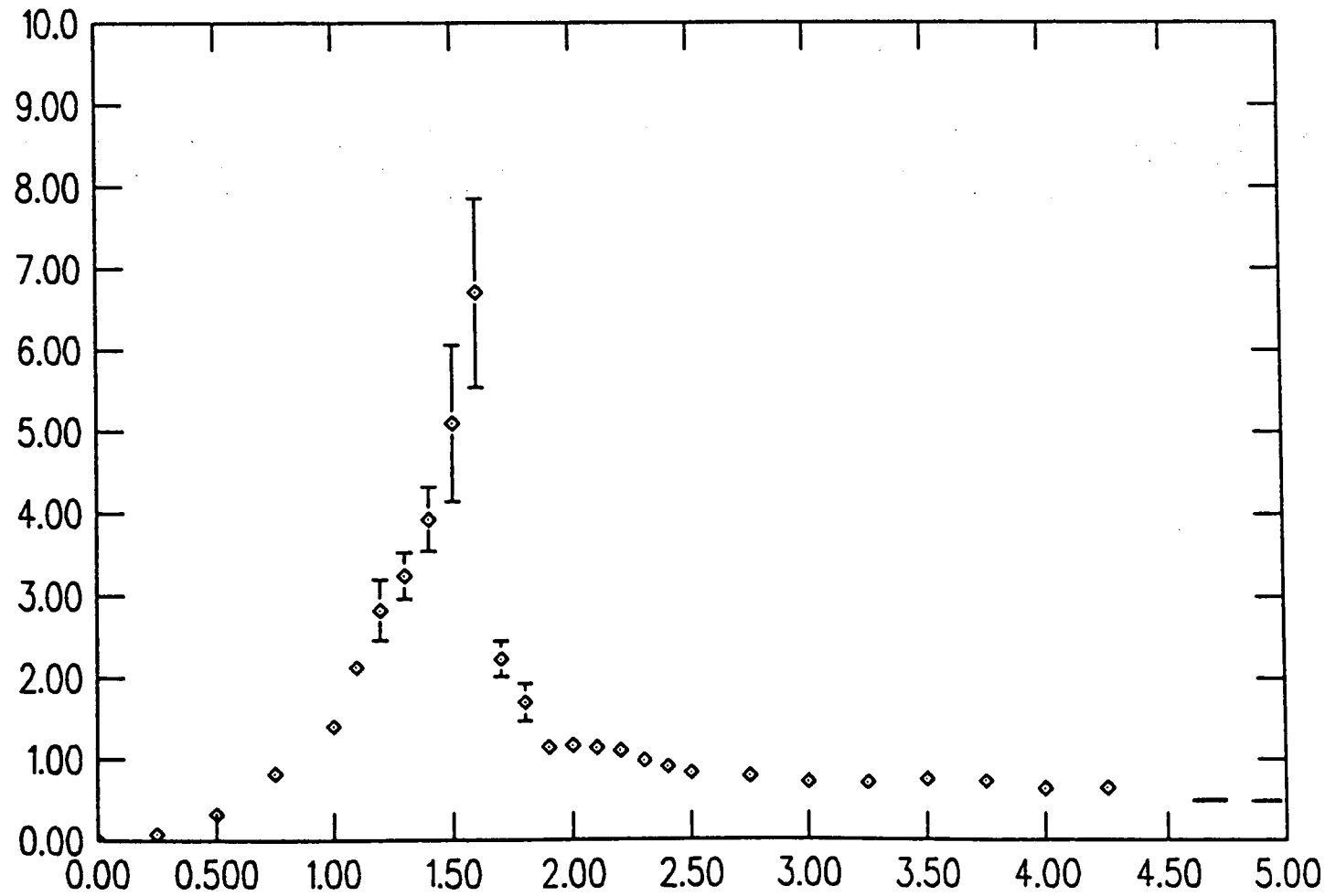

$N = 144(o)$, possesses a strong peak at this point, indicating a possible second order transition there. This result is in agreement with the findings of Kantor and Nelson [19]. They considered models of tethered surfaces of fixed connectivity with a square well potential between lattice sites and a type 2. rigidity term. They found a second order phase transition in the model. This crumpling transition, as it has come to be called, would constitute a new zero of the β- function and a point of at least global scale invariance.

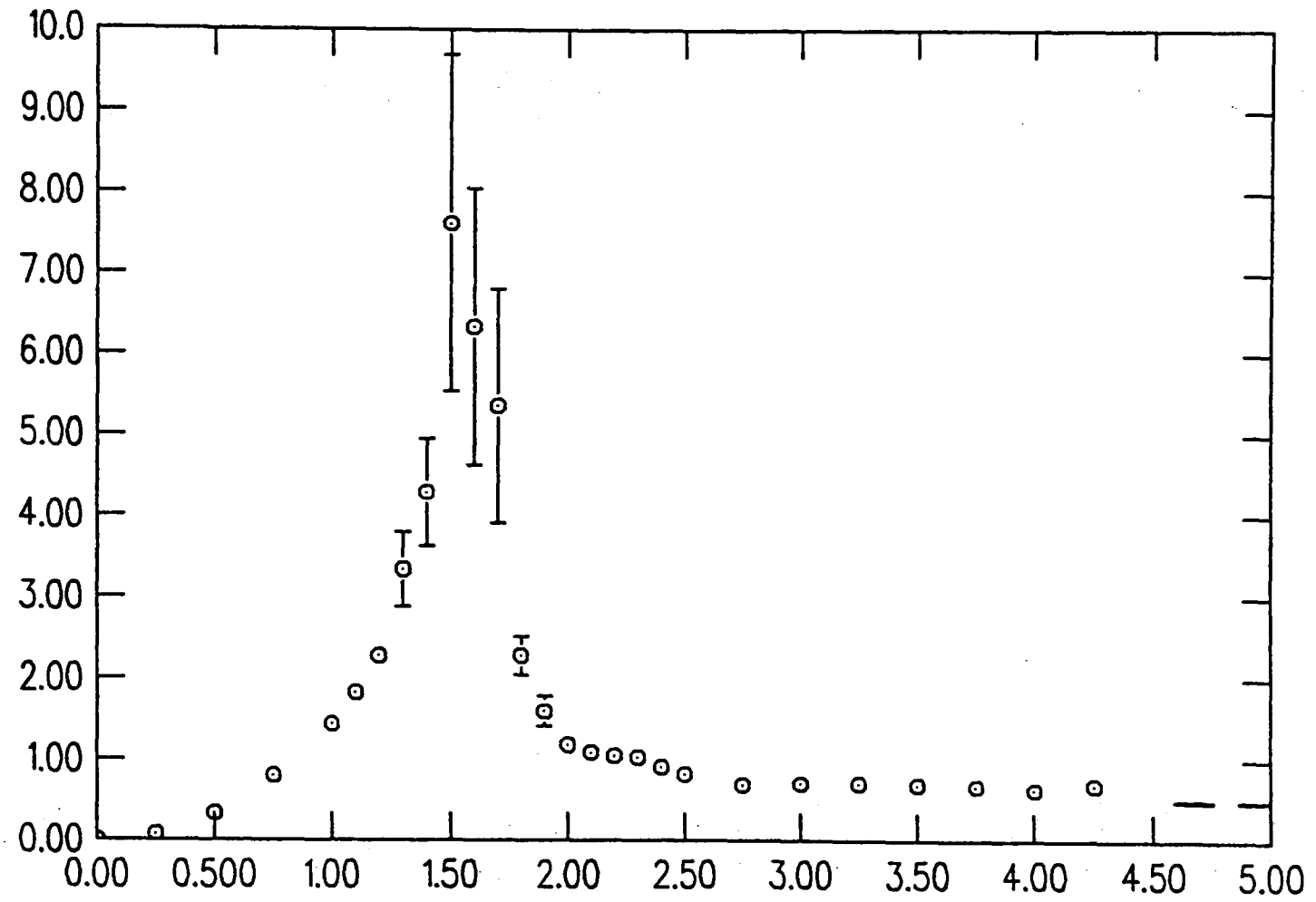

Figure 3.11. $C - D/2$ for type 2. models with N=144.

We examined the specific heat (3.24) in figs.(3.9-3.11) on $N = 72(\times)$, $N = 96(\diamond)$, and $N = 144(o)$ site lattices. A strong peak is seen, with height increasing with system size, at $\beta \sim 1.5$, confirming the presence of a second order phase transition. Note that as $\beta \to \infty$ the specific heat falls again to approach the mean-field result. The effect of summing over triangulations of the surface and employing

a gaussian action, apparently has not changed the critical behaviour of the type 2 term. We checked that increasing f (the link to vertex updating frequency) by an order of magnitude does not wash out the transition. The peak height remains constant, whilst the width increases only marginally. This latter observation is merely a consequence of the fact that the critical coupling will, in general, depend on triangulation. Hence one expects a smearing effect when one sums over all possible triangulations.

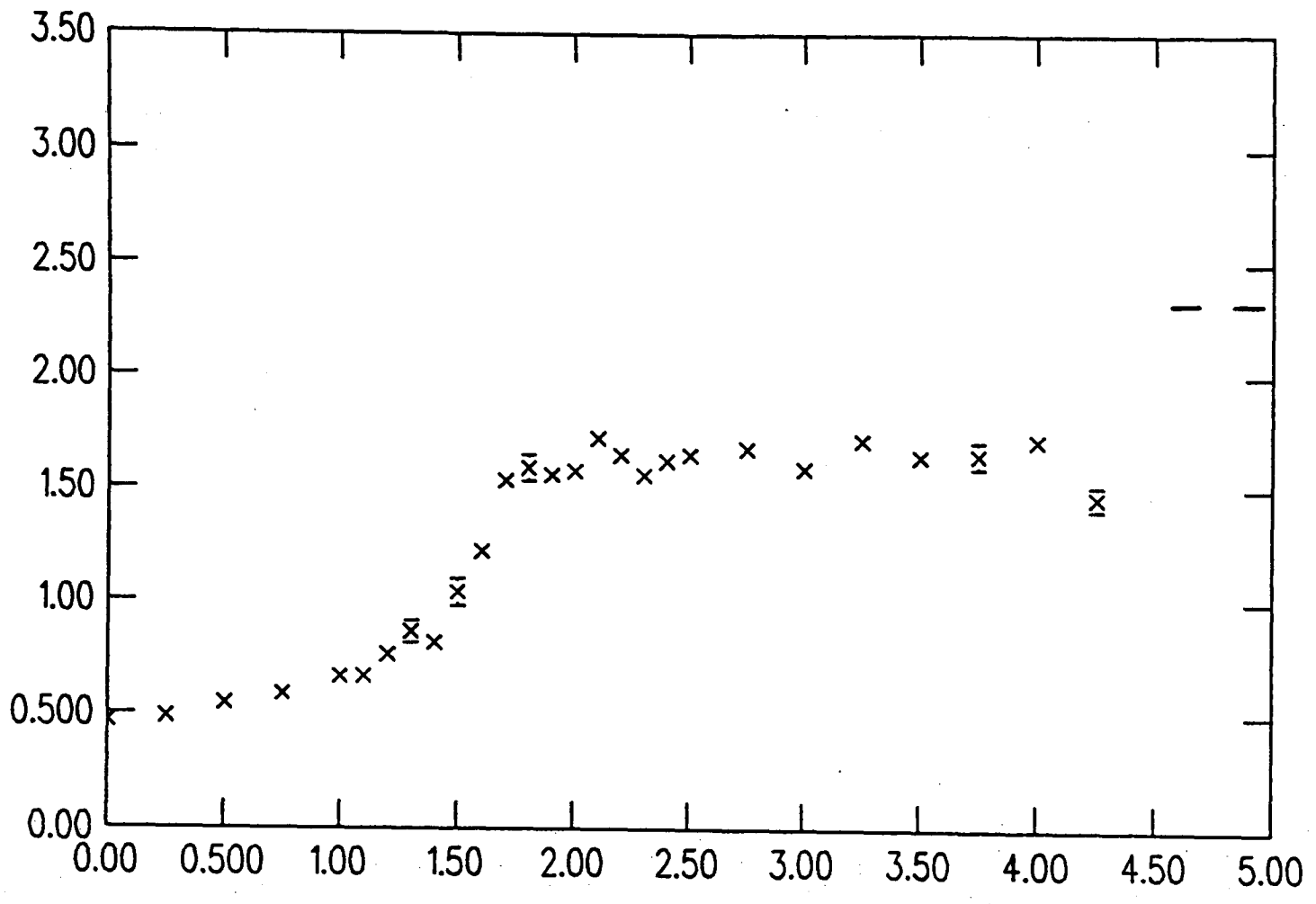

Figure 3.12. $\langle X^2 \rangle$ *vs* β *for type 2. with N=72.*

In figs.(3.12-3.14) the mean square gyration radius is shown as a function of β for the three lattice sizes $N = 72(\times)$, $N = 96(\diamond)$, $N = 144(\circ)$. Two distinct regimes are seen. From $\beta \sim 2.0$ onwards, the curves are essentially flat and correspond to a dominant contribution of smooth surfaces, whilst for $\beta \leq 1.0$ $\langle X^2 \rangle$ falls smoothly to its value at zero coupling. The transition between these two regimes is increas-

Figure 3.13. $\langle X^2 \rangle$ *vs* β *for type 2. with* $N=96$.

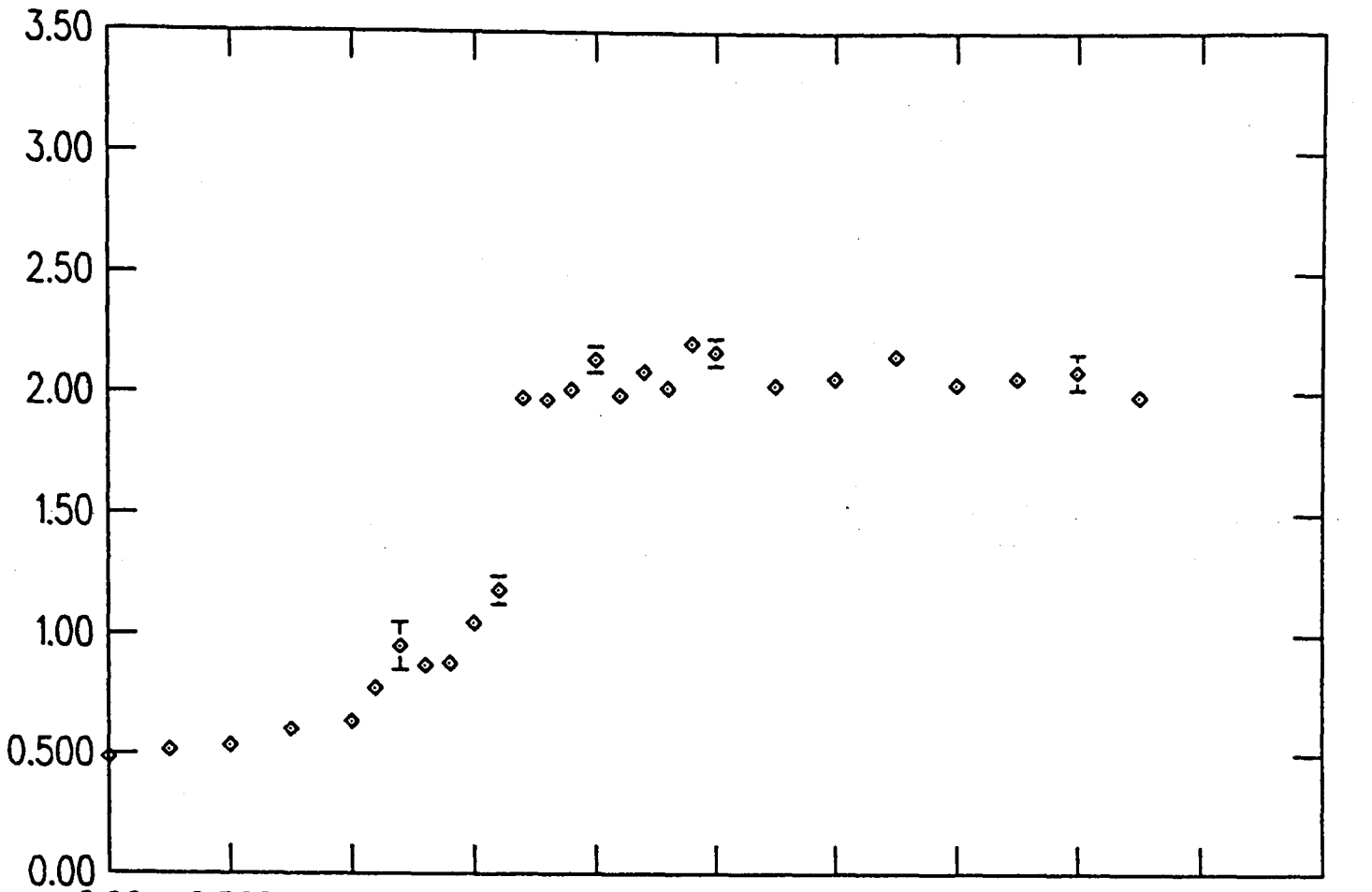

Figure 3.14. $\langle X^2 \rangle$ *vs* β *for type 2. with* $N=144$.

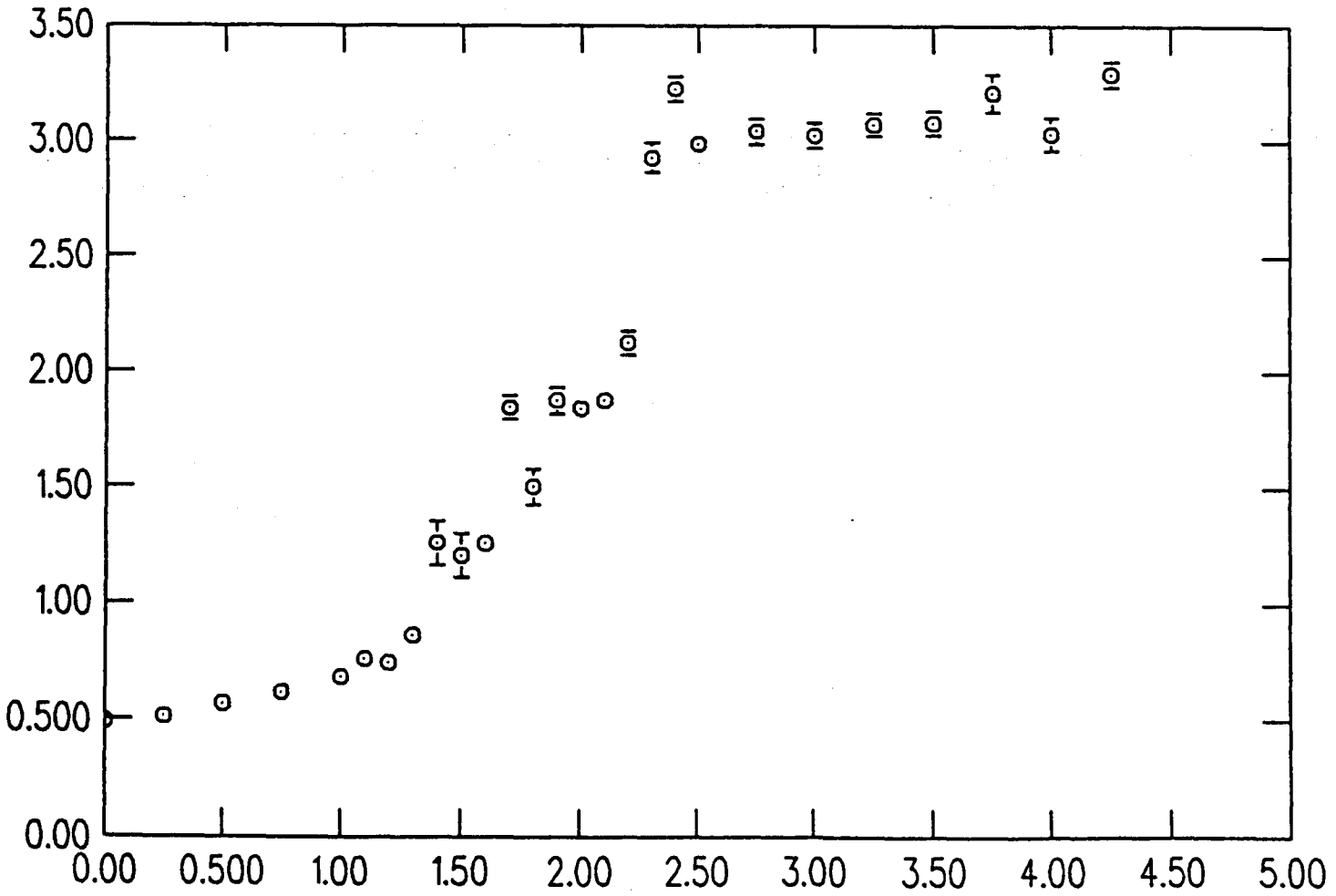

ingly abrupt as N increases, which is presumably due to the presence of the phase transition. Asymptotically $\langle X^2 \rangle$ scales like N, but its absolute value is significantly different from the rigid sphere prediction. It is possible that much larger β are needed in order for this to approach its asymptotic value. Alternatively it may be evidence for a significant renormalisation of the bare string tension in the smooth phase. Finally in fig. (3.15) we present a scatter plot of the inverse Hausdorff dimension vs β which summarises these conclusions. Notice that there appears to a fairly rapid transition from scaling behaviour characterised by $d_h \sim O(10)$, to one which possesses a d_H close to 2.

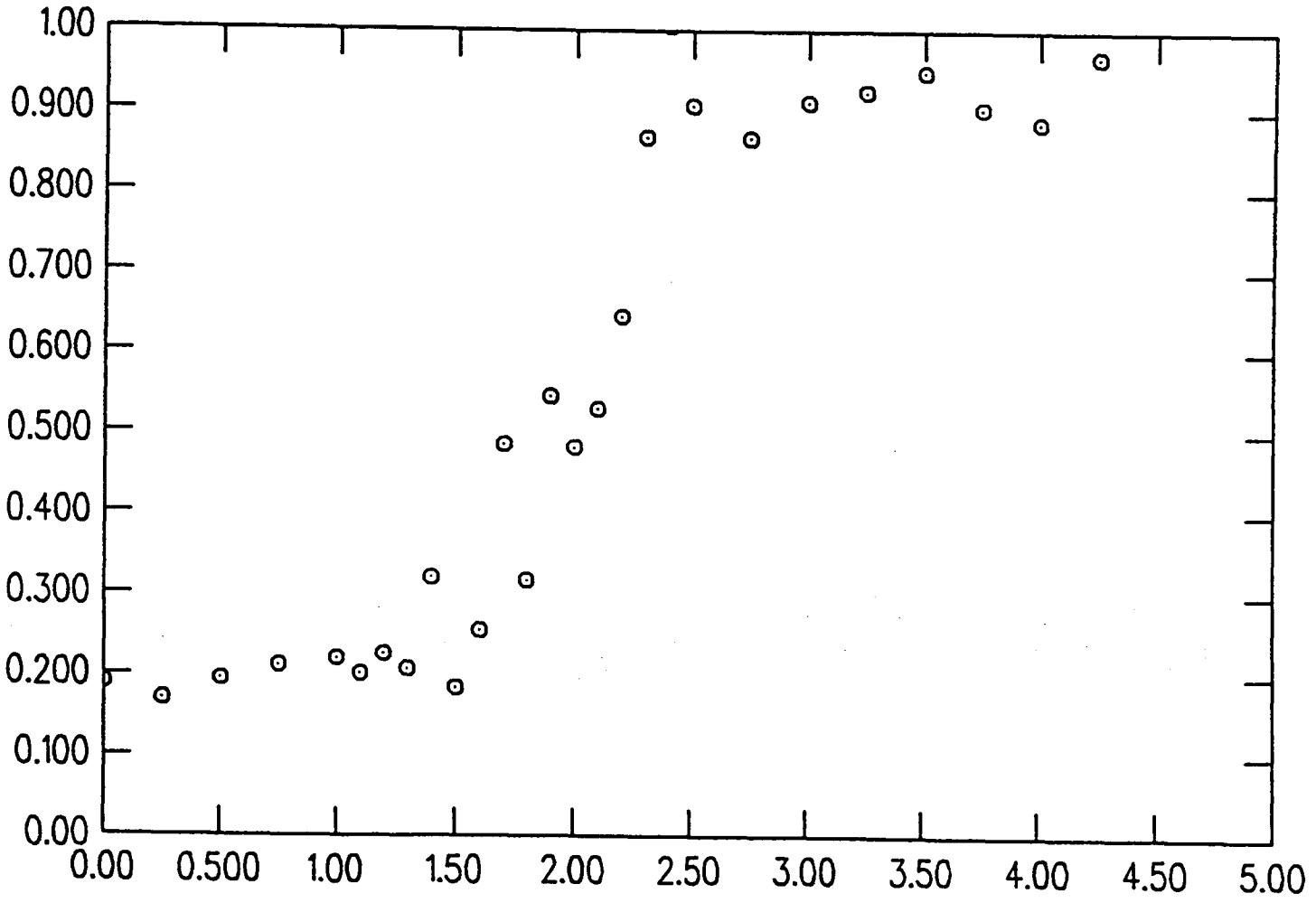

Figure 3.15. Scatter plot of $2/d_H$ vs β for type 2. models.

Figure 3.16. $\langle R_1 \rangle$ *vs* β *for lattices N=48(+), N=72(×), N=96(◇), and N=144(○) with mean-field limits.*

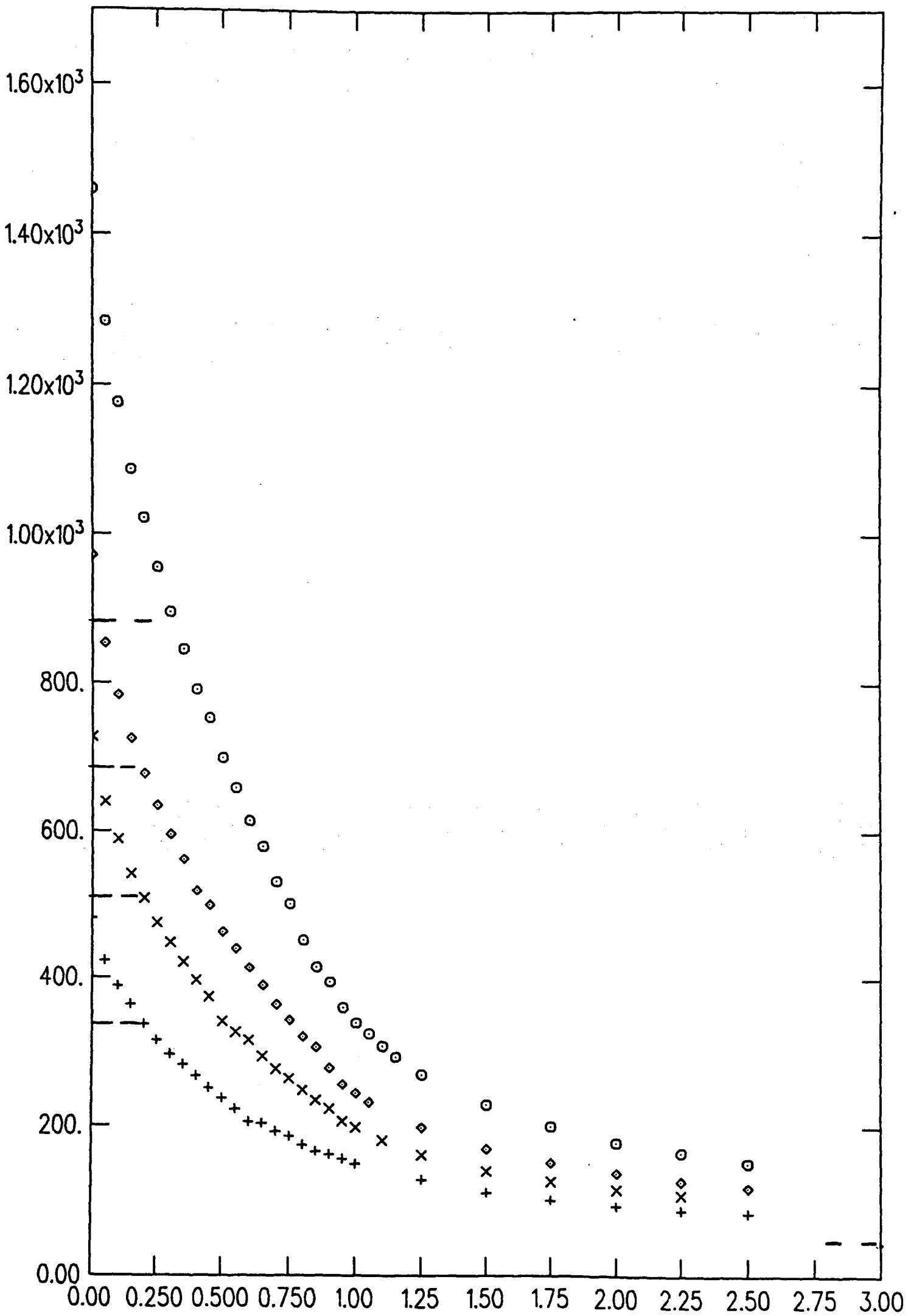

3.8.2 Type 1.

The situation for the type 1. case is markedly different. In fig.(3.16) we show the mean extrinsic curvature $\langle R_1 \rangle$ vs β for the same four system sizes $N = 48(+)$, $N = 72(\times)$, $N = 96(\diamond)$, $N = 144$ (o). A smooth decrease to approach the continuum result as $\beta \to \infty$ is seen, indicating as before the absence of any first order transitions. At $\beta = 0$ we see that there is substantial renormalisation of the mean-field predictions, which is not altogether surprising in such small dimension.

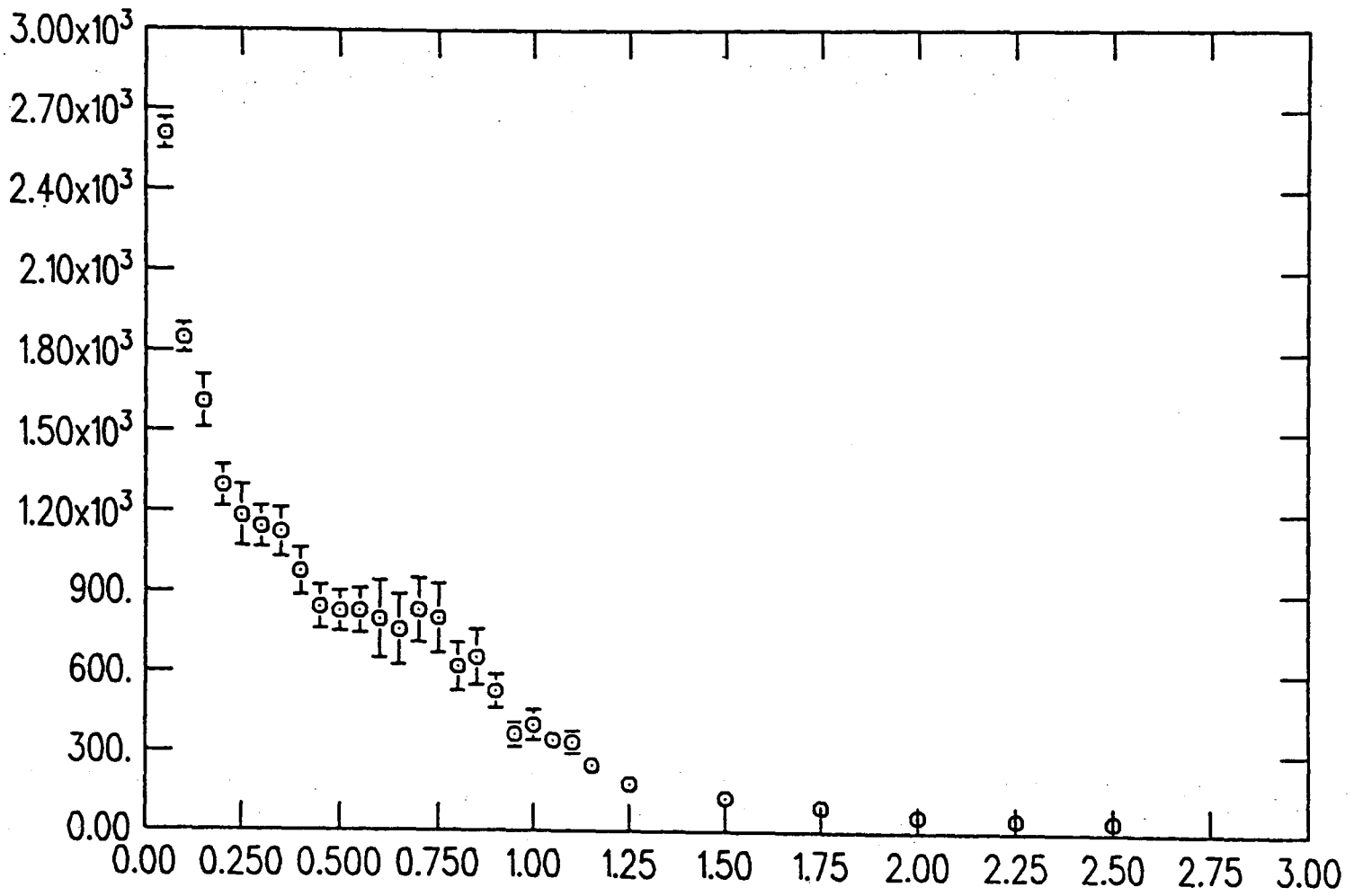

Figure 3.17. $\langle \frac{\partial R_1}{\partial \beta} \rangle$ *for N=144.*

When the variance $\langle \frac{\partial R_1}{\partial \beta} \rangle$ is examined (fig.(3.17),$N = 144$(o))there is now no peak in the curve at finite β. However we notice a slight plateauing around $\beta \sim 0.5 \to 0.8$ which may indicate the presence of some interesting physics (a higher order transition).

In order to clarify the situation we examined the specific heat, $C - D/2$. The

Figure 3.18. Specific Heat $C - D/2$ with mean-field limit $\beta \to \infty$ for N=72.

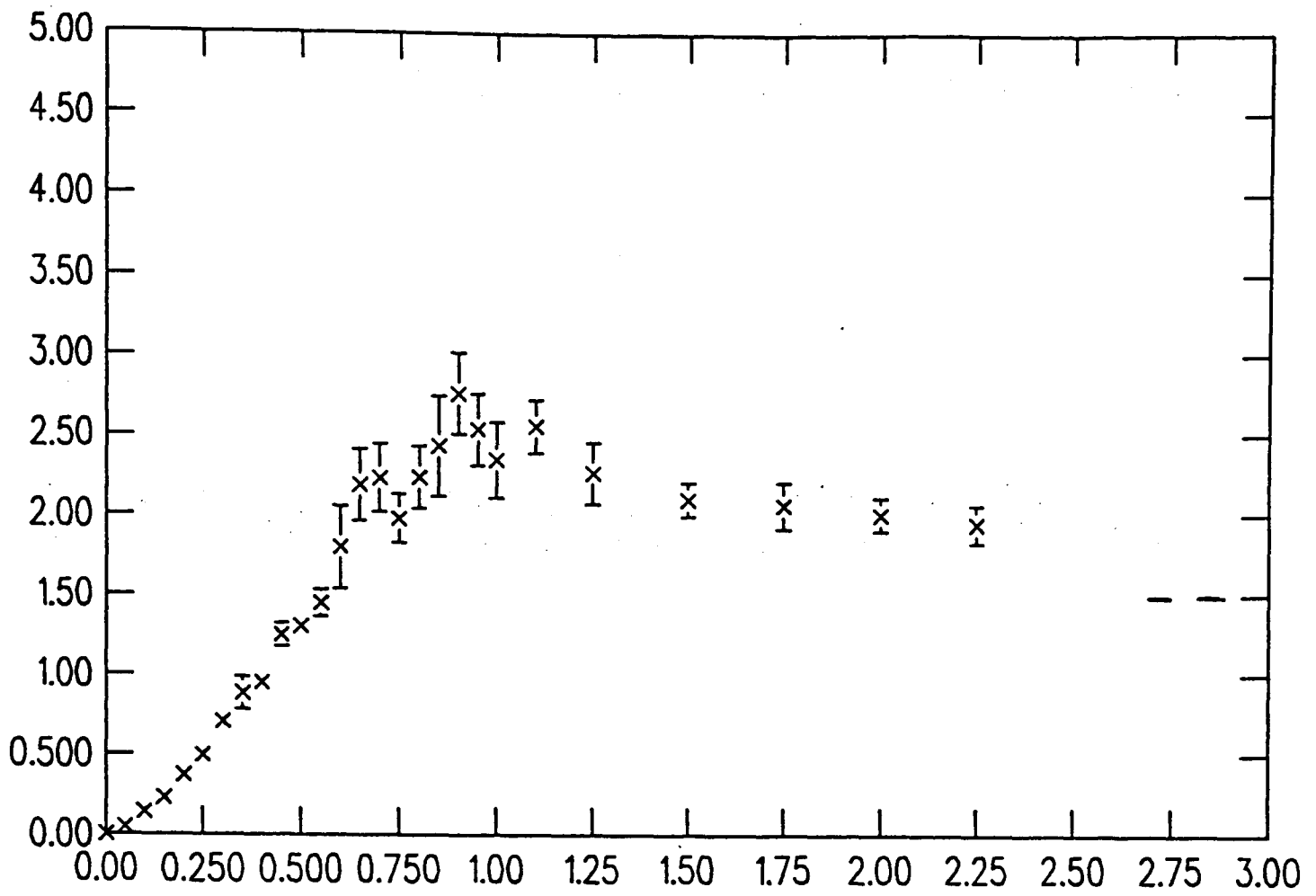

Figure 3.19. $C - D/2$ for N=96.

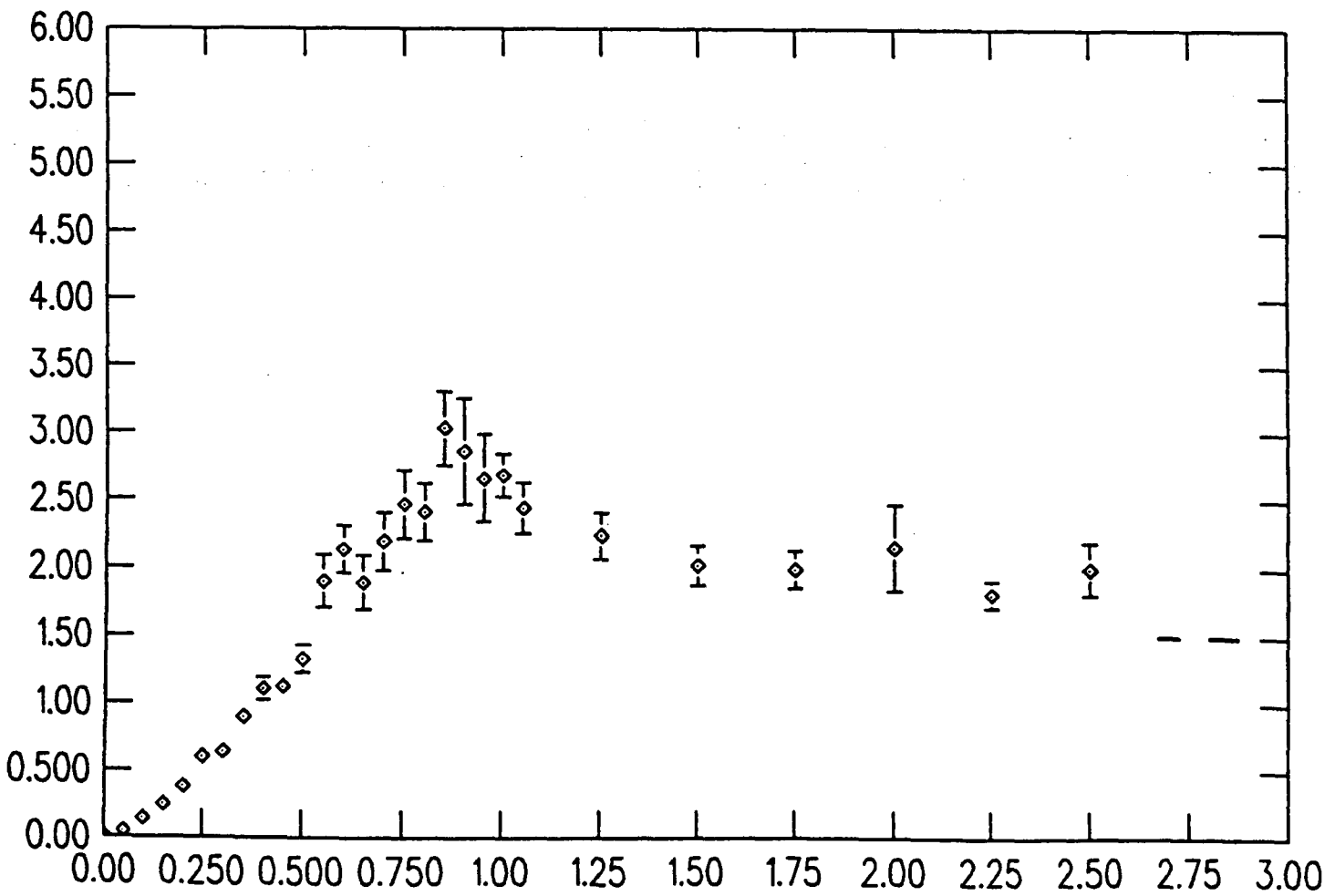

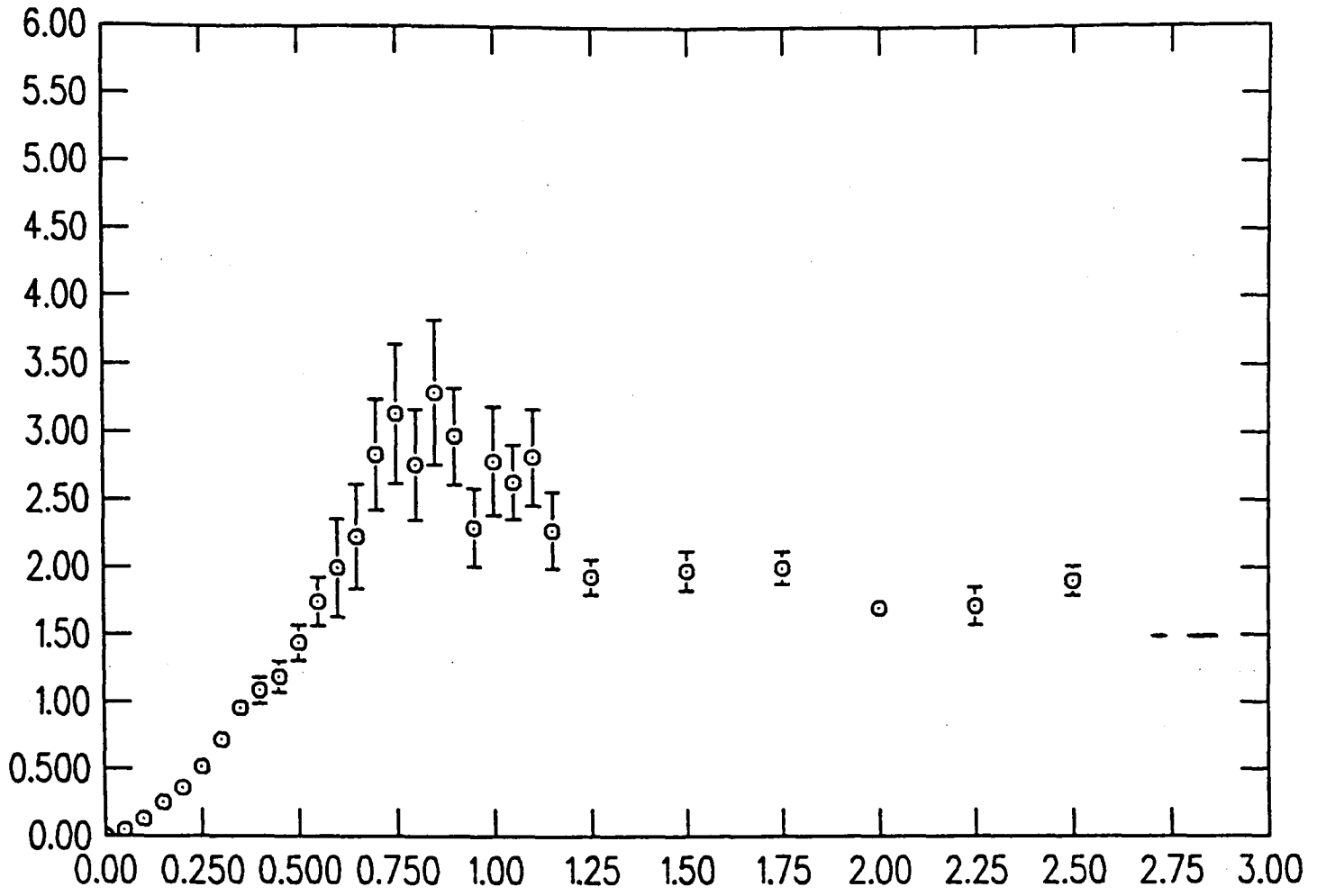

Figure 3.20. $C - D/2$ for N=144.

data for lattices $N = 72(\times)$, $N = 96(\diamond)$, and $N = 144(\circ)$ is shown in figs.(3.18-3.20). A prominent bump or cusp is visible around $\beta \sim 0.7$, whose height is constant as we vary the number of sites. This is strongly reminiscent of a third order phase transition. Again this result is compatible with other Monte-Carlo results by J.F.Wheater et al. [17], who considered a fixed triangulation model with this form of extrinsic curvature. They discovered a probable third order transition in the vicinity of which there was a rapid, but finite, increase of the correlation length. Thus, although we have discovered a possible phase transition of a high order (a rarity in itself), it appears there is no new zero of the β-function here, and hence the long-distance physics of such a model is governed by the gaussian term.

Finally the mean gyration radius $\langle X^2 \rangle$ is shown for all the lattices ($N = 72$, $N = 96$, $N = 144$) in figs. (3.21-3.23). It shows a much smoother (relative to

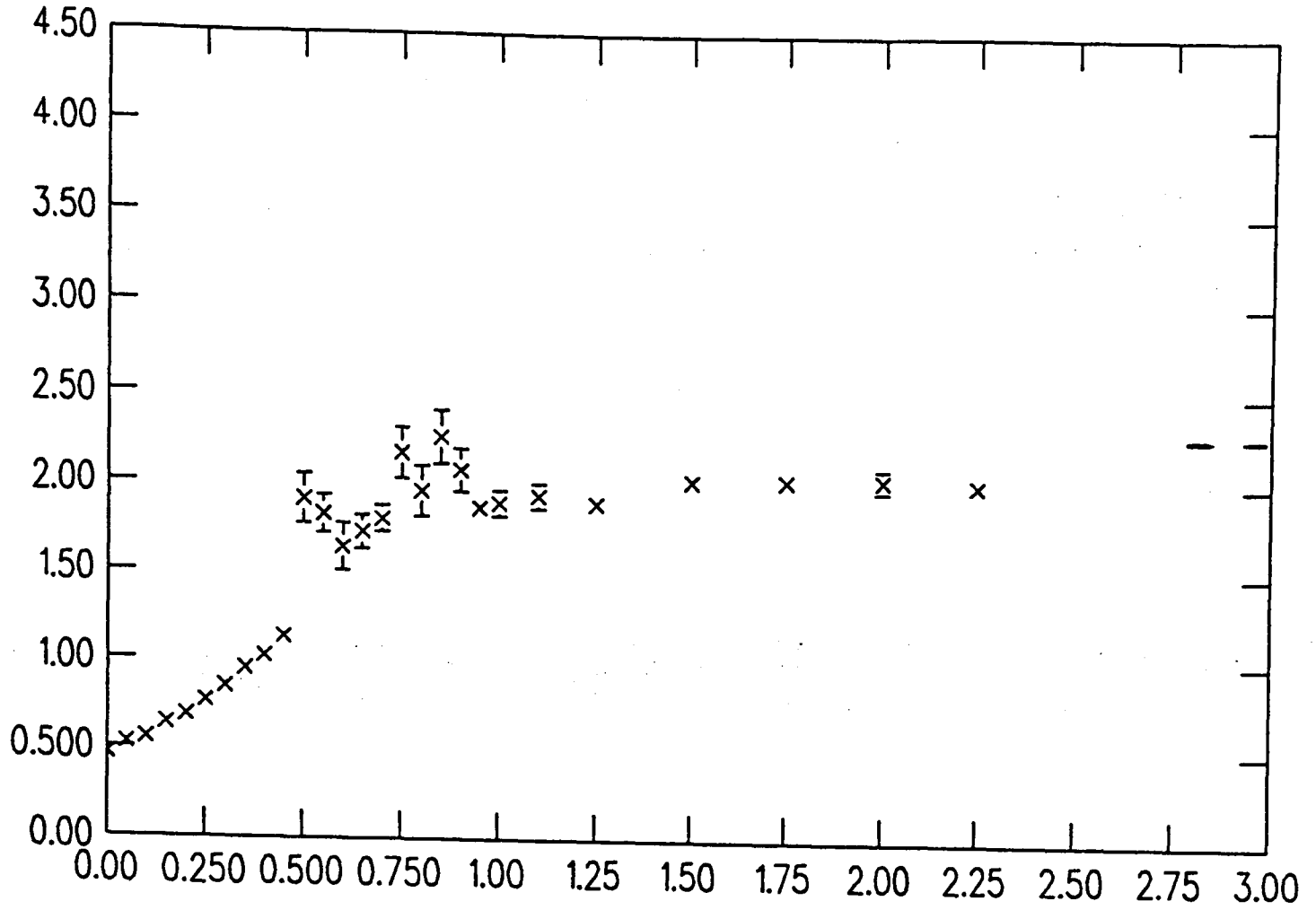

Figure 3.21. $\langle X^2 \rangle$ *vs* β *for type 1. with* $N=72$.

type 1.) evolution to asymptotic values close to those predicted on the rigid sphere model. It is not clear whether the oscillations, evident near $\beta \sim 0.7$ on the smaller lattices, are merely finite size effects, or signals for a rapidly decreasing mass gap at the third order transition. The scatter plot fig.(3.24). shows the inverse Hausdorff dimension $2/d_H$ increasing smoothly from ~ 0.2 to values close to unity.

Fig.(3.25). shows a plot of the naive order parameter $\langle n.n \rangle$ vs β for the largest system $N = 144$. The data indicate a continuous evolution to the asymptotic, smooth sphere result. The slight increase in the size of the error bars at intermediate β may again be signalling the presence of the larger fluctuations associated with a higher order crumpling transition.

Figure 3.22. $\langle X^2 \rangle$ *vs* β *for type 1. with* $N=96$.

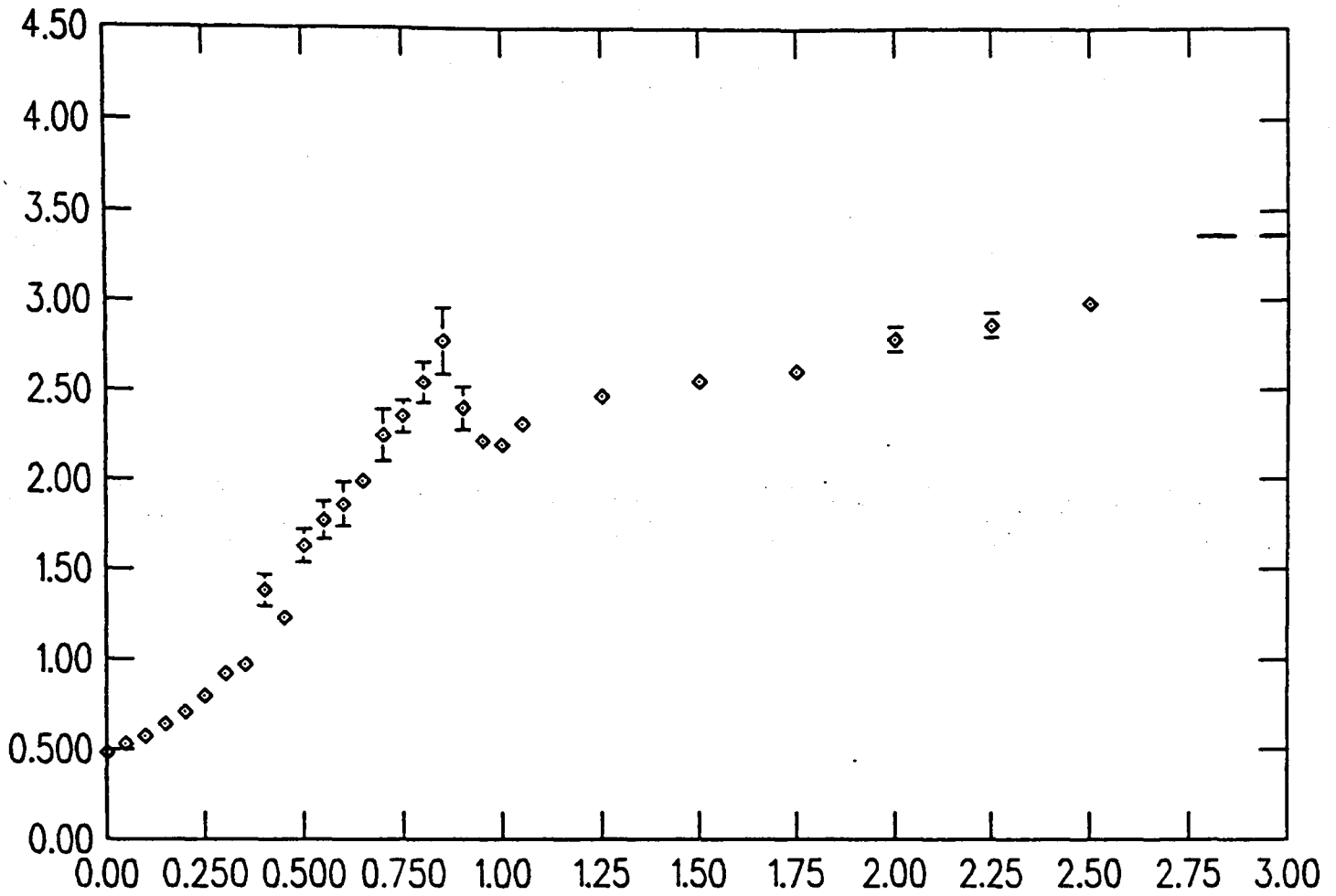

Figure 3.23. $\langle X^2 \rangle$ *vs* β *for type 1. with* $N=144$.

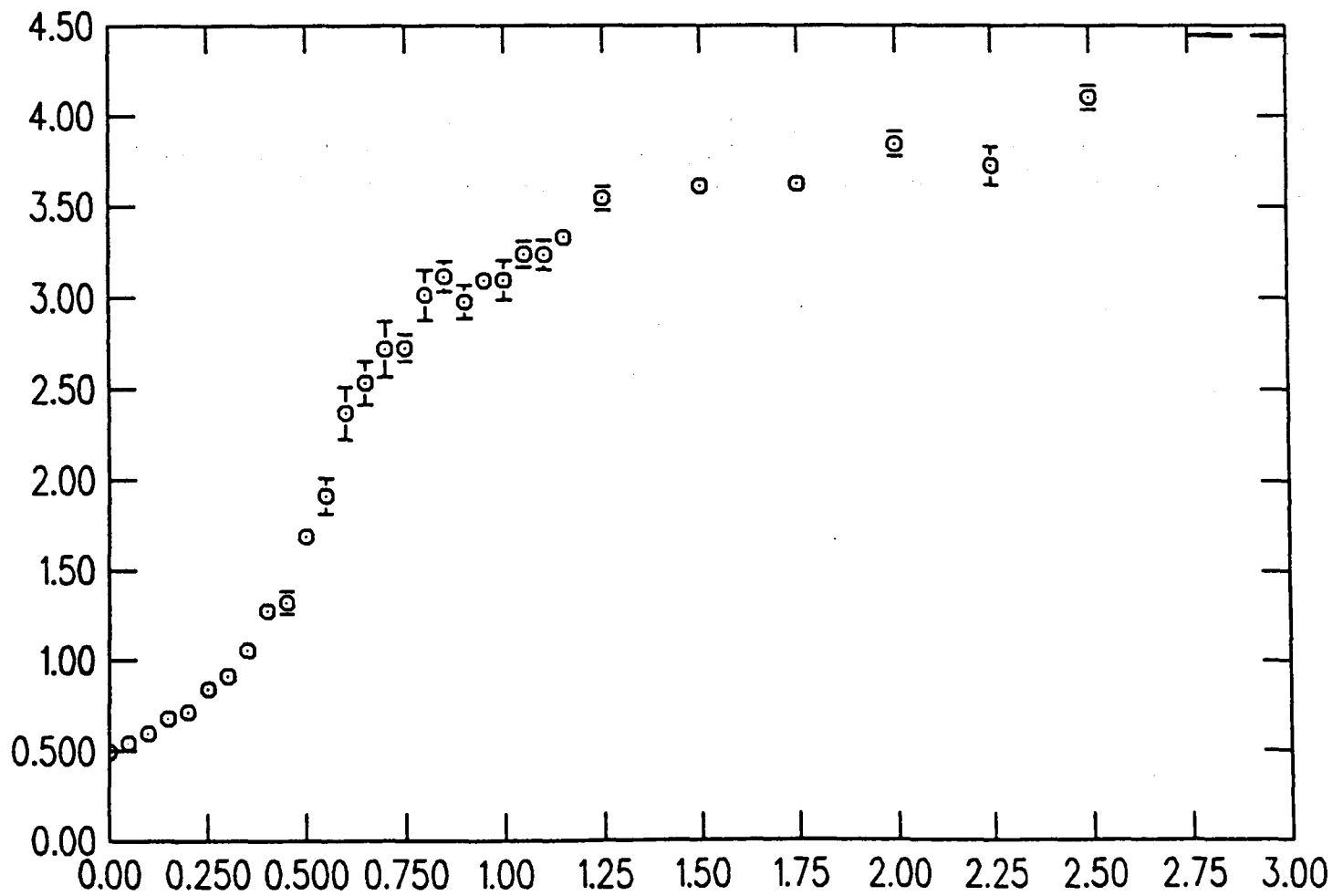

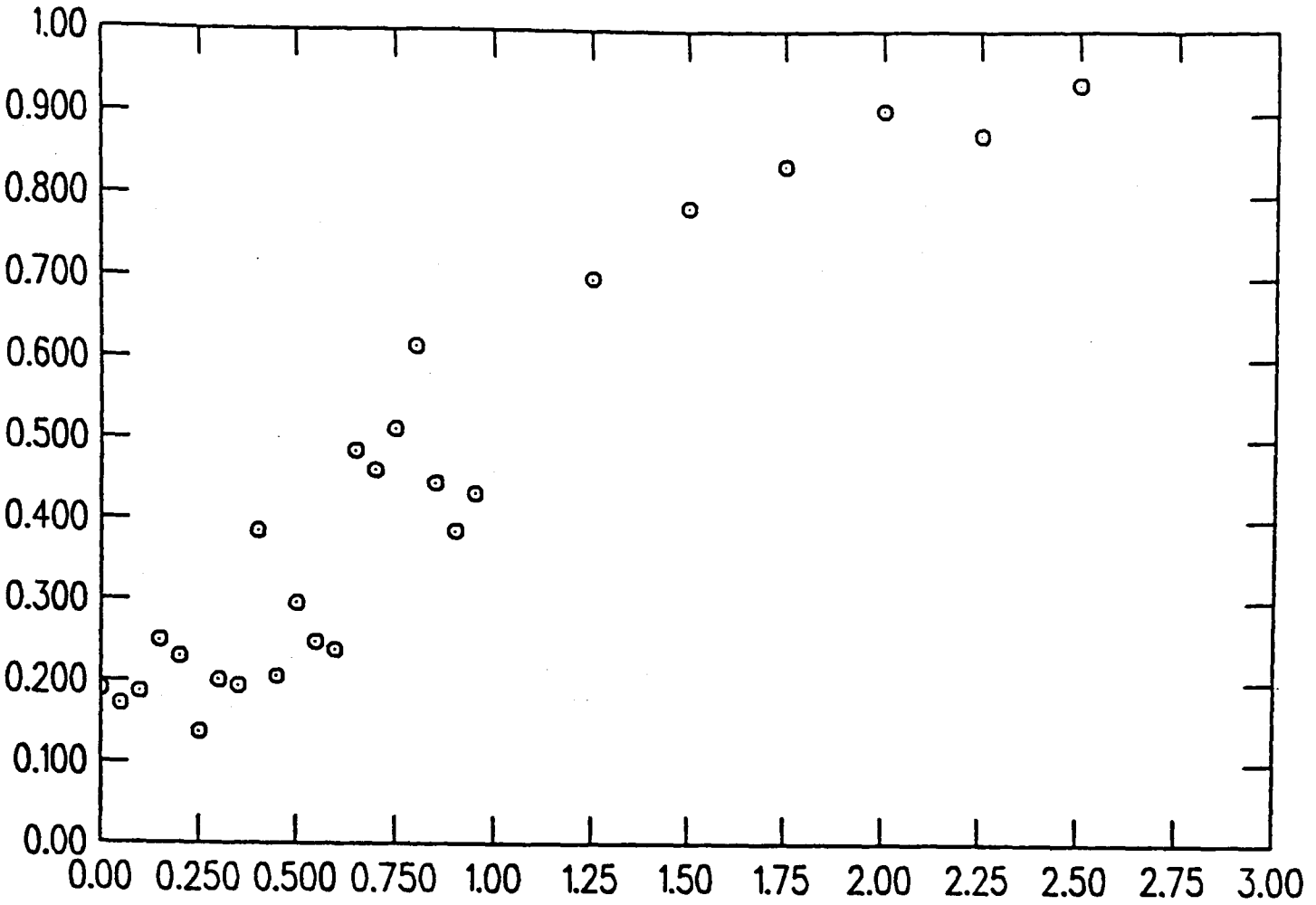

Figure 3.24. Scatter plot of $2/d_H$ vs β for type 1. models.

3.9 Conclusions and Discussion

The results reported here have concerned themselves with the task of trying to examine the phase structure of models based on a discretisation of the partition function for Polyakov's string with the addition of various curvature terms. Principally we examined two types of extrinsic curvature term, both possessing a global minimum corresponding to a smooth surface (in the continuum they are equivalent modulo total divergences). For one (type 1.) we find no evidence for first or second order phase transitions, but there seems to be a evidence of a higher order transition for finite coupling. The beta-function for such a model possesses only two zeros at $\beta = 0$ and $\beta = \infty$, which are infra-red and ultra-violet stable respectively. The surface is smooth at short distance and crumpled at long distance with a continuous evolution between these regimes. In terms of the inverse curvature coupling

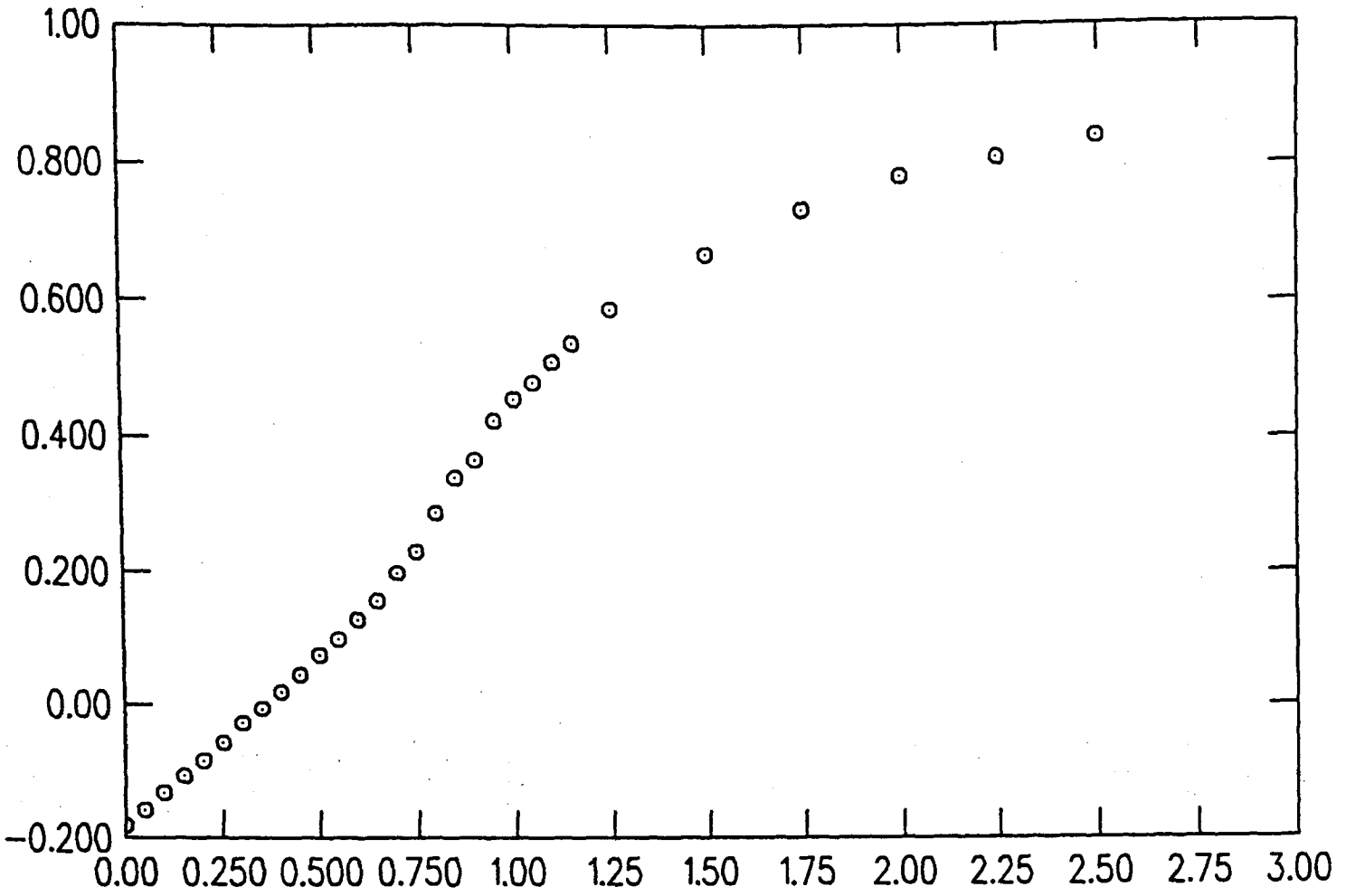

Figure 3.25. Order Parameter $\langle n.n \rangle$ vs β type 1.

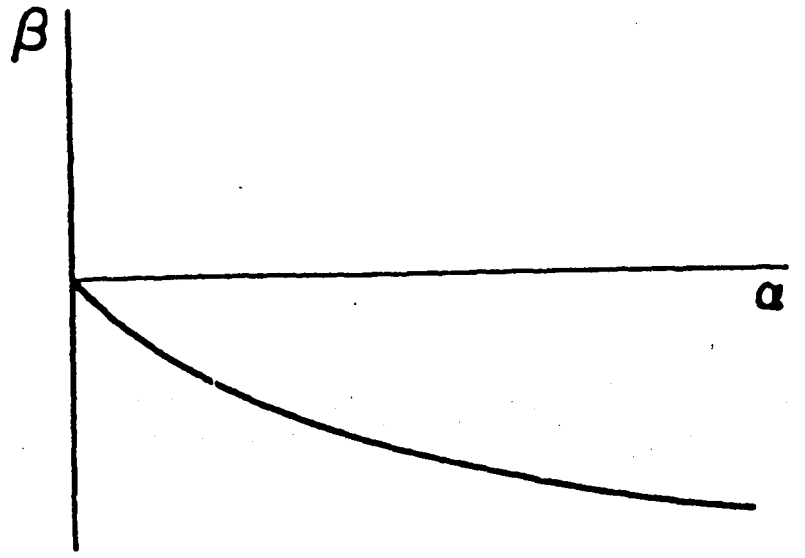

Figure 3.26. Beta function for type 1.

$\alpha = 1/\kappa$ the β-function

$$\beta(\alpha) = \Lambda \frac{\partial \beta(\alpha)}{\partial \Lambda}$$

appears as shown in figure (3.26)

In contrast, the other form (type 2.) possesses a very strong second order transition separating weak and strong coupling, giving rise to a new zero of the beta-function. This is in agreement with more recent work by J.Ambjorn et al. [21] who found that the transition observed by Kantor and Nelson continues in fixed triangulation models with gaussian actions . Their simulations were done with precisely the R_2 rigidity term. The behaviour of the model at low and high energy scales now depends on where in the phase diagram the bare theory sits. It appears possible to define a continuum model, which possesses a finite renormalised curvature coupling, and presumably corresponds to a smooth string. Of course, it remains to be shown that one finds the correct scaling behaviour for the string tension near the critical point. The corresponding β-function is sketched in fig. (3.27)

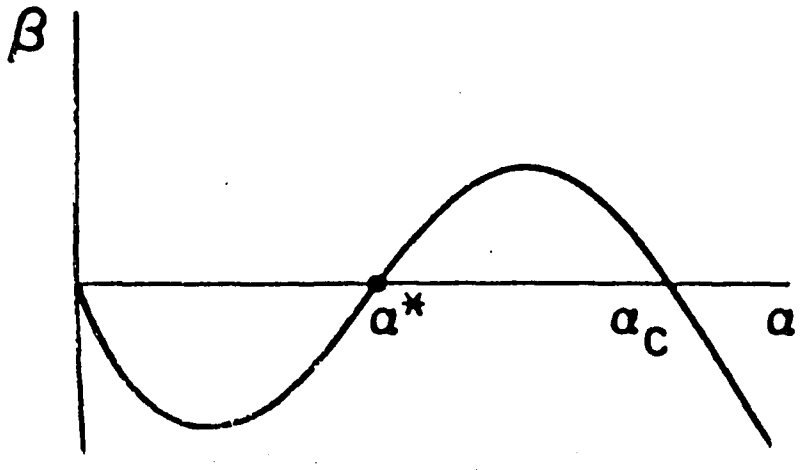

Figure 3.27. Beta function for type 2.

In our simulations we have only been able to consider lattices possessing a maximum of 144 sites. This is forced upon us by the very heavy computational requirements of models encorporating such dynamical retriangulation. Nevertheless we believe that our conclusions capture the qualitative features of the models correctly. It is interesting to speculate on the reasons for the differing phase structure in the two models. Both terms possess equivalent minima which correspond to smooth surfaces, and up to level of quadratic terms, the same fluctuation terms.

Hence their behaviour for small fluctuations will be the same. However the presence of higher order terms for the type 2. form may well yield different behaviours when the surfaces are very crumpled. This is analogous to the situation with compact and non-compact Q.E.D [22].

We have little to say about the restoration of the local symmetries in the models near the critical points. Clearly a proof of the restoration of full Weyl and Reparametrisation invariance will be very hard. Anticipating continuum results it may only be possible in certain critical dimensions. Clearly there is still much useful work to be done in determining critical exponents in the vicinity of the second order transition, and in developing an R.G approach to investigate the long range properties of the models near their critical points.

References:

[1] D.Weingarten Phys. Lett. B90 (1980) 280;
B.Durhuus, J.Frohlich and T.Jonsson Nucl. Phys. B 225 (1983) 185

[2] T.Eguchi and H.Kawai Phys. Lett. B114 (1982) 247

[3] J.M.Drouffe, G.Parisi and N.Sourlas Nucl. Phys. B 161 (1979) 397;
G.Parisi and N.Sourlas Phys. Rev. Lett 46 (1981) 871;
S.Redner J. Phys. A 18 (1985) L273

[4] B.Durhuus, J.Frohlich and T.Jonsson Nucl. Phys. B 240 (1984) 453;
B.Durhuus, J.Frohlich and T.Jonsson Nucl. Phys. B 257[FS14] (1985)779

[5] A.Billoire, D.J.Gross and E.Marinari Phys. Lett. B 139 (1984) 751;
B.Duplantier Phys. Lett. B 141 (1984) 239;
D.J.Gross Phys. Lett. B138 (1984) 185;
M.Bander and C.Itzykson Nucl. Phys. B 257[FS14] (1985) 531

[6] D.Espriu Phys. Lett. B 194 (1987) 271

[7] J.Ambjorn, B.Durhuus and J.Frohlich Nucl. Phys. B 257[FS14] (1985)433

[8] D.V.Boulatov, V.A.Kazakov, I.K.Kostov and A.A.Migdal
Nucl. Phys. B 275[FS17] (1986) 641

[9] A.Billoire and F.David Nucl. Phys. B 275[FS17] (1986) 617

[10] J.Jurkiewicz, A.Krzywicki and B.Petersson Phys. Lett. B177 (1986) 89

[11] A.Krzywicki LPTHE Orsay 87/71

[12] F.David Nucl. Phys. B 257[FS14] (1985) 543

[13] J.Ambjorn, B.Durhuus and J.Frohlich Nucl. Phys. B275[FS17] (1986)161

[14] S.J.Anthony, C.H.Llewellyn-Smith and J.F.Wheater Phys. Lett B116 287

[15] A.Polyakov Nucl. Phys. B 268 (1986) 406

[16] F.Alonso and D.Espriu Nucl. Phys. B 283 (1987) 393

[17] M.Baig, D.Espriu and J.F.Wheater Oxford University preprint

[18] J.Ambjorn, B.Durhuus, J.Frohlich and T.Jonsson
Nucl. Phys. B 290[FS20] (1987) 480

[19] Kantor and Nelson Harvard University preprint

[20] S.M.Catterall in preparation

[21] J.Ambjorn, B.Durhuus and T.Jonsson NBI-HE-88-61

[22] J.B.Kogut, E.Dagotto and A.Kocic ILL-(TH)-88-31

Figure Captions

Figure 3.1 Elementary link flip

Figure 3.2. $\ln X^2$ vs $\ln N$ for $\alpha = 0, 1.5, 3.0, 4.5, 6.0, 9.0, 15.0$.

Figure 3.3. Inverse Hausdorff dimension $(2/d_H)$ as a function of α.

Figure 3.4. $\langle X^2 \rangle$ vs N for random $(\times)$ and biased

$(\circ)$ update.

Figure 3.5. Histogram showing distribution of coordination number at $\alpha = 0$.

Figure 3.6. Distribution of coordination number for $\alpha = 15.0$.

Figure 3.7 $\langle R_2 \rangle$ on lattices with N=48(+),N=72($\times$),

N=96($\diamond$), and N=144($\circ$) sites. Mean-field predictions

are also shown at $\beta = 0$ and $\beta \to \infty$.

Figure 3.8. $\langle \frac{\partial R_2}{\partial \beta} \rangle$ for N=144 sites.

Figure 3.9. $C - D/2$ for type 2. models with N=72.

Figure 3.10. $C - d/2$ for type 2. models with N=96.

Figure 3.11. $C - D/2$ for type 2. models wi=th N=144.

Figure 3.12. $\langle X^2 \rangle$ vs β for type 2. with N=72.

Figure 3.13. $\langle X^2 \rangle$ vs β for type 2. with N=96.

Figure 3.14. $\langle X^2 \rangle$ vs β for type 2. with N=144.

Figure 3.15. Scatter plot of $2/d_H$ vs β for type 2. models.

Figure 3.16. $\langle R_1 \rangle$ vs β for lattices N=48(+), N=72($\times$),

N=96($\diamond$), and N=144($\circ$) with mean-field limits.

Figure 3.17. $\langle \frac{\partial R_1}{\partial \beta} \rangle$ for N=144.

Figure 3.18. Specific Heat $C - D/2$ with mean-field limit $\beta \to \infty$ for N=72.

Figure 3.19. $C - D/2$ for N=96.

Figure 3.20. $C - D/2$ for N=144.

Figure 3.21. $\langle X^2 \rangle$ vs β for type 1. with N=72.

Figure 3.22. $\langle X^2 \rangle$ vs β for type 1. with N=96.

Figure 3.23. $\langle X^2 \rangle$ vs β for type 1. with N=144.

Figure 3.24. Scatter plot of $2/d_H$ vs β for type 1. models.

Figure 3.25. Order Parameter $\langle n.n \rangle$ vs β type 1.

Figure 3.26. Beta function for type 1.

Figure 3.27. Beta function for type 2.

Appendix B

Here we detail the important data structures used in the Pascal code, and give some example procedures.

```
 (* data structures used in holding lattice information *)
 (* consider the creation of the records for link and triangle *)
 (* information *)


Program surface(input,output,.....)

const
 numofpts=144;              (* define constants *)
 dim=3;           (* equivalent to FORTRAN parameter statement *)
 ...;

type
 lpoint=^links;
 links=record         (* set up the data structures by defining *)
     endpt:integer;  (* the content of the link records *)
     trione:integer; (* here endpt contains the integer labelling *)
     tritwo:integer; (* the end of a link attached to some site i *)
     nextlink:lpoint (* trione,tritwo the endpoints of the complement *)
     end;            (* nextlink is a pointer to next link attached to i*)
     ....;

var
  linkhead:array[1..numofpts] of lpoint;  (* linkhead is an array *)
                                          (* of pointers *)
  .....;                                  (* to the first member of each*)
                                          (* linked list labelled by the*)
                                          (* site i *)


        (* now consider procedure to insert a link *)

procedure linkinsert(i1,i2,i3,i4:integer);

(* allows us to insert a new link at beginning of linked list *)
(* attached to site i1 *)

 var
   dum:lpoint;    (* local variable *)
   begin          (* start of routine *)

   dum:=linkhead[i1];
   new(linkhead[i1]);    (* access a portion of memory for new link *)
    with linkhead[i1]^ do
       begin
       endpt:=i2;        (* write data i2-i4 into record of this new *)
       trione:=i3;       (* data item *)
       tritwo:=i4;       (* connect pointers *)
       nextlink:=dum
       end
 end;
```

```
        (* now routine to delete item from linked list *)


   procedure linkdelete(i1,i2:integer);
(* routine searches down linked list attached to site i1 and deletes it *)

  var
    ref,refprevious:lpoint;
    located:boolean;

  begin
   (* locate entry *)

   ref:=linkhead[i1];
   located:=false;

  while (ref<>nil) and (not located) do  (* scan to end of list i.e nil *)
                                          (* until located *)
         with ref^ do
          if endpt=i2 then
           located:=true
          else
           begin
           refprevious:=ref;
           ref:=nextlink
           end;

    if not located then
    writeln(' couldn't find link to delete --error');

    if located then
     begin
      if ref=linkhead[i1] then

          (* deleting first element of linked list--redirect linkhead *)
      linkhead[i1]:=ref^.nextlink
     else
                      (* redirect previous entry *)
      refprevious^.nextlink:=ref^.nextlink;
      dispose(ref)    (* release data item *)
     end
end;

.............;
```